MOLECULAR IMPRINTING FOR SENSOR RECOGNITION ELEMEMENTS

SIMON MARK STANLEY

A thesis submitted in partial fulfilment of the requirements of The Nottingham Trent University for the degree of Doctor of Philosophy

September 2002

LCN= 10362536

C

S.L.C.

KEF

PH.D/CP/02 SrfA

This thesis is, to the best of my knowledge, original except where due reference is made.

Simon Mark Stanley

September 2002

SARAH

You'll remember me when the west wind moves
Upon the fields of barley
You'll forget the sun in his jealous sky
As we walk in fields of gold
So she took her love for to gaze awhile
Upon the fields of barley
In his arms she fell as her hair came down
Among the fields of gold
Will you stay with me, will you be my love
Among the fields of barley?
We'll forget the sun in his jealous sky
As we lie in fields of gold
See the west wind move like a lover so
Upon the fields of barley
Feel her body rise when you kiss her mouth
Among the fields of gold
I never made promises lightly
And there have been some that I've broken
But I swear in the days still left
We'll walk in fields of gold
We'll walk in fields of gold
Many years have passed since those summer days
Among the fields of barley
See the children run as the sun goes down
Among the fields of gold
You'll remember me when the west wind moves
Upon the fields of barley
You can tell the sun in his jealous sky
When we walked in fields of gold
When we walked in fields of gold
When we walked in fields of gold

Sting

Acknowledgements

Firstly, I would like to thank my supervisors at Nottingham Trent University, Dr Alan Braithwaite and Dr Mike Coffey for all the help, advice and encouragement throughout my PhD. Thanks are also due to Dr Wayne Hayes for getting this project off the ground.

I am indebted to the laboratory staff, Bob, Jim, Rob and Mick Wood for all their skilled assistance and technical advice. Thanks are also due to Professor Glen M^{c}Hale and Dr Mike Newton for the opportunity to collaborate on recognition elements for mass sensors.

I have been very fortunate to have been a member of a vibrant and stimulating research department and would like to thank my fellow PhD students Eileen, Max, Asan, Jenny, John, Will, James, Jo, David, and of course Claire and Becky, knowing you has deeply enriched me, three years is not long enough to spend amongst such fine people.

Three years is a fair slice of time and inevitably life doesn't always go to plan. I would like to say a very personal thank you to Dr Carl Percival, your support during trying times has touched me deeply. Thank you for your guidance, advice and the odd kick in the right direction, you have the patience of a saint.

Mum, thank you for all your love and support I could not have done any of this without you.

Finally, I would like to dedicate this thesis to my wife Sarah, you are everything to me, I love you.

Abstract

Molecular recognition is a highly efficient and essential feature of biological systems in nature and as such has found increasing application in biosensors. Natural recognition systems, whilst highly selective, are of limited use because of poor chemical and thermal stability, limited assay range and lifespan. The use of artificial recognition materials has been examined in order to address these shortfalls.

The development and application of molecularly imprinted polymers (MIPs) as artificially generated recognition materials is described. MIPs are highly cross-linked polymers, inherently stable and capable of selectivities approaching their natural counterparts. This thesis describes, in the first instance, the design, development and application of a range of MIP recognition materials as recognition elements applied to quartz crystal microbalances (MIP-QCM).

Initially non-covalent imprinting is employed to produce a recognition element for an important source of ozone producing VOCs, namely the monoterpene L-menthol. The MIP film is cast directly onto the surface of a quartz crystal microbalance (QCM) and enantioselective rebinding of the analyte over its analogues is observed as a frequency shift quantified by piezoelectric microgravimetry. The lower limit of detection to L-menthol was 200 ppb with the device giving a linear response between 0 and 1.0 ppm. This is the first report of an enantioselective MIP utilizing a single monomer-functional moiety interaction.

Non-covalent imprinting has been further examined to produce an MIP-QCM capable of the enantioselective rebinding of the aminoacid L-serine. It is envisaged that such a device could be employed in the identification of chirally active amino acids of importance to the pharmaceutical industry. The lower limit of detection to L-serine was 2 ppb with a linear response range of 0-0.4 ppm. The enantioselectivities of the L-menthol and L-serine sensors are compared and conclusions drawn regarding the importance of functional groups within the recognition site and on the analyte.

The use of covalent imprinting in the production of an artificial receptor for topical abuse steroid. The development of a screening device for nandrolone is reported. Rebinding of the analyte over its analogues is observed as a frequency shift quantified by piezoelectric microgravimetry. The limit of detection of the resultant device to nandrolone is 6 ppb with a linear response range of 0-1.0 ppm.

An alternate approach to recognition element design has been developed to produce a chemically coated piezoelectric sensor for the determination of PAHs in the liquid phase. An organic monolayer attached to the surface of a gold electrode of a quartz crystal microbalance (QCM) has been produced. Selective binding of anthracene via π-π-interaction has been observed as a frequency-shift subsequently quantified by piezoelectric microgravimetry with the QCM transducer. The lower limit of detection of the target analyte was 2 ppb with a linear response range of 0 – 50 ppb. The sensor was able to distinguish between different PAHs despite π-π-interaction being the sole communication between recognition element and analyte. It is envisaged that these techniques could be employed to create recognition elements for different PAHs.

Chapter one

Introduction

1.1 Introduction

Weak non-covalent interactions afford nature a reliable mechanism for the assembly of a diverse range of stable key functional entities such as DNA or the tobacco mosaic virus.[1,2] Non-covalent interactions are also essential during stereospecific reactions in natural systems for example the transamination of keto-acids to produce amino acids. Molecular recognition is fundamental to biological activity within natural systems such as antibodies and enzyme receptors with the enzyme catalysing a reaction once a particular substrate is bound within the recognition site.

Weak non-covalent interactions must be controlled in order to employ natural recognition phenomena in the production of artificial or biomimetic selective recognition systems capable of binding analytes with the same selectivity and efficiency as their natural counterparts.

As in nature high selectivity is obtained if the recognition site is complimentary to the target analyte in size, shape and arrangement of analyte specific functional groups. Ideally the specificity should be such that the entry of erroneous substrates is unlikely. In common with enzyme action a high degree of selectivity is obtained in a synthetic receptor if it possesses a complimentary three dimensional cavity for the desired substrate, and in addition features chemically specific binding sites organised in the correct spatial arrangement within the receptor cavity.

Artificial recognition materials have been produced within synthetic polymers in a process conceptually similar to Emil Fischer's 'lock and key' concept.[3] Artificial

recognition systems have also been produced using for example crown ethers,[4] cryptates,[5] cyclodextrins[6] and calixarenes.[7]

Synthetic mimics of natural enzymes and antibodies have been reported that do successfully replicate their natural counterparts whilst offering the added advantage of functioning in organic solvents and at elevated temperatures.[8,9] One successful approach to biomimetic recognition systems is the formation of molecularly imprinted polymers (MIPs). These synthetic polymers have the potential to act as enzyme mimics or highly selective adsorption media.

The binding of the analyte to such a recognition element occurs because of non-covalent intermolecular interactions between the analyte and the binding site of the receptor. This molecular recognition or supramolecular chemistry has excited the interest of researchers since Fischer postulated the lock and key hypothesis for the specific nature of enzyme substrate interaction. Essential to the understanding of this work is the concept of preorganisation developed independently by Pedersen, Cram and Lehn who in recognition of their incite received the 1987 Nobel prize for chemistry.

1.2 Interactive forces

The study of molecular recognition has provided us with an understanding of the interactive forces employed in nature and subsequently in its mimics. These interactive forces include Van der Waals forces, hydrogen bonding, secondary hydrogen bonding, electronic π- π stacking and solvation effects.

1.21 Dipole-dipole interactions

The high electronegativity of heteroatoms such as oxygen and nitrogen, present in many organic molecules, results in an uneven distribution of electrons in the bonds connecting them to the carbon skeleton. Consequently partial charges arising from this uneven distribution of electron density produce permanent electronegativity within the molecule. Attractive forces can occur because of these dipoles with an attractive force of 8 – 12.5 kJ mol^{-1}. Figure 1.1 shows such an interaction. The effect of such dipole-dipole interactions can be quite profound for instance the boiling point of acetone is 56°C whilst that of butane with an identical molecular weight of 58 is 0°C as a consequence of the dipole possessed by acetone.

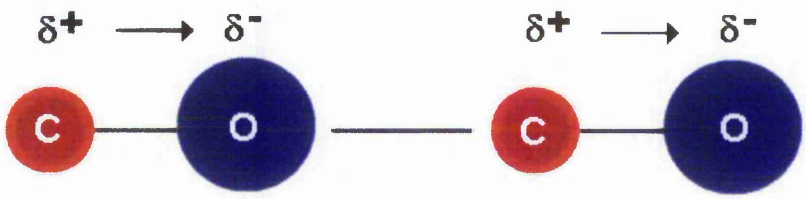

Figure 1.1: Dipole dipole interaction.

1.22 Van der Waals forces

Van der Waals forces are weak attractive forces between molecules not in possession of a permanent dipole. In this case a neutral molecule undergoes spontaneous polarisation that induces a complimentary dipole on a neighbouring molecule, as shown in Figure 1.2. These forces are small with the more electron rich species producing a larger force. The effect is more pronounced the closer the interacting species are to one another. This effect is exemplified by the observation that branched chain alkanes have a lower boiling point than their straight chain counterparts.

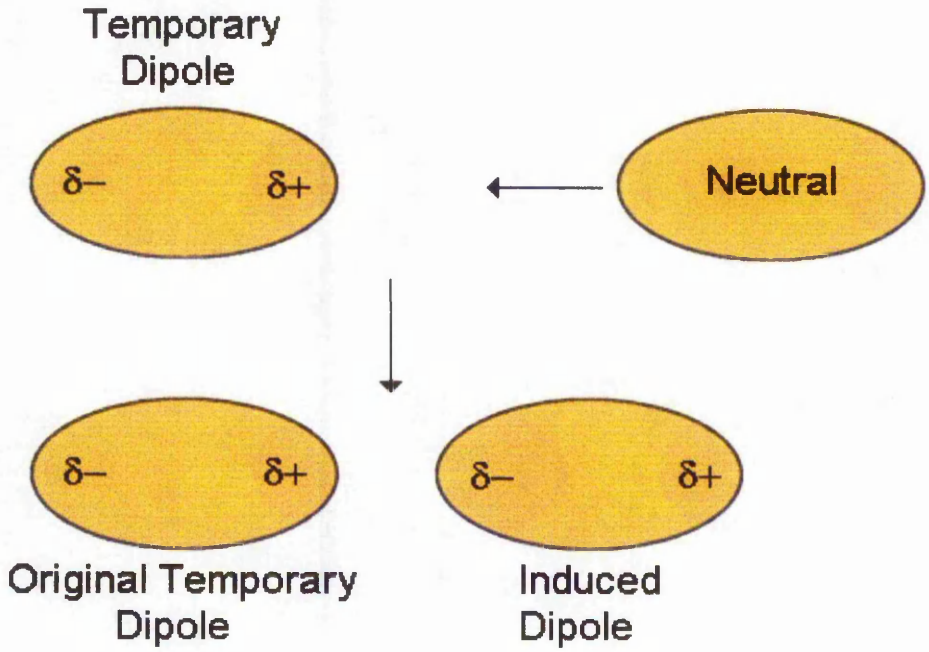

Figure 1.2: Induced dipole.

1.23 Hydrogen bonding

Hydrogen bonding is a result of a specific type of dipole-dipole interaction. Hydrogen bonding occurs as a result of the polarisation of a hydrogen atom and another electronegative atom. With an interactive force of 8-33.5 kJ mol^{-1} the hydrogen bond is stronger than dipole-dipole interactions. As shown in Figure 1.3.

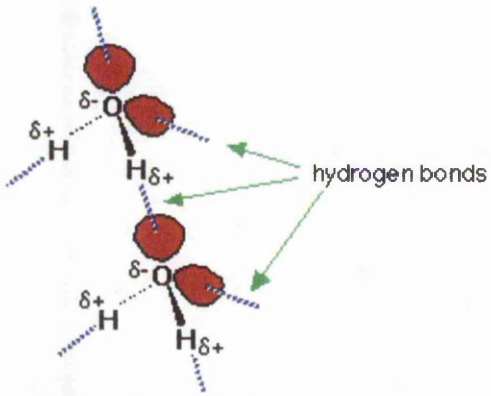

Figure 1.3: Hydrogen bond between water molecules.

1.24 Secondary hydrogen bonds

Secondary hydrogen bonds result when an electron deficient hydrogen bond donor repels a similar electron deficient hydrogen bond donor within another molecule. The same is true for electron rich hydrogen bond acceptors. The effect of secondary hydrogen bonding are evident when the binding energy between guanine/cytosine and uracil/guanine are compared. In the former the net effects of the secondary interactions are zero and the binding energy is 92 kJ mol^{-1}. In the latter, shown in Figure 1.4, there are 2 weaker secondary hydrogen bond interactions and consequently the binding strength between the two is much lower.

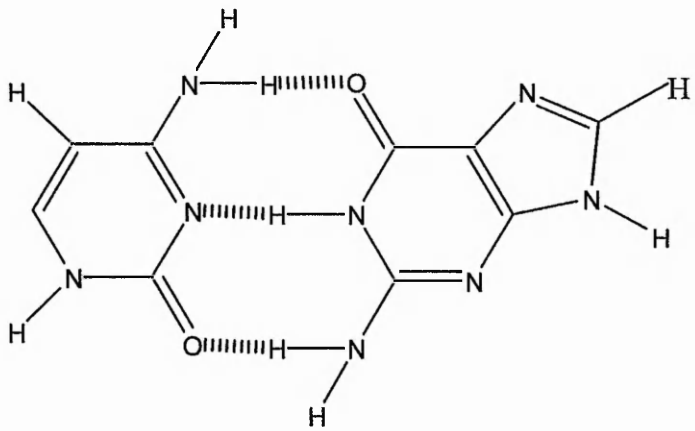

Figure 1.4: Secondary hydrogen bonding between uracil and guanine.

1.25 Electronic π-π interactions

Electronic π-π interactions generally occur in aromatic systems. The polyaromatic hydrocarbon (PAH) sensor described in Chapter 5 utilises such interactions as the sole means for the selective binding of specific PAHs in the liquid phase. Consider benzene, as shown in Figure 1.5, the π-bonds in one benzene molecule undergo a spontaneous polarisation which in turn induces a second dipole in a neighbouring benzene molecule forcing water molecules out of the solvation sphere thus a gain in entropy.

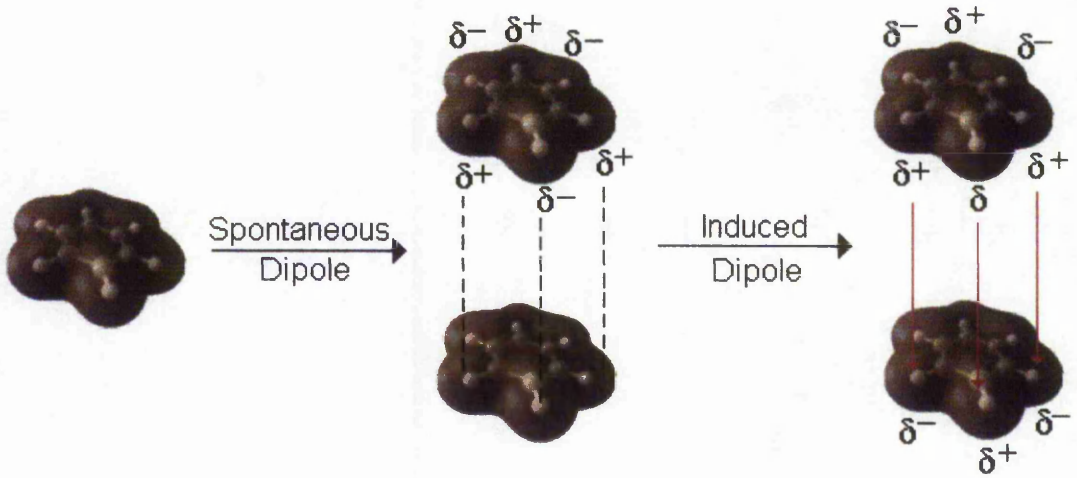

Figure 1.5: Electronic π-π interactions in benzene.

1.3 Molecular imprinting

Since their inception in the early 1970's MIPs have become well established[10,11], and have found application in many areas. Molecular imprinting or template polymerisation employs molecular recognition in the formation of novel porous polymers and has received significant attention[12] in the scientific community over recent years. The process of molecular imprinting is analogous to the mechanism of antibody formation, as shown in Figure 1.6, involving the mixing of functional monomers **1-3** with a *template* molecule **4** prior to polymerisation in the presence of a suitable cross-linking agent. Following polymerisation and subsequent removal of the template **4**, *imprinted* cavities that feature pre-disposed functional groups remain in the rigid polymer produced. The imprinted cavity possesses a shape and spatial arrangement of the functional groups that are complimentary to the template **4**.

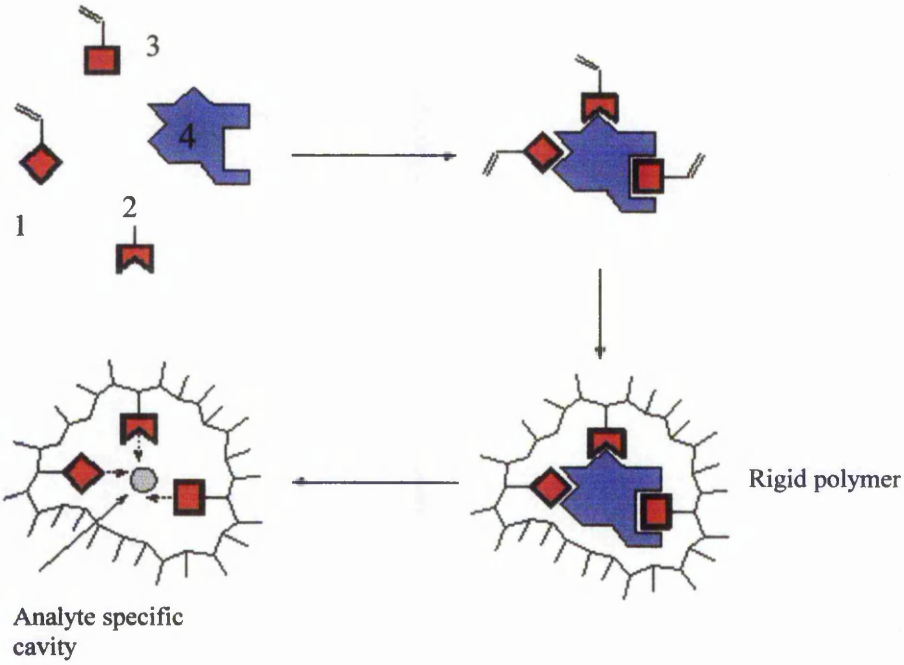

Figure 1.6: The molecular imprinting process.

Essentially the process involves the formation of cross linked polymers formed around a target analyte functioning as a template molecule which is, subsequent to polymerisation, removed. An imprint of the target analyte remains within the polymer matrix containing reactive groups with binding capability.

The structure of the polymer matrix is crucial in the imprinting process with an ideal polymer matrix having the following properties.

A. Stiffness, in order that the imprint cavity retain its shape subsequent to template removal inferring high selectivity.
B. Flexibility, essential for kinetics (equilibration K = mp/mip where K is the partition coefficient and mp the solvent and mip the imprint) but working against the benefits associated with stiffness.
C. Good accessibility of as many cavities as possible in the highly cross-linked polymer can be achieved by forming a particular polymer morphology.
D. Mechanical stability of the polymer particles is essential in many applications if for example they are to survive the high pressures associated with HPLC.
E. Thermal stability of the polymers enables their use at elevated temperatures where kinetics are more favourable.

Macroporous polymers are most commonly used for MIPs and are obtained if polymerisation of monomers is carried out with a high content of cross-linking agent (50 - 90%) in the presence of a suitable porogenic solvent. During the polymerisation, phase separation occurs, removal of the porogen and drying reveals a permanent pore structure. The large pores (10 - 60 nm) and large surface area 50 – 600 $m^2 g^{-1}$ ensure

that the specific microcavities formed by the imprinting process (0.5 - 1.5 nm) are accessible to the target analyte. If sufficiently crosslinked the cavities retain their shape after template removal. The cross-linker concentration is of paramount importance in the optimisation of the selectivity of an imprinted polymer. Figure 1.7.

Original MIPs were relatively poor in terms of selectivity, α, (α1.03- α 1.80) for the resolution of racemates.[10,13] Extensive optimisation by Wulff brought great improvements.[12] Wulff found that the ratio of porogen to monomer should be approximately 1:1 (mL:g) and that the type and quantity of the cross-linking agent used in the production of the macroporous polymers was decisive for achieving high selectivity.

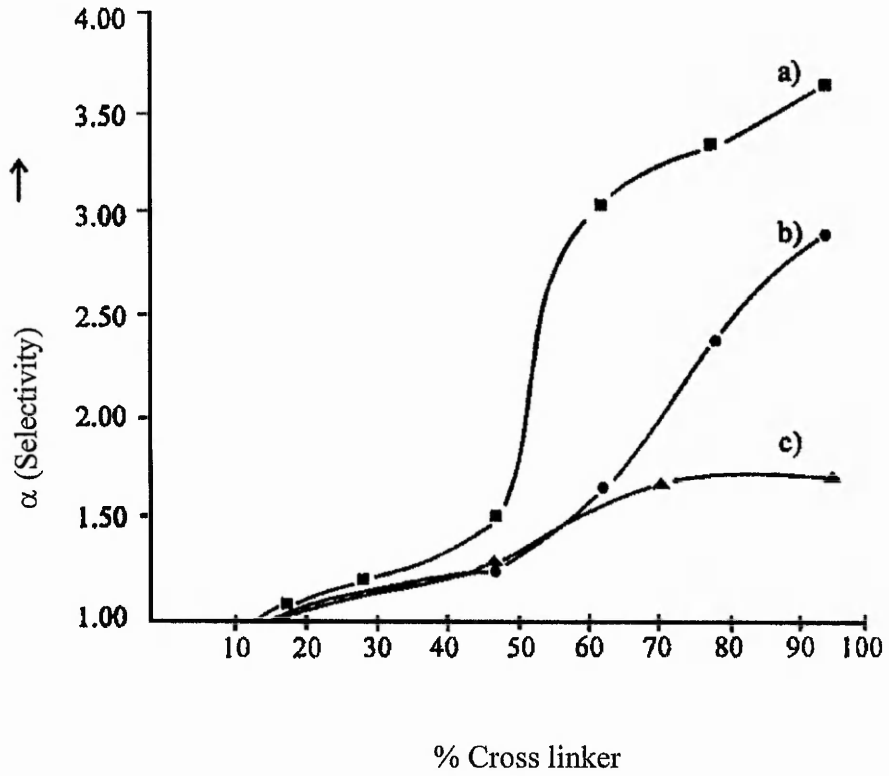

Figure 1.7: Effect of cross-linker concentration on selectivity factor α.

Where a is ethylene glycoldimethacrylate, b is trimethylolpropane and c is divinylbenzene. Figure 1.7 shows the relationship between percentage cross-linker and separation factor, α, for the resolution of phenyl-D,L- mannopyranoside. When the cross linker employed is ethylene glycoldimethacrylate (EDMA). The cross linker shows no specificity below about 10%. The shape of the cavities cannot be stabilised unless the matrix is adequately cross linked. As the percentage of cross linker increases from 10 - 50% the α value increases from 1.0 to 1.5. then increasing the cross linker further from 50 - 70% causes a dramatic increase in the α value from 1.5 - 3.0% corresponding to a four fold increase in selectivity. Further increase in cross-linker causes only moderate increases in selectivity α up to about 3.7. Selectivities of up to 6.0 can be achieved by reducing the ratio of racemate to polymer and by equilibration at higher temperature. EDMA has been identified as one of the most suitable cross-linking monomers because of its relative cheapness, ease of purification and hence the most widely employed monomer in imprinting.[12] The thermal and mechanical stability of polymers with higher EDMA concentration is very good and as a result chromatographic columns based on this material have been reported exhibiting no loss in selectivity at up to 80°C and high pressure for many months.[14] The cavities in EDMA type polymers have been demostrated to be readily accessible. Consequently if the template is fixed by readily hydrolysable or covalent bonds, over 90% of the template can be removed. Of the empty cavities about 80 - 90% have the potential for re-occupation on subsequent equilibration with an excess of the template molecule. If the templates are bound by non-covalent bonds this figure is 10-15%. Thus almost 90% of the cavities from which the template is removed cannot be re-occupied.[15]

Two different imprinting strategies exist the non-covalent or self assembly approach and the covalent or pre-organised route.

1.4 Non-covalent imprinting

The non-covalent route is the conceptually simpler of the two methods and involves the formation of host-guest complexes formed by intermolecular interactions (i.e. ionic or hydrophobic interactions, hydrogen bonding and metal co-ordination) between the analyte and monomer precursors.

In non-covalent imprinting monomers that can undergo non-covalent interactions are brought together with the template and a suitable cross linker to form well defined aggregates of template and monomer. Intuitively one can see that these monomers ligated to the template are in rapid equilibrium with monomers in solution. In order that the highest possible number of interactions occur during the polymerisation, the ratio of ligand monomer to template in the solution must be at least 4:1.[16] As a result the binding groups within the polymer matrix adopt a more random arrangement. This is illustrated by the reduced binding affinity of a non-covalently prepared MIP for the steroid nandrolone compared with its covalently prepared counterpart, outlined in Chapter 4. However, removal of the template in such a polymer is far easier and reversible interactions with substrates are rapid. The nature of the template determines which strategy is most suitable. For the purposes of MIP chromatographic stationary phases non-covalent interactions are usually preferred as an excess of binding groups does not appear to exert an adverse effect on separations.

With non-covalent interactions it is beneficial to carry out the polymerisations at low temperature, as these conditions favour the association equilibrium.[15,17,18]

Ideally the non-covalent interaction of binding groups with template molecules must undergo a stoichiometric reaction (e.g. 1:1, or 2:1). In this way the unspecific distribution of binding groups within the polymer matrix post polymerisation and subsequent to template removal will be reduced.

The non-covalent templating approach employs specific weak intermolecular interactions between a template and functional monomers to self-assemble highly defined stable pre-polymerisation complexes. The bulk reaction mixture containing the self-assembled complexes, excess monomer and cross-linking agent is then polymerised, typically using free radical initiation, to create a macroporous polymer featuring highly organised cavities incorporating the complexed template. The template is then removed from the polymer matrix by elution of a suitable solvent through the macroporous polymer, leaving vacant recognition sites specific to the template used. This approach has been extensively developed by Mosbach and coworkers and offers several key advantages over other routes to MIPs, the main practical benefit being the ease of sample preparation and polymer clean up. The non-covalent templating approach to molecular imprinting is shown in Figure1.8.

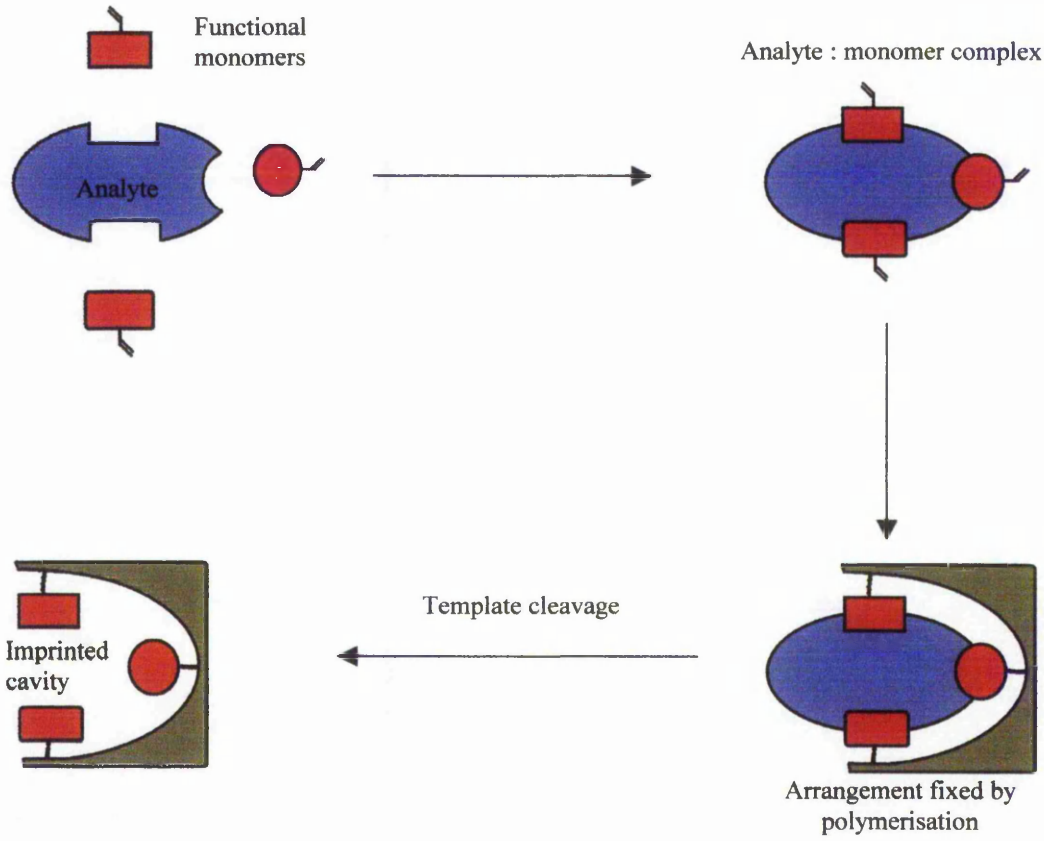

Figure 1.8: Non-covalent templating approach to molecular imprinting.

A notable example of a non-covalently imprinted polymer that employs hydrogen bonding interactions has been reported by Stanker, whereby the herbicide template, atrazine binds with the functional monomer methacrylic acid to form a stable pre-polymerisation termolecular complex, as shown in Figure 1.9.[19] The analyte molecular complex is then polymerised under free radical conditions in chloroform employing ethylene glycol dimethacrylate (EDMA) as the cross-linking agent and following template removal, a macroporous polymer is produced that is capable of extracting the herbicide template from beef liver residues.

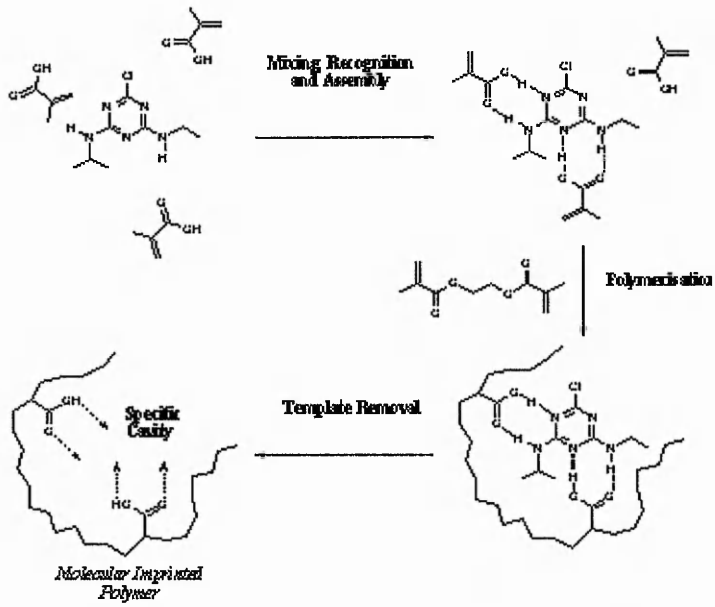

Figure 1.9: Non-covalent templating approach to a MIP capable of extracting the herbicide atrazine.

1.5 Covalent imprinting

In contrast to the non-covalent templating method, the technique of covalent imprinting produces macroporous polymers that incorporate the template by covalent bonds. Covalent interactions have the advantage that the binding groups remain precisely fixed in space during the polymerisation process resulting in a more homogeneous population of binding sites.

The primary requirement of the covalent imprinting method is that a functionalised monomer system must first be synthesised that features the desired template. The template system must therefore be stable to the coupling conditions used to link it to the

polymerisable unit. After polymerisation, in order to reveal the desired shape specific cavities, template cleavage strategies have to be employed before the macroporous polymer can be used for its intended function. Therefore, the linkage employed to couple the polymerisable unit to the template is a key factor to be considered when trying to develop covalently imprinted polymers. The covalent strategy is depicted in Figure 1.10.

Clearly the need to produce a polymerisable derivative of the template or an analogue contrasts sharply with the simpler non-covalent approach. However, in the preparation of an MIP catalyst the advantages associated with the covalent strategy, namely precision of binding site functionality pre and post polymerisation, can still favour this route.

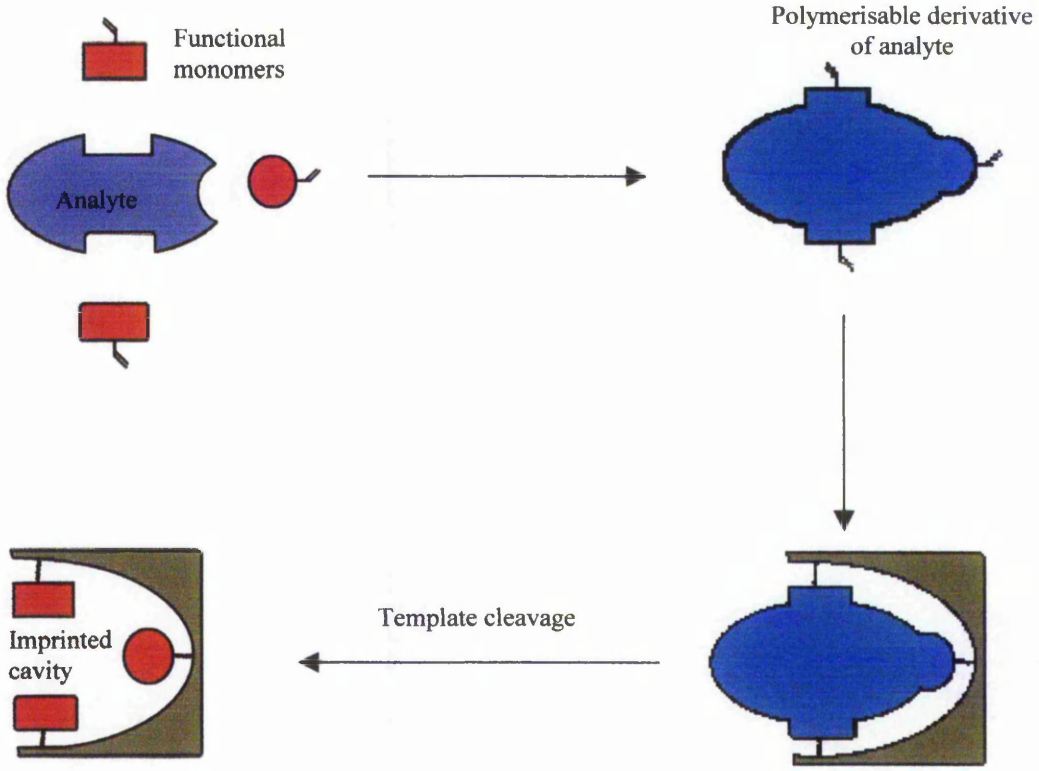

Figure 1.10: Covalent templating approach to molecular imprinting.

Extensive studies have been performed by Wulff and coworkers in the area of covalent imprinted polymers. An example of covalent MIP is shown in Figure 1.11, whereby the bisvinylboronic ester of phenyl-α-D-mannopyranoside is copolymerised in the presence of EDMA to form a rigid polymer that covalently incorporates the sugar unit.[12] Subsequent cleavage of the boronic esters by methanol releases the sugar unit to reveal highly sugar specific cavities possessing boronic acids units held in highly defined orientations capable of the selective rebinding of the target analyte through hydrogen bonding interaction.

Macroporous polymers of this type have been reported[12] that are able to effect baseline separations of racemic mixtures, exhibiting chromatographic selectivity factors α between 4 – 8.

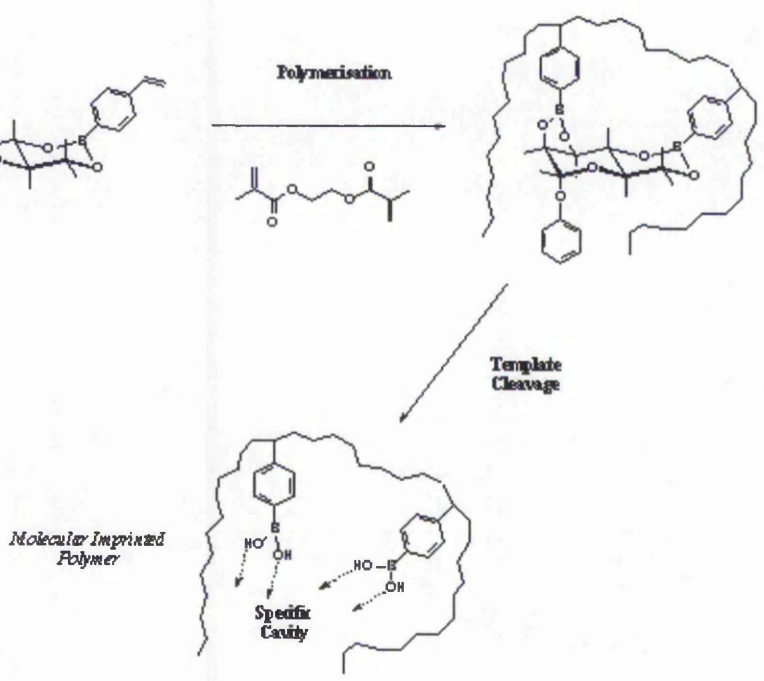

Figure 1.11: Molecular imprinting processes employing a covalent approach.[12]

The majority of the covalent imprinting studies[10,16] have involved bulk polymerisations in conjunction with a suitable porogenic agent[20] to produce a macroporous polymer block that is subsequently crushed, sieved and finally packed into clean HPLC columns for chromatographic evaluation.[21]

The covalent approach to molecular imprinting macroporous polymers has been successfully utilised to develop novel separation media exhibiting extremely high selectivities for a range of substrates, both organic[22] and inorganic[23] in nature.

This thesis concentrates on the synthesis and application of polymer type MIPs as artificial recognition materials. Alternatives to imprinting within the confines of a polymer matrix do exist and are outlined below.

1.6 Imprinting in biopolymers

As an alternative to imprinting within polymeric matrices Keyes *et al.*, [24] have converted proteins via an imprinting process into semi synthetic enzymes. The protein is initially denatured and a modifying agent is used. This may for example be an inhibitor for the enzyme to be modelled. The protein is then cross-linked around this modifier/template which is then removed. The starting materials Keyes used had no activity in the case of albumin or completely different activity in the case of a ribonuclease. Subsequently products with new types of enzymatic activity were obtained with the partially denatured protein assumed to bind the template. Bio imprinting was also examined by Mosbach *et al.*,[25] Here α chymotrypsin was allowed

to self assemble in the presence of N-acetyl-D-phenylalanine with 1 propanol and then dried. After the template removal the α chymotrypsin demonstrated good selectivity for the formation of D-phenylalanine ethyl ester in non-aqueous solution. An enzyme treated analogously in the absence of the template exhibited no selectivity.

1.7 Imprinting in carbohydrates

Shinkai *et al.*,[26] cross-linked water soluble starch with cyanuric chloride in the presence of methylene blue. The insoluble products subsequent to the removal of methylene blue were able to absorb methylene blue better than a starch cross-linked in its absence. The reason for this observation is the greater number of accessible sites within the imprinted starch compared to its non-imprinted counterpart.

1.8 Imprinted cavities with inorganic carriers.

Thin layers, 5-10 nm, of macroporous polymers can be produced on the surface of wide pore silica gels. Methacrylate groups are bound covalently to the surface of the silica gel, for example, by reaction with 3-(trimethoxysilyl) propyl methacrylate. The surface is then coated with a monomer mixture typical for the imprinting process and polymerised by free radical initiation. The result is a highly selective adsorbent consisting of non-swelling particles. These are especially suitable for the chromatographic separation of racemates.[27]

1.9 Imprinted silica gels

The foundations for molecular imprinting were arguably laid by Dickey.[28] In an extension of Emil Fischers lock and key hypothesis Dickey precipitated silica gel in the presence of dyes (methyl orange and its analogues). Once the dyes were removed the gels showed an increased affinity for the template dye. It would appear that during the formation of the matrix, silanol groups arrange themselves around the dye template. This work was subsequently extended to include racemate resolution and the separation of pesticides.[29] In the case of pesticides the separation observed was poor and consequently this work was not pursued.

1.10 Applications of imprinted polymers

The main applications of MIPs has traditionally been as either chromatographic type stationary phases or more recently as recognition elements in sensor devices.

1.11 Chromatographic type stationary phases

Imprinted macroporous polymers have found extensive application as stationary phases in chromatography, most usefully as chiral stationary phases. Macroporous polymers are ideally suited for chromatographic application for a number of reasons.

Despite numerous advantages such as high column efficiency, packed bed HPLC chromatographic columns have associated with them inherent limitations. The most

significant limitation being the slow diffusional mass transfer of high molecular weight solutes from stagnant mobile phase present in the pores of the separation medium and the large void volumes between the particles of sorbent. Molecular transportation within the pores and interparticular voids of packed bed columns is controlled predominantly by diffusion processes. Consequently, low molecular weight entities possess mass transfer coefficients several orders of magnitude greater in comparison to large molecules, such as polymers and proteins. The so-called 'resistance to mass transfer' is further promoted by the discontinuity inherent to packed bed columns. This phenomenon is highly detrimental to processes such as HPLC analysis, where the speed of mass transfer limits the overall separation rate.

The lowest interparticulate volume in a perfectly packed column of uniformly sized beads is theoretically 27% of the total column volume. However, in practice, a void volume of about 40% is obtained typically using modern column packing methods. Localised interparticulate void volumes can be decreased by reducing the size of the particles used, but this action in turn increases the mass transfer coefficient of analytes. Thus, columns possessing smaller porous particles exhibit high efficiency coefficients. In contrast to polymers that become porous in solvents (so-called 'gel-type' polymers), macroporous polymers are characterised by a permanent rigid porous structure that exists even in the dry state. The internal structure of macroporous polymers is produced in the polymerisation process only in the presence of specific inert diluents ('*porogens*') and consists of many interconnected pores of different sizes possessing a structural rigidity secured through significant crosslinking.

Many types of macroporous polymers have been developed as a result of the search for mechanically resistant ion-exchange resins possessing improved osmotic shock resistance and enhanced kinetics.[30] Polymers of this type have subsequently attracted significant attention with regard to their application in chromatographic analysis, ranging from size exclusion separations of polymers to their employment in capillary column chromatography. Chemists are most familiar with this class of polymer in the form of spherical 'beads' produced by suspension polymerisation processes that were invented by Hofman and Delbruck in 1912.[31]

A notable advance in the field of polymeric separation media has been reported by Fréchet and Svec,[32] who described an efficient approach to producing continuous macroporous *monolithic* columns. These monolithic systems are obtained by performing the polymerisation directly within a mould to afford, after removal of unwanted by-products and porogens, a macroporous rod-like column that can be immediately utilised for chromatographic purposes. Figure 1.12.[32]

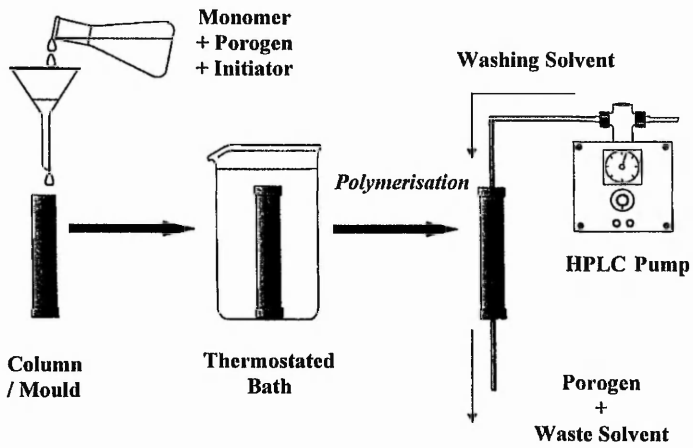

Figure 1.12: The moulding process used to produce monolithic macroporous polymer rods.

The mould, typically a tube or empty HPLC column, is sealed at one end and filled with the polymerisation mixture and then sealed at the other end prior to polymerisation.

A significant advantage of these monolithic columns is their pore size characteristics, typically dominated by a large number of flow-through pores and a connected network of smaller pores, as shown in Figure 1.13. These characteristics allow for rapid convective mobile phase flow through the monolith. As a direct consequence, columns of this nature have been found to be suitable for processes in which rapid mass transfer is required, such as the separation of polymeric mixtures.[33] The porous nature of these continuous columns can be extensively tailored to suit the desired application by altering porogen compositions and the temperature of the polymerisation.[32,33]

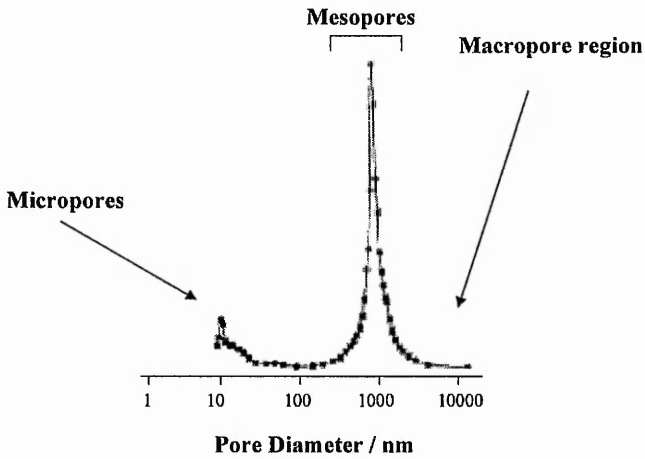

Figure 1.13: A typical bimodal pore size distribution of a monolithic column.

By combining the obvious benefits associated with macroporous polymers with those potentially available through molecular imprinting chromatographic stationary phases have been produced for the separation of a variety of analytes.

Molecular imprinting offers the promise of tailor made enantioseparation materials. MIPs have had notable success as chiral stationary phases in chromatography. The significance of molecular asymmetry in the pharmacological activity and pharmacokinetics of chiral compounds is well known with examples including the well documented horrific consequences of enantiomeric contamination observed in the case of thalidomide in the 1960's.[34] MIPs, used as chiral stationary phases in HPLC, have been prepared for a variety of analytes including N-Acetyl-L-Phe-L-Trp-Ome,[35] Cbz-L-Aspartic acid[36] and Propranolol.[37]

1.12 Sensor recognition elements

There is an increasing need to monitor all aspects of our environment in real time. Growing awareness and concern over pollution and its effect upon our health and safety, biomonitoring for the assessment of disease or substance abuse could both benefit from the development of rapid in situ screening devices capable of selectively responding to a specific analyte at ppb levels. The determination of contaminants and analytes with ever lower detection limits with improved accuracy and precision has led to the development of a wide range of fast and portable sensing systems which are increasingly replacing heavy and expensive apparatus. Chemical sensing is part of an information acquisition process where the chemical composition of a system is elucidated, at least in part, in real time. A chemical sensor interacts with a particular analyte via a chemical reaction and can ideally be employed for both qualitative and quantitative analyte determination.

Chemical sensors and biosensors are of great importance within modern analytical chemistry and as a result the search for highly selective, cheap, stable and facile chemical sensors for a huge array of environmental industrial analytes has attracted increasing interest in recent years with greater and greater specificity being sought. Molecular recognition is as outlined previously, a highly efficient and essential feature of biological systems in nature and as such has found application in biosensors.[38] Natural biological recognition systems, whilst highly selective, are of limited use, however, as a result of poor chemical and thermal stability, limited assay range, lifespan and expense. The use of artificial recognition materials has been proposed as a means of addressing some of the limitations inherent in biosensors. In biosensors, employing MIPs a signal is generated when an analyte is bound to the recognition element.

There are two parts to a chemical sensor. The region responsible for selective chemical interaction, the receptor region and the interrogative transducer or reporter region. The recognition element is responsible for the production of a signal such as fluorescence or change in oscillator frequency and the transducer for the conversion of this signal to a measure of the analyte. When the target analyte or guest molecule forms a complex with the receptor region a physical change occurs in or around the reporter region of the device. The change in the reporter region as a result of the analyte interaction with the receptor region can be subsequently monitored by utilising a suitable analytical technique, such as fluorescence emission, UV spectroscopy or in the case of a QCM microgravimetry. A schematic representation of a chemical sensor is given in Figure 1.14.

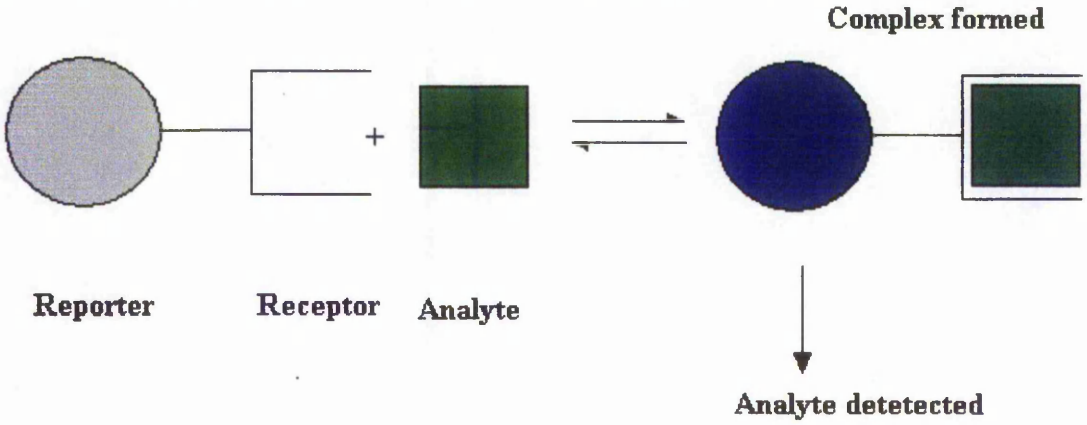

Figure 1.14: A schematic representation of a chemical sensor.

Gravimetric sensors, such as the quartz crystal microbalance (QCM), are well suited as transducer elements for chemical sensors, being portable, rapid and sensitive. For applications in chemical sensing, a recognition element is added to the acoustic wave device capable of selectively binding the analyte to the device surface. The response of these devices is then based on a decrease in their resonant frequency as mass is attached to the device or the recognition element.

MIPs as recognition elements for sensors are attracting increasing attention and reports of MIP-QCM devices have started to appear in the literature.[39-41] Initially these studies concentrated on analyte rebinding in gaseous media, however, recently an MIP-QCM sensor has been reported for the detection of the chiral β-blocking drug S-propranolol in the liquid phase.[42]

1.13 Quartz Crystal Microbalance sensors

Piezoelectric (PZ) devices such as the gravimetric quartz crystal microbalance (QCM) have the potential for "real-time" or "near-time" measurement of a large numbers of measureands including temperature, pressure, magnetic field strength and analytes in both the liquid and gas phases. Most sensor applications of acoustic waves are based on the ability of acoustic wave device to detect very small changes in mass on their surface.

The Curie brothers were the first to describe the piezoelectric effect in 1880 when they observed that a mechanical force applied to the opposite faces of a slice of α quartz resulted in the production of an electrical potential between them.[43] Subsequently Lippmann demonstrated the converse effect whereby the PZ material undergoes elastic deformation when an electric field is applied.[44] Alternating the electric field causes the PZ material to oscillate. The amplitude of this oscillation is maximum when the frequency of the applied field is equal to the resonant frequency of the PZ material, itself governed by the PZ material, its dimensions and the surrounding material.

The oscillation gets very large when the oscillating frequency corresponds to matching the thickness of the crystal with a whole number of half wavelengths so for plate thickness d, wavelength λ and where n is an integer:

$$\lambda = 2d/n \qquad 1.1$$

For AT cut quartz crystals this corresponds to a thickness of

$$d = 1.67/f \quad 1.2$$

where f is measured in MHz and d in mm. A 5MHz crystal operated with n=1 (fundamental) the thickness will be 0.334 mm. The resonant frequency of oscillation is a function of the mass of the sensor, including any attached recognition elements.

The deposition of any substance on the surface of the oscillating quartz causes a change in the frequency of oscillation. The Sauerbrey equation (1957) predicts the change of the crystals resonant frequency in relation to the change in rigid mass on the crystal surface. [45] For AT cut quartz,

$$\Delta f = - 2.26 \times 10^{-6} F^2 \Delta m/A \quad 1.3$$

Δf (Hz) is the change in frequency that occurs for an increase in mass Δm (g) on the surface of area A (cm^2) with a crystal resonant frequency of F (Hz); the constant reflects material properties of the crystal. From the Sauerbrey equation a 1Hz frequency shift observed with a PZ device operating at 10's of MHz corresponds to a sensitivity of 10^{-10} gcm^{-2}. Thus very low detection limits to analytes are offered as a result of the high sensitivity to nano mass changes at the device surface.

Mass sensitivity S_m of an acoustic wave device is defined as the incremental signal change in response to an incremental mass increase per unit area on one surface of the sensor device.

$$S_m = \text{limit}(\Delta f/F_o/\Delta m) \quad 1.4$$

$\Delta f/F_o$ is the frequency change relative to the fundamental frequency. S_m has units of (Hz/MHz)/(ng/cm^2). A common unit in the literature is cm^{2}g^{-1} with the two related by;

$$cm^2g^{-1} = (Hz/MHz)/(ng/cm^2) \times 1000 \quad 1.5$$

Analyte sensitivity is the incremental signal change per unit concentration change of the analyte.

The first devices used by Sauerbrey were Quartz Crystal Microbalances, an example of which is shown in Figure 1.15.

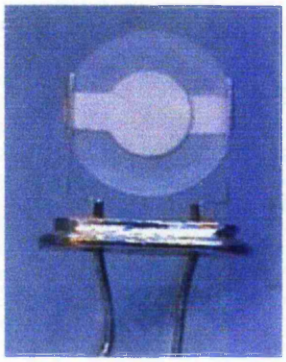

Figure 1.15: A typical QCM device.

QCMs consist of a thin piezoelectric plate with an electrode attached to each side, across which is generated a wave by the application of a voltage between the electrodes. This wave has a longitudinal and a shear component, with the latter commonly used for QCMs in the thickness shear mode; hence the term "thickness shear mode resonator" (TSM) often applied to such devices. QCMs as outlined above are limited in their highest fundamental frequency of oscillation by the thickness of the piezoelectric plate, the thinner the plate the higher the fundamental oscillating frequency. In practise an operating frequency of 10 MHz is the highest practable since this requires a QCM of about a fifth of a millimetre thick. Thus as a consequence these devices have a limited mass detection capability.

Acoustic wave devices are non-selective responding generally to surface mass changes. The use of sorptive or molecularly selective surface modifying layers such as an MIP can convert the devices into sensors that are capable of selective binding of a target analyte. Indeed, the major feature of PZ chemical sensors is the response of sensors with specific coatings applied to their surface. Whilst PZ devices have attracted increasing attention since the 1970's the majority of publications have concentrated on their application under very controlled conditions rather than in the environment at large. The basic relationships for mass sensitivity of the QCM oscillator resonator were derived with the assumption of air or vacuum contact with the device surface. However these devices are now employed in gaseous, liquid and aerosol sensing applications.

1.14 Application of QCM sensors

1.15 Gas analysis

If a coating that selectively absorbs a gaseous species is applied to the surface of the crystal then the crystal will function as a monitoring device with its sensitivity dependent upon coating, analyte area, temperature, and response times governed by reaction kinetics which in turn are affected by gas flow, temperature and analyte concentration. The main difficulty with gas analysis using PZ chemical sensors is the difficulty in producing an adsorbate selective for a single analyte gas.

1.16 Piezoelectric aerosol sensors

Aerosols are defined as liquid or solid particulate matter dispersed in a gaseous media. The particulate size of aerosols is of great interest in health and safety and within industrial clean rooms in the semiconductor industry. Particles of < 7.5 μm diameter fall within the respirable range and are consequently of particular interest. Diesel particulates offer a significant source of concern both because of their size and their toxicology/chemistry. Of recent interest are the sub 2.5 μm particles resulting from catalyst emissions. PZ systems are currently being developed for real-time dust measurement.

The PZ surface interaction with a dust or aerosol particle clearly differs from gas or liquid interactions and is related to the size and binding capacity of the analyte particle.

In the case of gaseous or liquid analytes sorption and desorption or reversible chemical reactions can occur with a suitable chemical coating on the PZ. This is not possible with dust, but alternatives include sorption on to silicon oil and electrostatic precipitation. Dust charging techniques offer the best hope for near real-time nanogram dust sensors.

The principle problems observed are a lack of dynamic linear range and deviation from Sauerbrey theory. This is associated with varying particle size range and a lack of particle binding with the surface of the PZ. As a deposit becomes thicker a point is reached where the observed frequency shifts are lower than the theoretical response. This is considered to be a result of a deviation from the monolayer requirement of the Sauerbrey equation, non-binding of dust or bounce-off of dust at the PZ surface, as a consequence there is a departure from linear response. This point is reached at 1.5 - 6.0 $\mu g\ mm^{-2}$ for ambient and pollution source aerosols so is clearly limited. Once again temperature and humidity can result in erroneous measurements.

1.17 Piezoelectric crystal liquid phase sensors

Two problems hindered the early use of PZ devices in the liquid phase namely, damping out and a lack of immobilised surface-active coatings. For analysis in the liquid phase the recognition element or selective coating should be insoluble and inert to liquid penetration and have dimensional stability i.e. resistant to shrinking or swelling. The MIPs introduced previously can possess the desired properties and have attracted increased attention recently as recognition elements for PZ devices. PZ sensing in the liquid phase is limited as signal loss occurs at frequencies above 10 MHz.

König and Gratzel[46] have produced a QCM based sensor for the detection of the herpes virus. Antibodies to five human herpes viruses were immobilized on the surface of a quartz crystal. Antigenic viruses introduced were then able to bind with the antibodies resulting in a mass increase and subsequently a frequency shift. They reported a detection limit of about 5 x 10^3 cells. The high selectivity associated with antibody-antigen interactions makes such an immunosensor highly selective. This result better than many others exemplifies the ability and suitability of molecular recognition as the primary source of selectivity. König and Gratzel found that the antigen-antibody binding was so strong that the analyte often resisted cleaving from the recognition element.

1.18 Outline of research

Analyte selective coatings have been prepared and evaluated as recognition elements appended to gravimetric transducers (QCM) for a range of analytes including monoterpenes, amino acids, topical steroids and organic hydrocarbons. Both covalent and non-covalent imprinting strategies have been studied and the results compared and contrasted with those reported in the literature.

Chapter two examines an MIP-QCM prepared by non-covalent imprinting for the detection of a significant source of biogenic VOCs, namely the monoterpenes. The relevance of monoterpenes in the production of ozone is also discussed.

Chapter three evaluates the response of an MIP-QCM with specific selectivity for the amino acid L-serine. The MIP is prepared by non-covalent imprinting, once again the response of this device to the target analyte and its analogues is examined. The importance of chirally pure compounds to the pharmaceutical industry is also discussed.

Chapter four describes the derivatisation of a topical steroid into a polymerisable analogue and the subsequent synthesis of a covalently prepared MIP for the detection of the steroid nandrolone. Screening for drugs of abuse within sporting activities is of topical interest. The response of the device is evaluated and its suitability for the screening of steroids in general is discussed.

Whilst Chapters 2, 3, and 4 have been concerned with recognition or selective binding as a result of hydrogen bonding and steric factors Chapter five reports the synthesis of a recognition element selective for polyaromatic hydrocarbons (PAH) employing Van der Waals interaction as the sole means of analyte discrimination. The selective coating is prepared by the addition of the recognition element directly onto the surface of a thiol coated QCM transducer. Two different synthetic strategies, an ionic and a covalent approach, for the attachment of the recognition element are examined and their relative merits compared. The response of the recognition elements to the target PAH and its analogues is reported and the importance of PAH monitoring discussed. The potential of the device to be retuned with a new recognition element selective for a different target is investigated.

Chapter six includes a discussion of the relative response of each of the devices to the target analyte and its analogues. In the case of the monoterpene L-menthol and the amino acid L-serine the observed enantioselectivity of the device is examined and compared with contemporary work. The ability of the covalently prepared nandrolone sensor to discriminate enantiomerically between isomers of testosterone is also evaluated and its import discussed. The suitability of the PAH sensor to identify the target PAH over its analogues is also considered and the advantages of both the covalent and ionically bound recognition elements is examined.

1.19 References

1. F. A.Jurnak, A. McPherson, *Biological Macromolecules and Assemblies*, John Wiley & Sons Ltd: Chichester, UK, **1985**.
2. W. Hayes, J.F. Stoddart, in *Large Ring Molecules*, J.A. Semlyen, Eds.; John Wiley & Sons Ltd: Chichester, UK, **1996**.
3. F.W. Lichtenthaler. *Angew. Chem., Int. Ed. Engl.*, **1994**, *33*, 2364.
4. D. J. Cram, *Angew. Chem.*, **1988**, 100, 1041; *Angew. Chem. Int. Ed. Engl.*, **1988**, 27, 1009.
5. J. M. Lehn, *Angew. Chem.*, **1988**, 100, 91; *Angew. Chem. Int. Ed. Engl.*, **1988**, 27, 89.
6. G. Wenz, *Angew. Chem.*, **1993**, 106, 851; *Angew. Chem. Int. Ed. Engl.*, **1994**, 33, 803.
7. D. Diamond, K. Nolan, *Anal. Chem.*, **2001**, 73, 22.
8. L.Ye, O.Ramstrom, K.Mosbach, *Anal. Chem.*, **1998**, 70, 2789.
9. M. Kempe, *Anal. Chem.*, **1996**, 68, 1948.
10. G. Wulff, A. Sarhan, K. Zarbrocki, *Tet. Lett.*, **1973**, 4329.
11. G. Wulff, A. Sarhan, *Angew. Chem.*, **1972**, 84, 364; *Angew. Chem. Int. Ed. Engl.*, **1972**, 11, 341.
12. G. Wulff, *Angew. Chem. Int. Ed. Engl.*, **1995**, *34*, 1812.
13. G. Wulff, R. Grobe-Einsler, W. Vesper, A. Sarhan, *Makromol. Chem.*, **1977**, 178, 2817.
14. G. Wulff, H. G. Poll, M. Minarik, *J. Liq. Chromatogr.*, **1986**, 9, 385.
15. B. Sellergren, K. J. Shea, *J. Chromatogr.*, **1993**, 635, 31.
16. B. Sellergren, M. Lepistö, K. Mosbach, *J. Am. Chem. Soc.*, **1988**, 110, 5853.

17. D. J. O'Shannessy, B. Ekberg, L. I. Andersson, K. Mosbach, *J. Chromatogr.*,**1989**, 470, 391.

18. B. Sellergren, *Chirality.*, **1989**, 1, 63.

19. L.H. Stanker, M.T. Muldoon, *Anal. Chem.*, **1997**, 69, 803.

20. K. Yoshizako, K. Hosoya, Y Iwakoshi, K. Kimata, N. Tanaka, *Anal. Chem.*, **1998**, 70, 386.

21. S. Rimmer, *J. Chromatogr.*, **1998**, 46, 470.

22. L. Fischer, R. Műller, B. Ekberg, K. Mosbach, *J. Am. Chem. Soc.*, **1991**, 113, 9358.

23. T. Rosatzin, L.I. Andersson, W. Simon, K. Mosbach, *J. Chem. Soc.* Perkin Trans., **1991**, 8, 1261.

24. S. Sarawathi, M. H. Keyes, *Enzyme. Microb. Technol.*, **1985**, 6, 98.

25. M. Stahl, U. Jeppsson-Wistrand, M. O. Mansson, K. Mosbach, *J. Am. Chem. Soc.*, **1991**, 113, 9366.

26. S. Shinkai, Yamada. T. Sone, O. Manabe, *Tetrahedron Lett.*, **1983**, 24, 3501.

27. O. Norrlöw, M. Glad, K. Mosbach, *J. Chromatogr.*, **1984**, 299, 29.

28. F. H. Dickey, *J. Phys. Chem.*, **1955**, 59, 695.

29. R. Curti, U. Colombo , *J. Am. Chem. Soc.*, **1952**, 74, 3961.

30. F. Svec, J.M.J. Fréchet, *Science.*, **1996**, 273, 5272.

31. F. Svec, J.M.J. Fréchet, *Anal. Chem.*, **1992**, 64, 820.

32. M. Petro, F. Svec, J.M.J Fréchet, *J. Chromatogr. A.*, **1996**, 752, 59.

33. F.C. Peters, F. Svec, J.M.J. Fréchet, *Chem. Mater.* **1997**, 9, 1898.

34. T. Adler, *Science News*, **1994**, 424.

35. O. Ramström, I. A. Nichols, K. Mosbach, *Tetrahedron: Asymmetry.*, **1994**, 5, 649.

36. L. I. Andersson, K. Mosbach, *J. Chromatogr.*, **1990**, 516, 313.

37. L. Fischer, R. Müller, B., Ekberg, K. Mosbach, *J. Am. Chem. Soc.,* **1991a**. 113, 9358.

38. R. S. Sethi, *Biosens. Bioelectron.*, **1994**, 9, 243.

39. F. L. Dickert, O. Hayden, *Trends Anal. Chem.,* **1999**, 18, 192.

40. K. Haupt, K. Mosbach, *Chem. Rev.*, **2000**, 100, 2495.

41. D. Kriz, O. Ramstrom, K. Mosbach, *Anal. Chem.*, **1997**, 69, 345.

42. K. Haupt, K. Noworyta, W. Kutner, *Anal. Commun.*, **1999**, 36, 391.

43. P. Curie, J. Curie, *Bull. Soc. Min. de France*, **1880**, 3, 90.

44. W. G. Cady, *Piezoelectricity*, Dover Publications, New York, **1964**.

45. G. Z. Saubrey, ZT Physik, **1959**, 155, 206.

46. B. König, M.Gratzel, *Anal. Chem.*, **1994**, 66, 341.

Chapter two

Sensor for L-menthol detection

2.1 Abstract

A piezoelectric sensor coated with an artificial biomimetic recognition element has been developed for the determination of L-menthol in the liquid phase. A highly specific non-covalently imprinted polymer (MIP) was cast in-situ on to the surface of a gold coated quartz crystal microbalance (QCM) electrode as a thin permeable film. Selective rebinding of the target analyte was observed as a frequency shift quantified by piezoelectric microgravimetry with the QCM. The detectability of L-menthol, quantified by a 1 Hz frequency shift, was 112 ppb with a linear response range of 0 - 1.0 ppm. The response of the MIP-QCM to a range of monoterpenes was investigated with the sensor binding menthol in favour of analogous compounds. The sensor was able to distinguish between the D- and L- enantiomers of menthol owing to the enantioselectivity of the imprinted sites. To our knowledge, this is the first report describing enantiomeric resolution within an MIP utilising a single monomer-functional moiety interaction. It is envisaged that this technique could be employed to determine the concentration of terpenes in the atmosphere. Monoterpenes represent a significant source of biogenic VOCs in the atmosphere and as such require quantification.

2.2 Introduction

The structure of the atmosphere is important when considering its chemistry. The atmosphere is divided into distinct regions identified by temperature, as shown in Figure 2.1. 80 - 90% of the atmospheres mass resides in the lower region the troposphere.

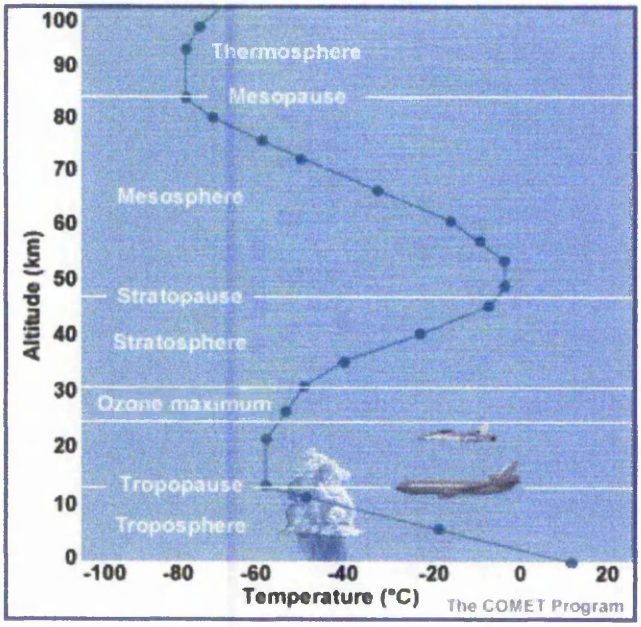

Figure 2.1: Structure and temperature of the atmosphere.

The temperature drop with altitude can be explained in terms of a radiative transfer model, i.e. hot air rises and in so doing performs work on the surrounding air mass and cools down. If it were to cool less than its surroundings, the air would not rise and the system would be convectionally stable, the troposphere is unstable but the mesosphere is stable. The criterion used to separate stable and unstable atmospheres is the adiabatic lapse rate. Vertical mixing within the troposphere occurs relatively quickly (~1 day), but horizontal mixing is slow taking approximately one year for an entire hemisphere to

thoroughly mix. The boundary between the troposphere and the stratosphere (the tropopause) is indicated by a change in the temperature gradient. The temperature of the tropopause is 220 K and acts as a cold trap causing the observed dryness of the air above it. The stratosphere has typically 2-3 ppm of water whilst the troposphere has a few thousand ppm. The height of the tropopause is determined by the latitude and the meteorological conditions but is typically 15 km.

In the stratosphere the temperature rises with altitude due to the photolysis of molecular oxygen to form ozone which absorbs strongly in the ultraviolet region of the electromagnetic spectrum.

$$O_2 + h\nu\ (\lambda \leq 240\ nm) \rightarrow O + O \qquad 2.1$$

$$O + O_2 + M \rightarrow O_3 + M \qquad 2.2$$

The photolysis of both O_2 and O_3 liberates thermal energy, which leads to a rise in temperature. As a consequence of the reversal of the temperature gradient warmer air lies on top of colder air and so the air mass is stable with respect to vertical mixing. At 50 km the temperature of the atmosphere starts to fall with altitude. The point at which the temperature starts to fall is called the stratopause. The region directly above this is known as the mesosphere. Eventually the atmosphere becomes so thin that the collisional frequency between gaseous species is so small that all the energy is not equilibrated between all the available degrees of freedom. As a result the translational thermal energy exceeds that of the rotational and vibrational energies resulting in a

temperature rise once more. This region is called the thermosphere and the boundary between this layer and the mesosphere is called the mesopause.

Mass transport between the troposphere and the stratosphere is of the order of 22-44 % of the total mass of the stratosphere every year.[1] Principally, transport to the stratosphere occurs in the tropics as a result of powerful convection currents generated by solar heating. The air then returns to the troposphere in the mid to high latitudes by tropospheric folding associated with low pressure systems.[1] This is considered a significant source of tropospheric ozone. However the extent of the contribution to the tropospheric ozone budget by transport of air masses from the stratosphere is hotly debated.[2]

2.21 Daytime Tropospheric Chemistry

The homogeneous daytime gas phase chemistry is dominated by the hydroxyl radical the major daytime oxidant, the major source of OH radical being the reaction of excited oxygen with water:

$$O(^1D) + H_2O \rightarrow 2\,OH \qquad 2.3$$

Where $O(^1D)$ is generated by the photolysis of ozone

$$O_3 + h\nu\ (\lambda<320\ nm) \rightarrow O(^1D) + O_2(^1\Delta_g) \qquad 2.4$$

Other sources of OH radicals are the photolysis of HONO and indirectly the photolysis of HCHO

$$HONO + h\nu\ (\lambda<320\ nm) \rightarrow OH + NO \quad 2.5$$

$$HCHO + h\nu\ (\lambda<320\ nm) \rightarrow H + HCO \quad 2.6$$

The source of HONO in the atmosphere is the thermolecular reaction of OH with NO.

$$HO + NO + M \rightarrow HONO + M \quad 2.7$$

If there are no other sources of HONO, reaction 2.5 does not lead to an overall net production of OH radicals. The sinks of the hydroxyl radical differ according to the ambient air quality and therefore to the characteristics of the area it is situated over. A remote rural area for example has lower concentrations of hydrocarbons (with some exceptions, CFCs, methane, CH_4, and methyl chloride). In this specific area the main reactions of the OH radical will be with CO and CH_4:

$$OH + CH_4 \rightarrow CH_3 + H_2O \quad 2.8$$

$$OH + CO \rightarrow CO_2 + H \quad 2.9$$

Reaction 2.8 is the start of an important series of reactions and products that indicate the degradation pathways prevalent in the tropospheric breakdown of volatile organic compounds (VOCs), as it is illustrated in Figure 2.2.[3] Both the above reactions produce reactive species that can subsequently react with oxygen to form peroxy species.

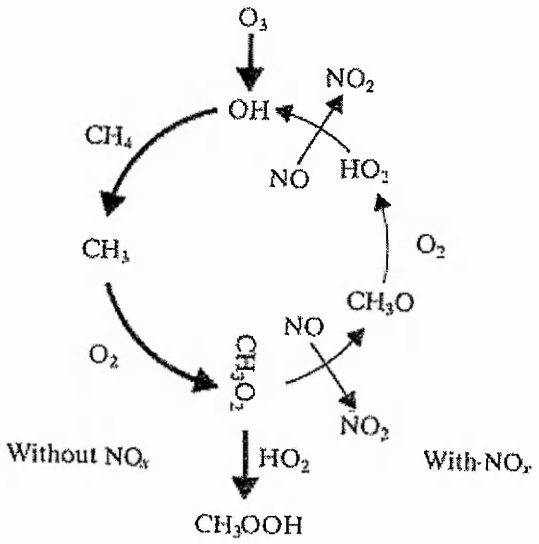

Figure 2.2: Essential steps in tropospheric methane oxidation. In absence of NO_X, the cycle stops on the bottom half.[3]

$$CH_3 + O_2 + M \rightarrow CH_3O_2 + M \qquad 2.10$$

$$H + O_2 + M \rightarrow HO_2 + M \qquad 2.11$$

In less polluted areas where the availability of trace species (e.g. NO or NO_2) is limited in the troposphere, it is possible for the peroxy species produced from the reactions 2.10 and 2.11 to undergo self or cross reactions:

$$HO_2 + HO_2 \rightarrow HOOH + O_2 \qquad 2.12$$

$$CH_3O_2 + HO_2 \rightarrow CH_3O_2H + O_2 \qquad 2.13$$

$$CH_3O_2 + CH_3O_2 \rightarrow 2\,CH_3O + O_2 \quad 2.14a$$

$$CH_3O_2 + CH_3O_2 \rightarrow CH_2O + CH_3OH + O_2 \quad 2.14b$$

The products of reactions 2.12 and 2.13 are readily soluble in water and therefore can be incorporated into cloud droplets and be washed out of the atmosphere by rain their main elimination process.

In areas with higher methane and NOx pollution levels the OH radical can react with a variety of organic species, RH, such as HFCs leading to the formation of peroxy radicals (RO_2)

The main loss mechanism for the peroxy radical is its reaction with NO:

$$RO_2 + NO \rightarrow RO + NO_2 \quad 2.15$$

Production of tropospheric ozone from the photolysis of the NO_2 subsequently occurs:

$$NO_2 + h\nu\ (\lambda<420\ nm) \rightarrow NO + O(^3P) \quad 2.16$$

$$O(^3P) + O_2 + M \rightarrow O_3 + M \quad 2.17$$

$$NO + O_3 \rightarrow NO_2 + O_2 \quad 2.18$$

When NO is plentiful the rate of the above reactions and consequently the rate of ozone production depends on the rate of formation of peroxy radicals which in turn depends on the rate of OH attack or photochemical dissociation of the VOCs present. Also a large fraction of the tropospheric peroxy species, RO_2, can react with HO_2 and to a lesser extent undergo self or cross reactions with other peroxy species.[4] Given that the global average of NO (about 2.5×10^8 molecule cm^{-3}) and HO_2 (about 2.5×10^8 molecule cm^{-3}) and that the rate constants for reaction of both species with RO_2 are of a similar magnitude, it is clear that there is a competition between NO and the HO_2 reaction with RO_2.[5] This competition is important with respect to the tropospheric ozone budget, and in the absence of NO, ozone loss occurs as can been seen from the following series of reactions:

$$HO_2 + O_3 \rightarrow OH + 2O_2 \qquad 2.19$$

$$CO + OH \rightarrow H + CO_2 \qquad 2.20$$

$$H + O_2 + M \rightarrow HO_2 + M \qquad 2.21$$

leading to a net reaction of:

$$CO + O_3 \rightarrow CO_2 + O_2 \qquad 2.22$$

As can be seen from the above simplified series of reactions the peroxy radicals play a significant role in the tropospheric ozone budget. Another source of ozone in the

troposphere can be the transport of air masses containing a high abundance of ozone, from the stratosphere (approximately 22 – 24 % of the mass of stratosphere).

2.22 Photochemical ozone creation potential (POCP)

Regional scale photochemical air pollution is a widespread phenomenon in many of the world's populated areas, with photochemical pollution episodes characterised by high levels of secondary pollutants such as ozone and peroxy acetyl nitrate.[5] The production of elevated levels of ozone is of particular concern, since it is known to have adverse effects on human health, vegetation and materials, and the formulation of control policies is therefore a major objective of environmental policy.[6]

It is well established that ozone is generated in situ from the sunlight-initiated oxidation of VOCs in the presence of NOx.[7] Whilst largely dependant upon geographical location the biogenic emissions of VOCs may exceed their anthropogenic counterparts by up to an order of magnitude.[8] Several thousand biogenic VOC's have been identified amongst the most important are the monoterpenes emitted by terrestrial plants. [9] The significance of VOCs of biogenic origin requires classification in terms of their ability to generate ozone, so compounds which make a greater contribution can be targeted preferentially in abatement strategies.

One well established method of defining such an ozone-formation index involves the use of boundary layer trajectory model, containing the appropriate detailed chemical

and meteorological mechanisms.[10] This allows all the main factors that can influence ozone production from a given VOC to be incorporated into a chemical mechanism.

The photochemical ozone creation potential, POCP, and the methods of calculation, has been described in detail previously, and is only briefly outlined here.[11] The indices are determined from the calculated formation of ozone over a period of almost five days in a boundary layer air parcel travelling along a straight line trajectory over northern Europe, using a photochemical trajectory model.[12] The production of ozone on such trajectories is believed to be predominantly limited by the availability of VOCs, such that the reduction in ozone levels is best achieved by control of VOC emissions.[10] Consequently the chosen trajectory is particularly appropriate for the definition of a comparative ozone formation index for VOCs.

The POCP for a particular VOC is determined by quantifying the effect of a small incremental increase in its emission on the integrated ozone formation along the trajectory, relative to that resulting from an identical increase in the emission of a reference VOC, which is taken to be ethene.[10] Thus the POCP 'i' for the given VOC is defined as follows:

$$POCP_i = \frac{\text{Ozone Increment with the } i\text{th VOC}}{\text{Ozone Increment with ethene}} \times 100 \qquad 2.23$$

With the value of ethene being 100 by definition.

2.23 Chemistry of Ozone Formation

The essential features of the VOC degradation mechanisms are illustrated in Figure 2.3. For almost all VOCs, the degradation is predominantly initiated by reaction with hydroxyl radical (OH). In the presence of NOx, this initiates a rapid sequence of reactions involving organic peroxy (RO_2) and alkoxy (RO) radicals, and the hydroperoxy radical (HO_2), ultimately leading to the regeneration of OH as shown in Figure 2.3. Since OH is regenerated, this mechanism is a catalytic cycle which oxidises the given VOC into its first generation carbonyl product (or products), with ozone generated as a by-product.[13] The radicals are mainly produced by photodissociation of stable molecules (e.g. ozone, aldehydes and ketones), such that sunlight, VOCs and NOx are the key ingredients for ozone formation.

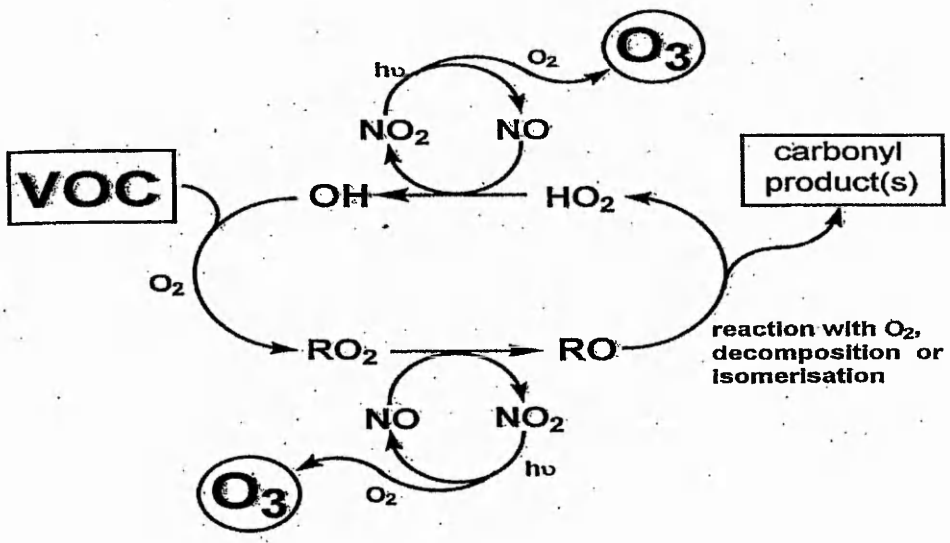

Figure 2.3: Schematic representation of the free radical catalysed oxidation of a VOC into its first generation carbonyl product(s) in the presence of NO_x and the associated generation of ozone.

The various classes of free radical all have important roles to play in the ozone formation process. Whereas the rates of reaction with OH govern the relative lifetimes and oxidation rates of VOCs, the reactions of the peroxy radicals, RO_2 and HO_2, provide the coupling with NOx chemistry by oxidising NO to NO_2.[14] The efficient photodissociation of NO_2 by near ultra-violet and visible radiation then generates ozone. (reactions 2.16, 2.17). As shown in figure 2.4, the RO radical is converted into HO_2 as part of the chain propagating process. The mechanism of RO $\rightarrow$ HO_2 conversion is strongly dependent on the structure of RO (and therefore on the structure of the parent organic compound), and also determines the identities of the first generation carbonyl products, which may vary considerably in structure and reactivity.[15] For simple RO radicals, conversion to HO_2 is achieved in a single step by reaction with O_2, also yielding a carbonyl oxidation product. More complex RO radical may also thermally decompose or isomerise (if they contain a carbon chain $>C_4$). In these cases, a sequence of reactions involving additional peroxy radicals may occur prior to the generation of HO_2. If a thermal decomposition process is involved, two smaller carbonyl products will be produced in conjunction with HO_2.[5]

Figure 2.3 shows the oxidation of a given VOC into its first generation carbonyl product (or products). The complete photochemical degradation of any VOC to carbon dioxide and water usually proceeds via a sequence of similar stages. The oxidation of the first, and subsequent, generation carbonyl compounds is also driven by reactions of the free radical intermediates by the general pattern described above, with ozone produced at each stage.

2.24 Simple Structure-Based Ozone Formation Index (γ_S)

A simple ozone-formation index may be derived by considering the total quantity of ozone formed as a by-product of the complete OH-initiated oxidation of a given compound to CO_2 and H_2O, catalysed by NOx. The detailed tropospheric chemistry for simple hydrocarbons such as methane and ethane may therefore, be represented by the following overall equations.[10]

$$CH_4 + 8O_2 \rightarrow CO_2 + 2H_2O + 4O_3 \qquad 2.24$$

$$C_2H_6 + 14O_2 \rightarrow 2CO_2 + 3H_2O + 7O_3 \qquad 2.25$$

$$C_2H_4 + 12O_2 \rightarrow 2CO_2 + 2H_2O + 6O_3 \qquad 2.26$$

Ozone formation from the oxidation of methane occurs via HCHO and CO as intermediate oxidised products, and involves well established radical propagating reactions involving CH_3O_2, CH_3O, HCO and HO_2 .[15] as shown schematically in Figure 2.4. According to equations 2.24 – 2.26, therefore, the complete oxidation of one molecule of each of the compounds leads to the production of 4, 7 and 6 molecules of ozone respectively. Interestingly the number of ozone molecules produced in each case is equivalent to the number of reactive bonds in the parent molecule (n_B), i.e. the number of C-H and C-C bonds, cleaved during complete oxidation to CO_2 and H_2O.[10]

A simple structure based ozone formation index (γ_S) is generated by further normalising the total ozone yields relative to a value of 1.0 for ethene.[10]

$$\gamma_S = (n_B / M) \times (28 / 6) \qquad 2.27$$

where M is the molecular weight of the given VOC and 28 and 6 are respectively the molecular weight and the number of reactive bonds in ethene. An example of the calculation of ozone formation index γ_S is:

Linalool: $\gamma_S = (n_B / M) \times (28 / 6)$ 2.27

$\gamma_S = (28 / 154) \times (28 / 6)$

$\gamma_S = 0.84$

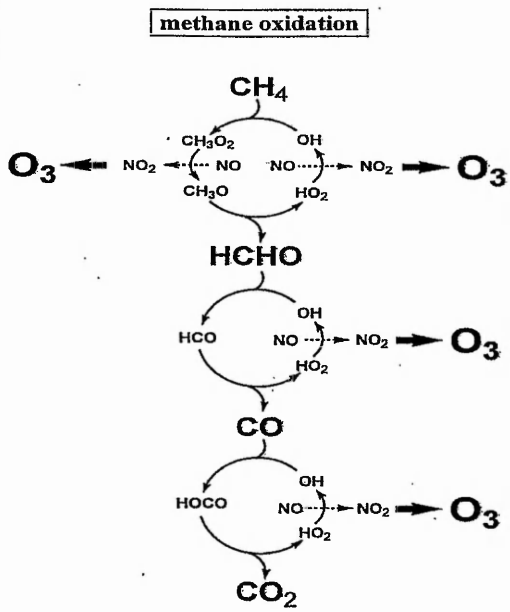

Figure 2.4: Schematic representation of the free radical and NOx – catalysed oxidation of methane to carbon dioxide, showing the associated production of ozone at each stage.[10]

Thus, it is well known that HO_x (the sum of OH and HO_2) plays an important role in the formation of tropospheric ozone. Recently, Wennberg *et al.*,[16] have noted that the levels of HOx in the upper troposphere are greater than previously modelled using just the oxidation of CH_4. The presence of non-methane hydrocarbons (e.g. C_2H_6) and other oxygenated species (e.g. $CH_3C(O)CH_3$) in the upper troposphere are now believed to significantly augment the rate of formation of CH_3O_2, which can lead to an autocatalytic formation of HOx.[16] Several thousand biogenic VOC's have been identified amongst the most important are the monoterpenes emitted by terrestrial trees, plants and vegetation.[8] As a result terpenes clearly represent a significant natural source of oxygenated hydrocarbons in the Earth's atmosphere that need to be quantified.[3] There is an obvious need to measure oxygenated species in the atmosphere as a function of altitude, hence the fabrication of a monoterpene sensor described herein.

2.25 Measurement of VOCs in the atmosphere

Generally atmospheric hydrocarbons (such as terpenes) are collected and then pre-concentrated on a chromatographic type stationary phase prior to analysis by, for example, atmospheric thermal desorption-gas chromatography-mass spectrometry (ATD-GC-MS)[17] in order to separate and identify the components of the sample. An alternative approach involves identifying key marker compounds that might be used to assess the pollution potential problem to model and calculate the flux of these terpenes. The development of analytical techniques for measuring the marker compounds would therefore greatly simplify the monitoring and analysis process obviating the need for sample preconcentration and chromatographic separation. Such a technique involves the

use of chemical sensors such as thickness shear mode devices coated with a recognition element.

As outlined in chapter 1, gravimetric sensors, such as the quartz crystal microbalance (QCM), are well suited as transducer elements for chemical sensors, being portable, rapid and sensitive. For applications in chemical sensing, a recognition element is added to the acoustic wave device capable of selectively binding the analyte to the device surface. The response of these devices is then based on a decrease in their resonant frequency as mass is attached to the device or the recognition element.

The search for highly selective, cheap, stable and facile chemical sensors for a huge array of environmental industrial analytes has attracted increasing interest in recent years with greater and greater specificity being sought. Molecular recognition is as outlined previously, a highly efficient and essential feature of biological systems in nature and as such has found application in biosensors.[18] Natural biological recognition systems, whilst highly selective, are of limited use, however, as a result of poor chemical and thermal stability, limited assay range, lifespan and expense. The use of artificial recognition materials has been proposed as a means of addressing some of the limitations inherent in biosensors.

Acoustic wave microsensors have been gaining widespread recognition as sensors for a wide range of analytes with an excellent review recently published.[19] MIPs as recognition elements for sensors are increasingly of interest[20,21] and MIP-QCM have started to appear in the literature and work in this area has been recently reviewed.[22] Initially these studies concentrated on analyte rebinding in gaseous media however,

recently an MIP-QCM sensor has been reported for the detection of the chiral β-blocking drug S-propranolol in the liquid phase.[23] The preparation and development of a sensor device for the specific detection of the monoterpene L-menthol is described in the following sections. This device illustrates the potential specificity of MIP-QCM sensors and their applicability for in-situ monitoring of compounds having ozone precursor potential.

2.26 Experimental

2.27 Reagents

All terpenes and the functional monomer methacrylic acid (MAA) were purchased from Lancaster Synthesis (Lancashire, UK). The cross-linkers ethylene glycol dimethacrylate (EDMA) and trimethylolpropane trimethacrylate (TRIM) were supplied by Aldrich Chemicals (Dorset, UK). The initiator 2,2'-Azobis(2-methylpropionitrile) was supplied by Acros Chemicals (Loughborough, UK). All the solvents were of analytical grade and all reagents were used as supplied.

2.28 Quartz Crystal Microbalance

The quartz crystal microbalance was produced using unpolished AT-cut, 25 mm diameter, plano-plano Quartz crystals with Cr/Au contacts, operating at a fundamental resonant frequency of 5 MHz and with an electrode area of approximately 133 mm^2

(Maxtek model No. 149211-2). The crystals were mounted in a Maxtek CHC-100 crystal holder and the measurement system consisted of a Maxtek PLO10 phased locked oscillator and a Hewlitt Packard 53132A universal counter interfaced to a microcomputer.

Prior to the application of the polymer coating to the electrode area, the crystals were prepared using Pirannha etch solution (1:3 30% v/v H_2O_2: conc. H_2SO_4). The crystals were immersed in the etch solution for ten minutes, then rinsed with deionised water and ethanol then dried overnight.

2.29 Imprinted polymer films for the detection of L- menthol

Co-polymers of poly (EDMA-co-MAA) were used for the preparation of the molecular imprinted polymers. In a typical MIP synthesis, the polymerisation mixture consisted of L-menthol (1.5 mmol), Methacrylic acid (6.0 mmol), EDMA (10 - 40 mmol), chloroform (74 mmol) with AIBN (0.19 mmol) as the polymerisation initiator. The polymerisation mixture was degassed by sonication for 5 minutes and then cooled on ice for 5 minutes prior to use. The quartz crystals were coated with polymer using the sandwich casting method described by Kugimiya and Takeuchi.[24] The polymer film was cast by dispensing 2 μl of the polymerisation solution directly onto the surface of the Cr/Au electrode and then covered immediately with a 13 mm diameter microscope coverslip, treated with Sigma cote (Sigma, St. Louis, MO) to reduce unwanted adhesion of the MIP. Figure 2.5. Polymerisation was initiated by UV radiation using a 125 W medium pressure mercury lamp (Photochemical reactors 3012) under an inert

atmosphere for 30 minutes. Control samples of non-imprinted polymers were synthesised in a similar manner, without the addition of the L-menthol template to the polymerisation solution. The quartz crystals were washed for 10 minutes in ethanol and dried prior to use.

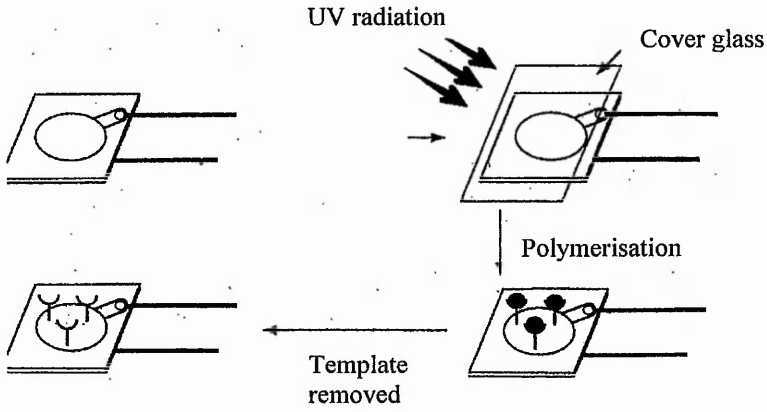

Figure 2.5: Preparation of polymer film.

2.3 Evaluation of sensor response

The coated crystals were tested by placing them in the crystal holder connected to an oscillator. The holder was immersed in a beaker filled with ethanol, which was placed in a large volume of water to prevent rapid temperature-changes during the experiment. Voltage and frequency were recorded for each crystal and the data transferred to a computer using the Labview programme (National Instruments Corporation, Austin, Texas). After connecting the crystal holder to the oscillator and eliminating the influence of the cable between them by adjusting the oscillator, the frequency was left to stabilize.

Solutions containing known amounts of the target analyte were prepared in ethanol. The coated quartz crystals were placed into a beaker of ethanol until a stable response was obtained, then 9 ml of the analyte solution of varying concentrations were added to the stirred bulk ethanol solution via successive additions of 1.0mL aliquots. The frequency was recorded until a stable response was obtained. After each 9 ml addition of analyte the coated quartz crystal was washed repeatedly with ethanol for 10 minutes and the experiment was repeated.

2.4 Results and Discussion

2.5 Effect of cross linker

The effect of cross linker concentration in the MIP was investigated by variation of the amount of cross linker employed in the polymerisation mixture. Cross linker concentrations were varied from 10 to 40 mmol (from 55 to 83 %) and of these, the 40 mmol cross linked co-polymer proved unsuccessful. On each attempt the 40 mmol cross linked MIP displayed considerable contraction and separated from the electrode. Yilmaz *et al.*[25] have reported similar results and suggest that high cross linker concentrations can lead to a rigid polymer film with significantly reduced adherence to the electrode surface. The 10 and 20 mmol cross linked EDMA co-polymer displayed no change in resonant frequency upon the addition of up to 2 ppm L-menthol. However, the lack of frequency shift of the lower concentrations of cross linker indicates that the increased flexibility of the polymer results in the relaxation of the imprinted sites so that no response is observed. The 30 mmol cross linked EDMA co-polymer displayed a

repeatable shift in resonant frequency on addition of L-menthol which is shown in Figure 2.6 (squares). The 30 mmol co-polymer is rigid enough to selectively rebind the template, yet retains suitable adherence to the electrode.

In light of the studies upon the effect of cross linker concentration control experiments were performed to assess the response of quartz crystals coated with the non-imprinted 'blank' 30 mmol cross linked EDMA polymer towards L-menthol. The data shown in Figure 2.6 (triangles) demonstrates that no change in resonant frequency was observed upon addition of up to 2 ppm of analyte. This result indicates that binding of the analyte to the 'blank' was insignificant.

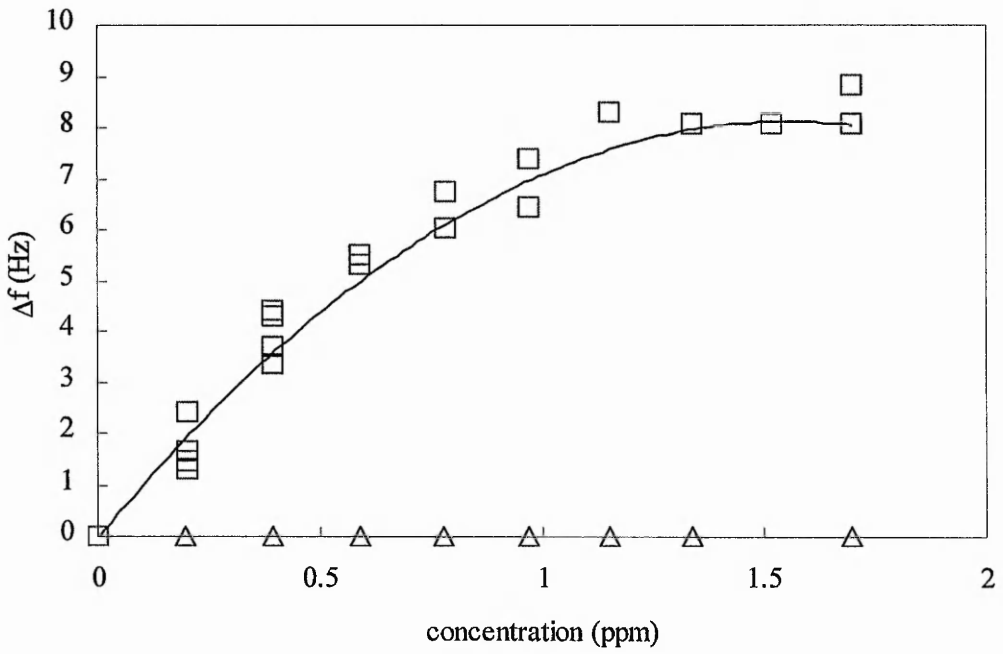

Figure 2.6: The response of the QCM sensors to L-menthol for the MIP coated (squares) and non-imprinted polymer coated (triangles). Using five repeat runs and the MIP film thickness was 2μm.

It can be seen from Figure 2.6 that, although the data for the imprinted polymer coated quartz crystals falls on a repeatable curve, some scatter in the data is observed. This may be attributed to the drift in resonant frequency that is caused by changes in the environmental conditions such as temperature. On the timescale of the experiment, the change in frequency caused by environmental conditions could be greater than that caused by the mass loading of the quartz crystal. In order to overcome this difficulty the frequencies of two quartz crystals immersed in the ethanol solution, one crystal coated with the MIP and one crystal coated with the non imprinted polymer, were measured simultaneously following the dual quartz crystal microbalance (DQCM) technique of Bruckenstein *et al.*,[26] The resultant difference in frequency between the two crystals can be used to assess the response of the crystal to mass loading of the analyte, as the non imprinted polymer displayed no change in resonant frequency with mass loading; all further experiments were performed in this manner.

2.6 Response of the sensors to mass loading of L-menthol

The change in resonant frequency of the MIP quartz crystal as a function of L-menthol concentration is shown in Figure 2.7. There is an initial linear decrease in frequency corresponding to increase in menthol concentration up to about 0.8 ppm with a gradient in the range $S_{D\text{-menthol}} = -8.9 \pm 0.6$ Hz ppm^{-1}, which reaches saturation at concentrations exceeding 1.1 ppm. The data presented in Figure 2.7 shows the response for 5 different quartz crystals each with a MIP coating produced in the same way. The agreement suggests that the methodology reported herein for coating the quartz crystals with MIP is not only reproducible between runs but also between different coatings.

Similar sorption isotherms have been observed by Haupt *et al.*,[23] for the binding of S-propranolol to a molecularly imprinted polymer and such sorption isotherms are expected for polymers that contain immobilised binding sites, typical of MIPs.

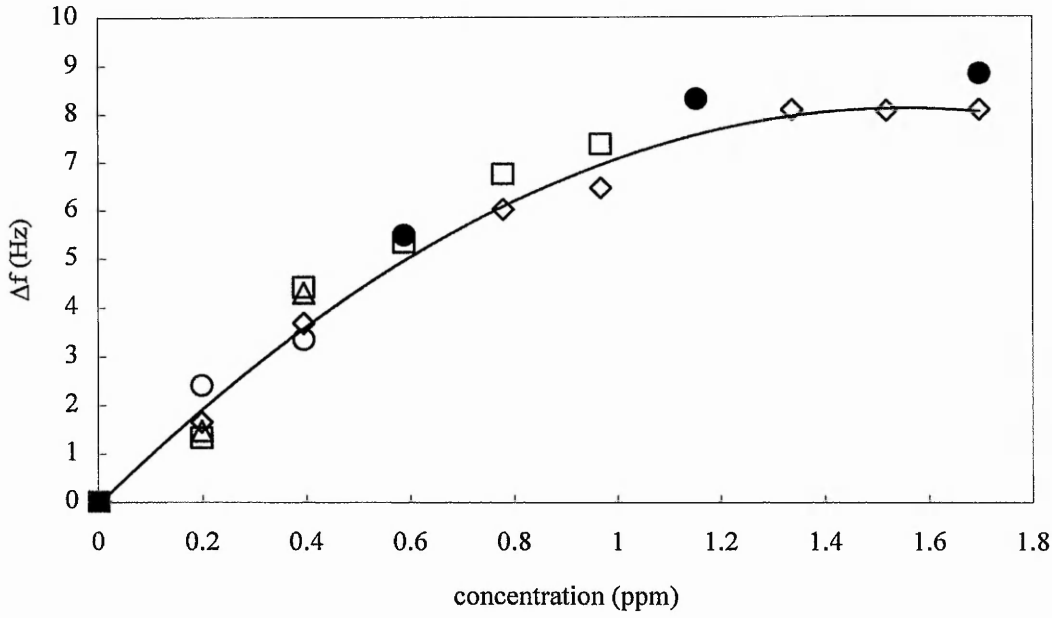

Figure 2.7: Resonant frequency change of the QCM with L-Menthol TRIM cross linked MIP coating number 1 (diamonds); EDMA cross linked MIP coating number 1 run 1 (squares); EDMA cross linked MIP coating number 1 run 2 (circles); EDMA cross linked MIP coating number 2 (solid circles) and TRIM cross linked MIP coating number 2 (triangles).

The affinity of the MIP polymers towards L-menthol can be evaluated using a one site Langmuir-type binding isotherm analysis.[22]

$$Kc\frac{\Delta f}{\Delta f_\infty}+\frac{\Delta f}{\Delta f_\infty}=Kc$$

Where K is the apparent dissociation constant, c is the free analyte concentration at equilibrium, Δf is the frequency change and Δf_∞ is the frequency change corresponding to complete coverage. Although this does not reflect the real situation in the polymer it allows for a comparison of binding between polymers. Using the data shown in figure 2.7, the calculated apparent association constant $K = 4.5 \pm 0.5\ \mu M^{-1}$. The calculated apparent dissociation constant are similar to those found in MIPs.[27] Affinity of recognition sites to other monoterpenes is given in next section.

2.7 Selectivity of Sensors

A number of other terpenes (limonene, menthone, citronellol, citronellal and D-menthol) were examined in order to investigate the selectivity of the MIP. No change in resonant frequency was observed upon the addition of up to 2 ppm for all terpenes that did not contain an OH moiety, as shown in Figure 2.8. The inability for the MIP-QCM to detect limonene, menthone and citronellal is demonstrative of the role of the functional monomer in analyte rebinding; non-covalent interactions between the carbonyl groups or double bonds of the analyte and the functional monomer (MAA) do not occur.

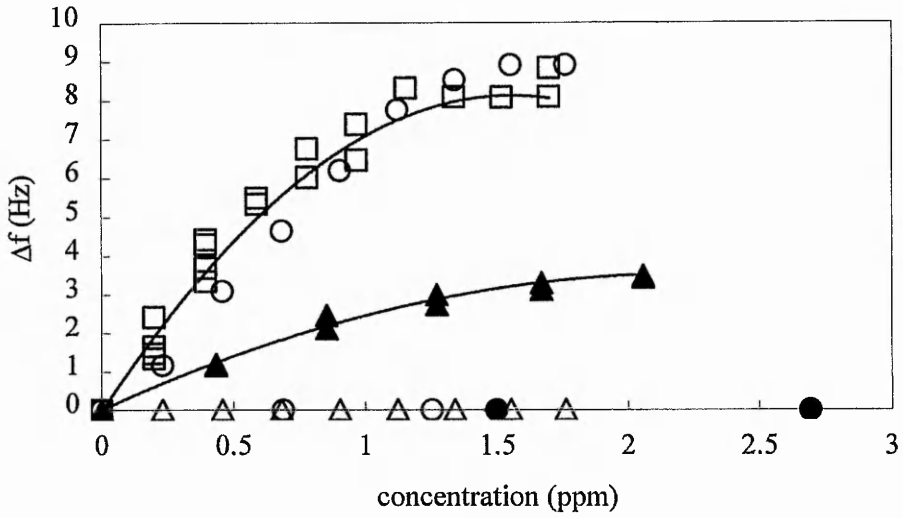

Figure 2.8: Response of MIP to other monoterpenes. D-menthol (solid triangles), L-menthol (open squares), citronellol (open circles) and limonene (open triangles).

The MIP used also responds to D-menthol as shown in Figure 2.8 (solid triangles). Analogous to L-menthol, there is an initial linear decrease in frequency corresponding to increase an in D-menthol concentration up to about 0.8 ppm with a gradient in the range $S_{L\text{-menthol}} = -2.4 \pm 0.2$ Hz ppm^{-1}. The enantioselectivity of the MIP coating can be assessed by evaluating the ratio of the initial linear change in frequency of L-menthol (squares) to D-menthol (solid triangles) $S_{D\text{-menthol}} / S_{L\text{-menthol}}$. Hence, the enantiomeric selectivity coefficient of the MIP used in this work was 3.6. Haupt *et al.*,[23] have also reported enantiomeric discrimination between R and S-propranolol using a non covalent imprint of S-propranolol with an the enantiomeric selectivity coefficient of 5. The lower selectivity coefficient of our MIP is considered to be a function of the number of sites available for non-covalent interaction in menthol compared with propranolol. The lower

selectivity of our MIP compared with that of S-propranolol is explained by the reduced number of binding sites within the menthol MIP. The L-

menthol MIP has one point of interaction with the OH functional group. The imprinting process produces a cavity that is selective in terms of size and shape as well as complimentary functionality. Therefore, a lower response of the quartz crystal towards D-menthol was observed as a result of the incorrect spatial orientation of the receptor sites for the OH group of D-menthol within the cavities. This is further supported by the observed change of resonant frequency for citronellol, shown open circles in Figure 2.8. Citronellol shares the same functional group as menthol but the overall size of the molecule is smaller and exhibits similar binding characteristics within the cavity. As a result the changes in resonant frequency of the MIP quartz crystal as a function of citronellol concentration are similar to that of L-menthol. The response of the imprinted sensors to the template, D-menthol and citronellol but not to limonene, menthone or citronellal demonstrates the molecular imprint effect. However, the enantioselectivity of the polymer matrix as a consequence of trapped menthol cannot be excluded. The importance of both the functional monomer in analyte rebinding and the observed shape selectivity support enantioselectivity of the binding site as the most probable reason for the observed chiral discrimination.

The one site Langmuir-type binding isotherm analysis described previously can also be used to determine the selectivity of the recognition element when exposed to other monoterpenes.

2.8 Conclusion

A MIP coated quartz crystal sensor can be used to selectively detect the monoterpene menthol in the liquid phase with a sensitivity of 112 ppb (as defined by a 1 Hz frequency shift). The natural extension of this work is to enhance the sensitivity of the sensors to enable the vapour phase detection of terpenes; this may be achieved in two ways. Firstly, it is may be possible to increase the concentration of binding sites in the MIP by increasing the ratio of the functional monomer to template and secondly, by increasing the mass sensitivity of the acoustic device. This may be achieved by increasing the resonant frequency of the sensor as the sensor response to mass loading is proportional to the square of the operating frequency. The upper limit for quartz crystal microbalances operating at the fundamental frequency is around 10 MHz; the higher the frequency the thinner the crystal. Alternatively, surface acoustic wave devices (SAWs) may be employed that will extend the range of operating frequencies to over 1 GHz.[28,29] The implementation of these enhancements should provide an increased sensitivity allowing the detection of atmospheric levels of gaseous terpenes.

2.9 References

1. I. M. Campbell, Energy and the atmosphere, John Wiley & Sons, New York. **1986**.
2. S. Karlsdottir, I. S. A. Isaken, G. Mhyre. T.K. Bernsten, *J. Geophys. Res.*, **2000**, 105 (D23), 28907.
3. R. P. Wayne, *Chemistry of Atmospheres*, Oxford Science Publications, Oxford, UK, **2000**.
4. C. J. Percival, *Studies on the Formation and Reactions of Peroxy Radicals of Tropospheric Relevance*, PhD, Oxford University. **1995**.
5. M. E. Jenkin, G. D. Hayman, *Atmos. Environ.*, **1999**, 33, 1275.
6. UNECE, **1992,1993,1994**.
7. P. A. Leighton, Photochemistry of Air Pollution, Academic Press, **1961**.
8. C. N. Hewitt, *Reactive Hydrocarbons in the Atmosphere*, Academic Press. **1999**.
9. R. Fall, *Biogenic Emissions of Volatile Organic Compounds*, Academic Press, 1999.
10. M. E. Jenkin, Report on the Contract EPG 1/3/ 70, **1998**, Photochemical Ozone and PAN Creation Potentials : Rationalisation and Methods of Estimation, Issue1, 1-7.
11. R. G. Derwent, M. E. Jenkin, S. M. Saunders, *Atmos. Environ.*, **1996**, 30, 181.
12. R. G. Derwent, M. E. Jenkin, S. M. Saunders, M. J. Pilling, *Atmos. Environ.*, **1998**, 32, 181.
13. Y. Anderson-Skold, P. Grennfelt, K. Pleijel : *J. Air Manage. Association*, **1992**. 42.

14. R. G. Derwent, M. E. Jenkin, *Atmos. Environ.*, **1991**. 25, 1661.

15. R. Atkinson, D. L. Baulch, R. A. Cox, R. F. Hampson, J. A. Kerr, M. J. Rossi, J. Troe, *J. Phys. Chem.*, **1997**. 26, 521.

16. P. O. Wennberg, T. F. Hanisco, L. Jaegle, D. J. Jacob, E. J. Hintsa, E. J. Lazendorf, J. G. Anderson, R.-S. Gao, E. R. Keim, S. G. Donnelly, L. A. Del Negro, D. W. Fahey, S. A. Mckeen, R. J. Salawitch, C. R. Webster, R. D. May, R. L. Herman, M. H. Proffitt, J. J. Margitan, E. L. Atlas, S. M. Schauffler, F. Flocke, C. T. McElroy, T. P. Bui, *Science*, **1999**, 279, 49.

17. M. R. Allen, A. Braithwaite, C. C. Hills, *Environ. Sci. Technol.*, **1997**, 31, 1054.

18. R. S. Sethi, *Biosens. Bioelectron.*, **1994**, 9, 243.

19. J. W. Grate, *Chem. Rev.*, **2000**, 100, 2627.

20. F. L. Dickert, O. Hayden, *Trends Anal. Chem.*, **1999**, 18, 192.

21. K. Haupt, K. Mosbach, *Chem. Rev.*, **2000**, 100, 2495.

22. D. Kriz, O. Ramstrom, K. Mosbach, *Anal. Chem.*, **1997**, 69, 345.

23. K. Haupt, K. Noworyta, W. Kutner, *Anal. Commun.*, **1999**, 36, 391.

24. A. Kugimiya, T. Takeuchi, *Electroanalysis,* **1999**, 11, 1158.

25. E. Yilmaz, K. Mosbach, K. Haupt, *Anal. Commun.*, **1999**, 36, 167.

26. S. Bruckenstein, M. Michalski, A. Fensore, Z. Li, A.R. Hillman, *Anal. Chem.*, **1994**, 66, 1847.

27. G. Vlatakis, L.I. Andersson, R. Müller, K. Mosbach, *Nature,* **1993**, 364, 645.

28. H. S. Ji, S. McNiven, K. Ikebukuro, I. Karube, *Anal. Chim. Acta.*, **1999**, 390, 93.

29. B. Jakoby, G. M. Ismail, M. P. Byfield, M. J. Vellekoop, *Sens. Actuators A.*, **1999**, 76, 93.

Chapter three

Sensor for L-serine detection

3.1 Abstract

An artificial biomimetic recognition element developed to selectively detect the amino acid L-serine has been synthesised in the form of a highly specific non-covalently imprinted polymer (MIP). This MIP has been cast in-situ upon the surface of a gold coated quartz crystal microbalance (QCM) electrode as a thin permeable film. The use of MIP's as recognition elements applied to sensor transducers is well established with recognition elements that are selective for a variety of analytes reported.[1] Recently enantioselectivity has been demonstrated with an MIP-QCM exhibiting chiral discrimination.[2] The application of our MIP-QCM in the identification of an amino acid has been investigated. Selective binding of the amino acid has been observed as a frequency shift quantified by piezoelectric microgravimetry with the QCM. The detection limit of L-serine is 2 ppb with a response range of 0 - 0.4 ppm. The sensor is able to discriminate between L and D- serine owing to the enantioselectivity of the imprinted binding sites. The results further demonstrate the importance of the shape and spatial orientation of functionality of the imprinted binding site in these materials. It is envisaged that this technique could be applied to the analysis of chirally active amino acids of importance to the pharmaceutical industry.

3.2 Introduction

The synthesis of enantiomerically pure organic compounds presents a major challenge to industry. The pharmacological and biological activities of chiral organic compounds is well known to be dependant upon their specific stereochemistry. Thus there is a clear need for sensors capable of enantiomeric discrimination. In peptide and protein synthesis enantiomerically pure compounds are essential and in the case of naturally occurring peptidic species, the majority of the amino acid building blocks possess the S-configuration. In asymmetric synthesis, starting materials containing racemic mixtures must be resolved prior to use or one enantiomer may be consumed in a preferential manner *via* enantioselective synthesis. Both of these approaches require significant methodological development, either involving the preparation of diastereoisomers that can then be separated by tedious fractional crystallization or the construction of highly selective chiral auxiliaries. As outlined in Chapter 1 MIPs have been successfully developed that do exhibit chiral discrimination.[1] Chiral recognition sites within MIP can be synthesised in a relatively direct manner and therefore the potential exists to remove enantiomers in a quantitative fashion from a racemic mixture. In addition to the difficulties in separating enantiomers, conventional identification of chiral substrates has involved expensive and time consuming derivatisation methods or optical studies such as circular dichroism. The development of an analytical technique for the real time analysis and quantification of one enantiomeric species in a racemic mixture would greatly simplify the monitoring and analysis process obviating the need for sample preconcentration and chromatographic separation.

As outlined in Chapter 1 MIP have become well established as a means of producing biomimetic recognition sites since first reported over 25 years ago with the selectivity and binding affinities of MIP being comparable to antibody-antigen interactions.[2,3] Two distinct imprinting strategies were introduced to the reader in Chapter 1 covalent and non-covalent template polymerisation. Covalent imprinting involves the conversion of the template (or an analogue) into a polymerisable derivative that is then copolymerised with a suitable cross-linker to afford a resin that covalently incorporates the template. Covalent interactions between the template and the functional monomer have the advantage that the binding groups remain precisely orientated during elevated temperatures that are often a feature of the polymerisation process. The stability of the covalent bond produces a homogeneous population of binding sites within the imprinted polymer. In part this stability of the 'covalent complex' is responsible for the high binding affinities (in comparison to non covalent MIP) associated with covalently imprinted polymers with in excess of 75% of print sites being re-occupied.[4] Covalent imprinting has been widely used to produce MIP that are selective for a range of analytes including, caffeine in human urine and serum, the plant hormone indole acetic acid, macromolecules, the chiral benzodiazepine and the steroid cholesterol.[5-10]

L-serine, with 4 functional groups, does not require the enhanced stability inferred upon the pre-polymerisation mixture by the use of a polymerisable derivative i.e. covalent imprinting. L-serine is an ideal imprinting template for use in the simpler non-covalent approach involving the self-assembly of suitable functional monomers around the template molecule. Following addition of a cross-linker this assembly is then 'fixed' by polymerisation. The subsequent removal of the non-covalently bound template to reveal

a vacant recognition site specific to the target analyte in terms of spatial and electronic environment. Non-covalent imprinting has inherent advantages over the covalent strategy as a consequence of the rapid and reversible nature of non-covalent interaction between the polymer and the template. Also the non-covalent strategy obviates the need for derivatisation of the target analyte or an analogue. Non-covalent imprinting has been reported with MIPs selective for many analytes including, R- and S-propranolol, the odorant methylisoborneol, steroids, carboxylic acids, nucleotide bases, enantiomeric resolution of amino acids, dyes and PAHs.[11-20] In this work a piezoelectric sensor coated with a non-covalently imprinted recognition element for the amino acid L-serine is presented. The enantioselectivity of the imprinted binding sites is investigated for discrimination between L- and D-stereoisomers of serine.

3.3 Experimental

3.31 Reagents

All amino acids and the functional monomer methacrylic acid (MAA) were purchased from Lancaster Synthesis. The cross-linkers ethylene glycol dimethacrylate (EDMA) was supplied by Aldrich Chemicals. The initiator 2,2'-Azobis(2-methylpropionitrile) was supplied by Acros Chemicals. All the solvents were of analytical grade and all reagents were used as supplied.

3.32 Quartz Crystal Microbalance

The quartz crystal microbalance consisted of a Maxtek PLO10 phased locked oscillator and an Hewlitt Packard 53132A universal counter interfaced to a microcomputer. The quartz crystals used were unpolished AT-cut, 25 mm diameter, with Cr/Au contacts, operating at a fundamental resonant frequency of 5 MHz. The electrode area was approximately 133 mm^2 (Maxtek model No. 149211-2) and the crystals were mounted in a Maxtek CHC-100 crystal holder.

3.33 Cleaning of crystals

Prior to the application of the polymer coating to the electrode area, the crystals were prepared using Pirannha etch solution (1:3 30% v/v H_2O_2: conc. H_2SO_4). The crystals were immersed in Pirannha etch solution for ten minutes, then rinsed with deionised water and ethanol and dried overnight.

3.34 Imprinted polymer films

Co-polymers of poly (EDMA-co-MAA) were used for the preparation of the molecular imprinted polymers. In a typical MIP synthesis, the polymerisation mixture consisted of L-serine (1.5 mmol), methacrylic acid (6.0 mmol), EDMA (30 mmol), 90:10 cyclohexanol:dodecanol (74 mmol) with AIBN (0.19 mmol) as the polymerisation initiator. The polymerisation mixture was degassed by sonication for 5 minutes and then cooled on ice for 5 minutes prior to use. The quartz crystals were coated as described by

Kugimiya and Takeuchi.[7] With a polymer film being cast by dispensing 2 µl of the polymerisation solution directly onto the surface of the Cr/Au electrode and then covered immediately with a 13 mm diameter microscope coverslip (see Figure 2.5). Prior to use the coverslip was treated with Sigma cote (Sigma, St. Louis, MO) to reduce the adhesion of the MIP to the coverslip. Polymerisation was initiated by UV radiation using a 125 W medium pressure mercury lamp (Photochemical reactors 3012) under an inert atmosphere for 30 minutes. Control samples of non-imprinted polymers were synthesized in a similar manner, without the addition of the L-serine template to the polymerisation solution. The quartz crystals were washed for 10 minutes in ethanol and dried prior to use.

3.35 Cross linker

Previously in Chapter 2 an examination of the effect of cross-linker concentration within the polymer was performed. Optimum imprinting conditions were identified.[2] Cross linker concentrations were varied from 10 and 40 mmol (from 55 to 83 %) and of these, the 10, 20 and 40 mmol cross linked co-polymers proved unsuccessful. The 30 mmol cross linked EDMA co-polymer displayed a repeatable shift in resonant frequency on addition of L-serine and was rigid enough to selectively rebind the template whilst adhering to the QCM. The 40 mmol cross linked MIP displayed considerable contraction and separated from the electrode. These findings were in agreement with previously reported results[21] and suggest that high cross linker concentrations can lead to a rigid polymer film with significantly reduced adherence to the electrode surface. As a result 30 mmol cross linked polymers were used throughout this study.

3.4 Evaluation of sensor response

Solutions containing known amounts of L-serine were prepared in 90:10 cyclohexanol:dodecanol. The coated quartz crystals were placed into a beaker of ethanol until a stable response was obtained, then 6 ml of analyte solution was added to the stirred bulk ethanol solution via successive 1 ml aliquots. The frequency was recorded until a stable response was obtained. After each 6 ml addition of analyte the coated quartz crystal was soaked in the porogenic solvent for 10 minutes and the experiment was repeated. Control experiments were performed to assess the response of quartz crystals coated with non-imprinted 'blank' polymers; no detectable changes in resonant frequency were observed upon the addition of up to 2 ppm of analyte. On the timescale of the experiment, the change in frequency caused by environmental conditions could be greater than that caused by the mass loading of the quartz crystal. In order to overcome this difficulty the frequencies of two quartz crystals immersed in the ethanol solution, one crystal coated with the MIP and one crystal coated with the non imprinted polymer, were measured simultaneously following the DQCM technique of Bruckenstein *et al.*,[22] The resultant difference in frequency between the two crystals can be used to assess the response of the crystal to mass loading of the analyte, as the non imprinted polymer displayed no change in resonant frequency with mass loading; all further experiments were performed in this manner. Figure 3.1 diagramatically depicts the experimental set up.

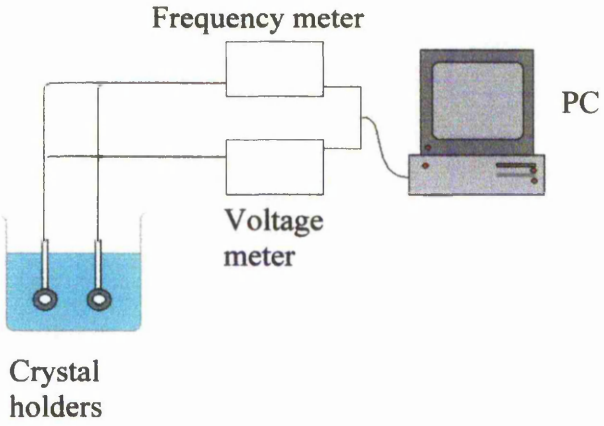

Figure 3:1 Experimental setup

3.5 Results and Discussion

The change in resonant frequency of the MIP quartz crystal as a function of L-serine concentration is shown in Figure 3.2. There is a linear decrease in frequency corresponding to increase in L-serine concentration up to about 0.2 ppm with a gradient in the range $S_{L\text{-serine}}$= 482 ± 16 Hz ppm^{-1}, which reaches saturation at concentrations exceeding 0.5 ppm. These sorption isotherms are expected for polymers that contain immobilised binding sites, such as those found within MIP and are consistent with those reported by Haupt *et al.*,[11] for the binding of S-propranolol. The data presented in Figure 3.3. shows the response for 4 different quartz crystals each with a MIP L-serine coating produced in the same way. The agreement suggests that our methodology for coating the quartz crystals with MIP is not only reproducible between runs but also between different coatings. The affinity of the MIP polymers towards L-serine can be evaluated using a one site Langmuir-type binding isotherm analysis.[23] Affinity is evaluated by the calculation of the apparent association constant Kc for a given concentration of analyte.

$$Kc\frac{\Delta f}{\Delta f_\infty}+\frac{\Delta f}{\Delta f_\infty}=Kc$$

where K is the apparent dissociation constant, c is the free analyte concentration at equilibrium, Δf is the frequency change and Δf_∞ is the frequency L-serine change corresponding to complete coverage. Although this does not reflect the real situation in the polymer it allows for a comparison of binding between polymers. Using the data shown in Figure 4, the calculated apparent dissociation K = 35.45 μM^{-1}. The calculated apparent dissociation constants are similar to those previously reported for MIP.[24]

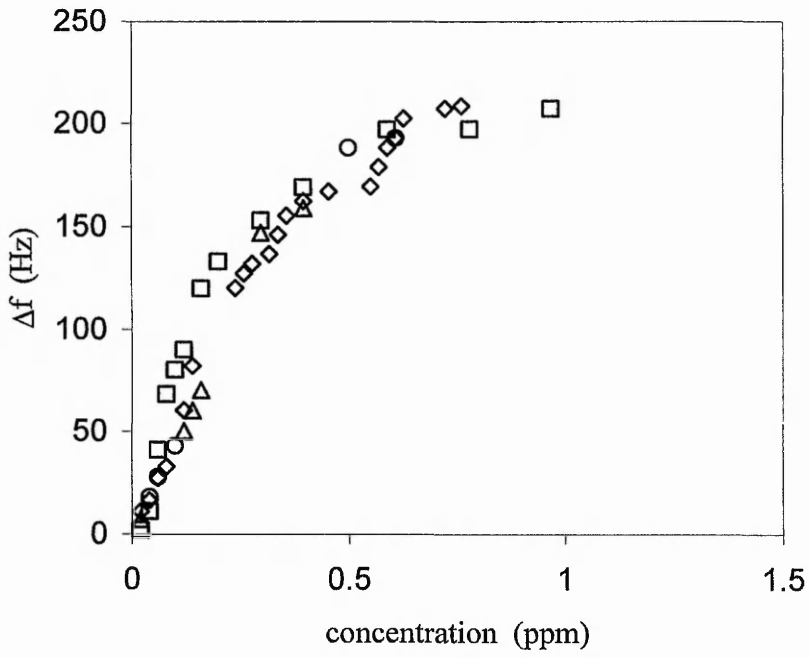

Figure 3.2: Response of sensor to L-serine. The resonant frequency change of the QCM as a function of concentration for L-serine (different coatings shown as squares, diamonds, circles and triangles).

The MIP used also responded to D-serine (open diamonds), as shown in Figure 3.3. Analogous to L-serine, there is an initial linear decrease in frequency corresponding to increase an in D-serine concentration up to about 0.4 ppm with a gradient in the range $S_{D\text{-serine}}$= 99.71 ± 7.10 Hz ppm^{-1}. The enantioselectivity of the MIP coating for L-serine compared to D-serine can be assessed by evaluating the ratio of the initial linear change in frequency of L-serine to D-serine $S_{L\text{-serine}}$ / $S_{D\text{-serine}}$. Hence, the enantiomeric selectivity coefficient of the MIP used in this work was 4.8. In Chapter 2 the enantiomeric discrimination between L- and D-menthol was reported. With the non covalent imprint of L-menthol exhibiting an enantiomeric selectivity coefficient of 3.6. The increased selectivity coefficient of the L-serine MIP is considered to be a function of the number of sites available for non-covalent interaction in L-serine compared to that of L-menthol. Haupt *et al.*, have also reported enantiomeric discrimination between R and S-propranolol using a non covalent imprint of S-propranolol with an the enantiomeric selectivity coefficient of 5.[11] Both L-serine and S-propranolol have three possible sites of interaction and show similar enatioselectivity, whereas L-menthol has only one possible site for interaction and shows a much smaller enantioselectivity. The imprinting process produces a cavity that is selective in terms of size and shape as well as complimentary functionality. Therefore, a lower response of the quartz crystal towards D-serine was observed as a result of the incorrect spatial orientation of the receptor sites for the NH_2, OH and COOH groups of D-serine within the cavities.

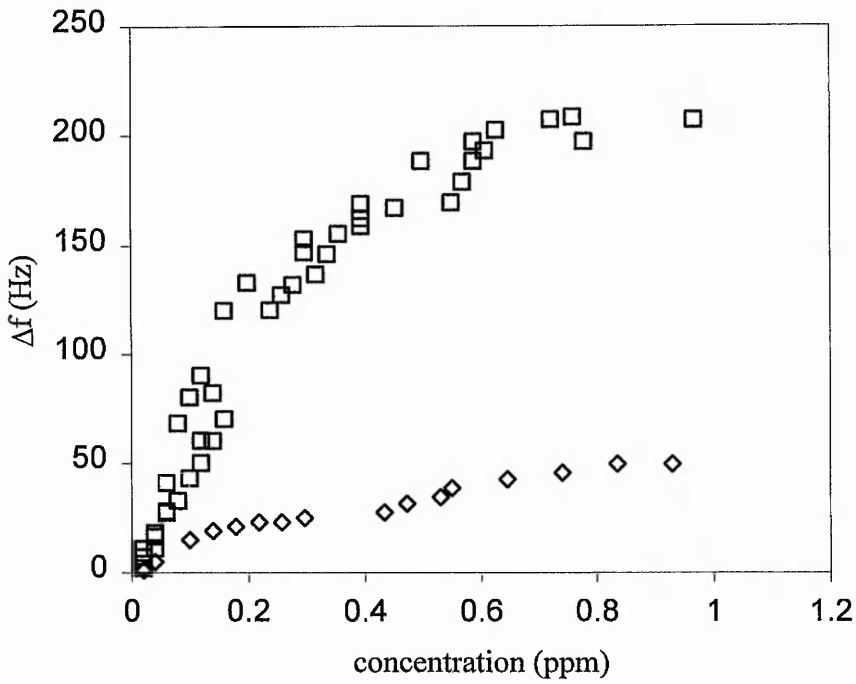

Figure 3.3: The resonant frequency change of the QCM as a function of concentration for L-serine (open squares) and D-serine (open diamonds).

3.6 Conclusion

An MIP selective for an amino acid and capable of enantiomeric discrimination has been produced via non-covalent imprinting. The MIP coated quartz crystal sensor can be used to detect the amino acid L-serine in the liquid phase up to 0.4ppm and with a sensitivity of 2 ppb. The enantioselectivity of the MIP coating has also been investigated for L-serine and D-serine giving an enantiomeric selectivity coefficient of 4.8. Further enhancing the sensitivity of the sensors would enable the chiral discrimination of ever smaller quantities of chiral actives. This may be achieved by increasing the concentration of binding sites in the MIP by increasing the ratio of the

functional monomer to template or alternatively by increasing the mass sensitivity of the acoustic device; the latter by increasing the resonant frequency of the sensor. The upper limit for quartz crystal microbalances operating at the fundamental frequency is around 10 MHz however, surface acoustic wave devices (SAWs) may be employed that would extend the range of operating frequency by more than an order of magnitude.[12,25] The results further demonstrate the importance of the shape and spatial orientation of functionality of the imprinted binding site in these materials. It is envisaged that this technique could be applied to the analysis of chirally active amino acids of importance to the pharmaceutical industry.

3.7 References

1. K. Haupt, *Analyst*, **2001**, 126, 747.
2. G. Wulff, A. Sarhan, *Angew. Chem. Int. Ed. Engl.*, **1972**, 11, 341.
3. G. Wulff, *Angew. Chem. Int. Ed. Engl.*, **1995**, 34, 1812.
4. B. Sellergren, *Anal. Chem.*, **1994**, 66, 1578.
5. G. Wulff, A. Sarhan, K. Zabrocki, *Tetrahedron Lett.*, **1973**, 44, 4329.
6. C. Liang; H. Peng, X. Bao, L. Nie, S. Yao, *Analyst,* **1999**, 124, 1781.
7. A. Kugimiya and T. Takeuchi, *Electroanalysis*, **1999**, 11, 1158.
8. K. J. Shea; E. A. Thompson, S.D. Pandey, P. S. Beauchamp, *J. Am. Chem. Soc.*, **1980**, 102, 3149.
9. B. R. Hart, D. J. Rush, K. J. Shea, *J. Am. Chem. Soc.*, **2000**, 122, 460.
10. M. J. Whitcombe, M. E. Rodriguez, P. Villar, E. N. Vulfson, *J. Am. Chem. Soc.*, **1995**, 117, 7105.
11. K. Haupt, K. Noworyta and W. Kutner, *Anal. Commun.*, **1999**, 36, 391.
12. H. S. Ji, S. McNiven, K. Ikebukuro, I. Karube, *Anal. Chim. Acta.*, **1999**, 390, 93.
13. O. Ramstrom, L. Ye, M. Krook, K. Mosbach, *Anal. Commun.*, **1998**, 35, 9.
14. O. Ramstrom, L.I. Andersson, K. Mosbach, *J. Org. Chem.*, **1993**, 58, 7562.
15. D. A. Spivak, K. J. Shea, *Macromoleculues*, **1998**, 31, 2160.
16. L. Andersson, K. Mosbach, *J. Chromatogr.*, **1990**, 516, 313.
17. L. I. Andersson, D. J. O'Shanessy, K. Mosbach, *J. Chromatogr.*, **1990**, 513,167.
18. M. Glad, O. Norrlow, B. Sellergren, N. Seigbahn , K. Mosbach, *J. Chromatogr.*, **1995**, 347, 11.

19. F. L. Dickert, M. Tortschanoff, W. E. Bulst ,G. Fischerauer, *Anal. Chem.*, **1999**, 71, 4559.

20. C. J. Percival, S. Stanley, M. Galle, A. Braithwaite, M. I. Newton, G. M^{c}Hale, W. Hayes, *Anal. Chem.*, **2001**, 73, 4225.

21. E. Yilmaz, K. Mosbach, K. Haupt, *Anal. Commun.*, **1999**, 36, 170.

22. S. Bruckenstein, M. Michalski, A. Fensore, Z. Li, A. R. Hillman, *Anal. Chem.*, **1994**, 66, 1847.

23. D. Kriz, O. Ramstrom, K. Mosbach, *Anal. Chem.*, **1997**, 69, 345.

24. G. Vlatakis, L.I. Andersson, R. Müller, K. Mosbach, *Nature*, **1993**, 364, 645.

25. B. Jakoby, G. M. Ismail, M. P. Byfield, M. J. Vellekoop, *Sens. Actuators* A, **1999**, 76, 93.

Chapter four

Sensor for nandrolone detection

4.1 Abstract

A piezoelectric sensor coated with an artificial recognition element has been developed for the determination of the steroid nandrolone in the liquid phase. One of the most widely abused classes of banned drugs in sports are the anabolic steroids (e.g. nandrolone). Anabolic steroids, which are related in structure and activity to the male hormone testosterone, are used by competitors to improve muscle strength and accelerate recovery times from exercise and so to extend their training effectiveness. The abuse of anabolic steroids in human and equine sports has led to a strict ban by national and international sports federations and by the medical commission of the International Olympic Committee (IOC). Urine analysis is recommended for the detection of all banned drugs on the current IOC list.[1] A wide variety of methods for the detection of anabolic steroids in urine have been described including immunoassay,[2,3] TLC and HPTLC methods[4-7] and GC-MS.[8-12] In this work an alternative cost effective technique, based on acoustic wave devices and molecularly imprinted polymers for the selective direct detection of nandrolone in aqueous media is presented. A highly specific covalently imprinted polymer (MIP) has been prepared and subsequently appended to the surface of a gold coated quartz crystal microbalance (QCM) electrode as a thin permeable film. Selective rebinding of the target analyte was observed as a frequency shift quantified by piezoelectric microgravimetry with the QCM. The lower limit of detection of nandrolone was 6 ppb with a linear response range of 0 – 1.0 ppm. The response of the MIP-QCM to a range of steroids has been investigated with the sensor binding nandrolone in favour of analogous compounds.

4.2 Introduction

Taking drugs by athletes to increase their chance of winning has reached pandemic proportions with estimates of the percentages of drug usage among athletes varying from 2% to 75% in certain sports.[13,14] Substance abuse to gain an advantage is not isolated to modern times having existed for thousands of years.

In pagan times bryony was used by witches as a purgative and is still widely regarded as a potent aphrodisiac. Bryony was according to the bible used to put Adam to sleep in order to remove one of his ribs. Bryony contains a number of atropine like alkaloids and is still used today to increase levels of testosterone in the body after anabolic steroid use. Runners in ancient Egypt ingested the ground up rear hooves of Abyssinian asses flavoured with rosehip in an attempt to improve their speed. By the third century B.C. drugs were reportedly being used in Olympic competition.[15] In the mid 200's A.D. the Romans, angered by early substance abuse discontinued the Olympics as a "devaluation of true athletic competition".

The modern era is in many ways history repeating itself, with drug abuse widespread. In 1968 Olympics in Mexico City drug testing was in use in part as a response to the very obvious drug abuse being practiced and the early demise of an increasing number of athletes in both the professional and amateur arenas.

One of the most important classes of performance enhancing drugs are the anabolic steroids. Anabolic steroids are a class of compounds structurally related to testosterone.

The steroid testosterone produced in the body from cholesterol is secreted by the testes from puberty and is largely responsible for the differences in muscle growth, fat mass and distribution and behavioral characteristics that distinguishes males from females. Testosterone can be converted to 27 compounds by enzymatic action within the body which in turn can be converted to at least another 540 compounds.[16] The modification of testosterone has led to the development of its synthetic analogues, the "anabolic steroids". The term "anabolic steroid" is something of a misnomer since none of these synthetically modified steroids has exhibited specific separation of anabolic from androgenic activity.[17] These compounds are now more correctly recognized as anabolic-androgenic steroids (AAS).

AAS exhibit anabolic activity by producing an increase in protein synthesis in the target tissues. The AAS interacts with receptor proteins within the target tissue to form hormone receptor complexes which in turn interact with receptor sites on the chromosomes eliciting gene transcription and the subsequent synthesis of messenger RNA and subsequently various proteins. Interestingly with regard to drug testing optimum muscle growth results when androgen levels are close to normal. The use of AAS results in an increase in body weight and strength of the athlete however, termination of steroid use can result in a loss of the gained weight but no accompanying loss of strength. This of course has implications for monitoring such substances of abuse since an athlete trying to evade detection may simply cease drug taking in advance of the event without loss of performance.

Perhaps the defining moment in the history of drugs in sport came in 1998 with a series of sport doping scandals highlighting the pervasive use of drugs and the inability of testing systems to deal with the problem. In January of 1998 a Chinese swimmer was found to be in possession of human growth hormone (Hgh). Hgh was a banned substance but an athlete could not be sanctioned for its use as there were no tests for monitoring its abuse available at the time. In the same year the German cancer researcher Werner Franke exposed a GDR state doping plan coupled with officially sanctioned testing to avoid detection. Later that year French customs officers seized a car filled with banned drugs belonging to Festina a top ranking cycling team taking part in the Tour de France. Subsequently the team was found to have a doping program monitored by doctors. As in the case of the Chinese swimmer the cyclists were using banned substances, hgh and also erythropoietin (EPO), for which no reliable tests had been introduced. Also found was perfluorocarbon (PFC) an experimental drug not even on the market. These cases provided clear illustration that the sophistication of the athlete using drugs has often been above that of the testing laboratory. There is clearly a need for increasingly more sensitive and selective testing to protect the athlete from false positives and to identify deliberate substance abuse.

In 1999 the British Olympic sprinter Linford Christy was accused of using the banned steroid nandrolone. He was subsequently found not guilty by the U.K. athletics federation. Athletes alleged that IOC tests did not differentiate between dopants and substances produced naturally within the body.

4.3 Monitoring drugs of abuse

Sensors selective for individual drugs of abuse could be employed to produce quick and accurate screening tests for an array of controlled substances. As outlined previously acoustic wave sensors such as the quartz crystal microbalance (QCM), are well suited as transducer elements for chemical sensors.[18] Again for applications in chemical sensing, a recognition element is added to the acoustic wave device capable of selectively binding the analyte to the device surface. The response of these devices is then based on a decrease in their resonant frequency as mass is attached to the device or the recognition element.

4.4 Nandrolone sensor

MIPs are well established as a means of producing biomimetic recognition sites since first reported over 25 years ago[19,20] with the selectivity and binding affinities of MIP being comparable to antibody-antigen interactions.

MIPs as recognition elements for sensors are increasingly of interest[21,22] and MIP-QCM have started to appear in the literature and work in this area has been recently

Reviewed.[23] Initially these studies concentrated on analyte rebinding in gaseous media however, recently an MIP-QCM sensor has been reported for the detection of the chiral β-blocking drug S-propranolol in the liquid phase.[24]

Two distinct imprinting strategies have evolved: i) covalent and ii) non-covalent template polymerisations. These two strategies have been discussed in detail in Chapter 1, a summary is presented here.

A nandrolone sensor has been developed using a covalent imprinting strategy, involving the conversion of the template (or an analogue) into a polymerisable derivative. This is then copolymerised with a suitable cross-linker to afford a resin that covalently incorporates the template. Covalent interactions between the template and the functional monomer result in binding groups that remain precisely orientated during elevated temperatures that are often a feature of the polymerisation process. The stability of the covalent bond produces a homogeneous population of binding sites within the imprinted polymer. In part this stability of the 'covalent complex' is responsible for the high binding affinities (in comparison to non covalent MIPs) associated with covalently imprinted polymers with in excess of 75% of print sites being re-occupied.[25] Covalent imprinting has been widely used to produce MIPs that are selective for a range of analytes including, caffeine in human urine and serum,[26] the plant hormone indole acetic acid,[27] macromolecules,[28] the chiral benzodiazepine[29] and the steroid cholesterol[30]. Whilst the non-covalent imprinting strategy does have advantages over its

covalent counterpart (see Chapter 1) the nature of the analyte nandrolone favors the latter.

The steroid nandrolone is characterized by a fused ring structure with two spatially separated functional groups. At first glance nandrolone does not offer promise as a prospective imprinting candidate possessing as it does a single carbonyl moiety separated from an alcohol group by the four fused rings of the sterol skeleton, Figure 4.1. The requirement for multiple heteroatom functionality is thought to limit, to a large extent the types of molecules which can be considered suitable for the imprinting process.[30] It is evident from Figure 4.1 that nandrolone is far from an ideal imprinting

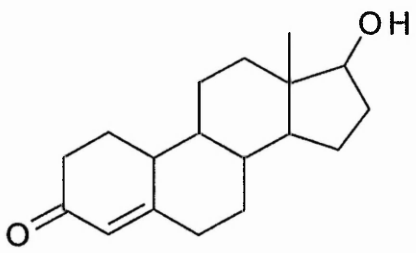

Figure 4.1: Nandrolone.

analyte in this regard, furthermore, with the exception 1,2- and 1,3-diols there is no general method for the imprinting of alcohols. For these reasons nandrolone clearly

presents a challenge to the imprinting process. The fused ring system of such steroid compounds however, could facilitate the imprinting process in that a polymer around such a template may be capable of analyte discrimination due to the shape of the cavity and weak Van der Waals forces present between the MIP cavity and the analyte. This is because the template monomer and any self-assembled functional monomers are fixed within the bulk polymer matrix by polymerization. The rigid fused structure of the polymer results in complimentary functional groups within the cavity adopting a more defined orientation than would possibly be the case with a more flexible template molecule. Incidentally this is also the advantage proffered by the covalent strategy compared to the non-covalent.

Whitcombe[30] has reported the covalent imprinting of the steroid derivative cholesterol chloroformate in 1995 to produce a binding site capable of rebinding cholesterol. Key to the imprinting of cholesterol and nandrolone is the use of the 4-vinylphenyl carbonate ester, Figure 4.2. 4-vinylphenyl carbonate ester functions as the labile covalently bound template monomer which is efficiently and readily cleaved hydrolytically with the loss of CO_2.

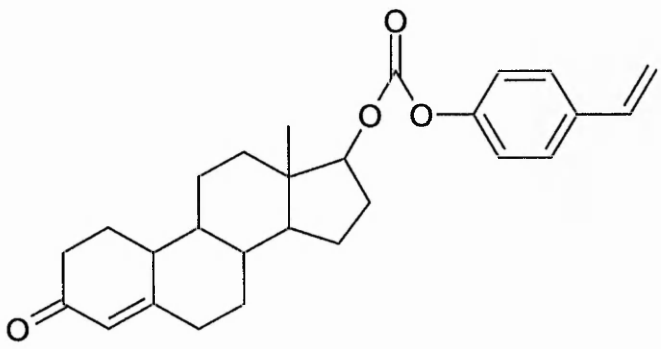

Figure 4.2: 4-Vinylphenyl carbonate ester of nandrolone.

Thus the carbonyl group of the nandrolone 4-vinylphenyl carbonate ester functions as a sacrificial spacer. The result is the formation of a non-covalent recognition site replete with phenolic residue capable of binding nandrolone. In this chapter the development and evaluation of a piezoelectric sensor coated with a covalently imprinted recognition element for nandrolone is presented.

4.5 Experimental

4.51 Chemicals

All steroids and the functional monomer methacrylic acid (MAA) were purchased from Lancaster Synthesis. The cross-linkers ethylene glycol dimethacrylate (EDMA) and trimethylolpropane trimethacrylate (TRIM) were supplied by Aldrich Chemicals

(Dorset, UK). The initiator 2,2'-Azobis(2-methylpropionitrile) was supplied by Acros Chemicals (Loughborough, UK). All the solvents were of analytical grade and were used as supplied.

4.52 Instrumentation

The quartz crystal microbalance was produced using unpolished AT-cut, 25 mm diameter, plano-plano Quartz crystals with Cr/Au contacts, operating at a fundamental resonant frequency of 5 MHz and with an electrode area of approximately 133 mm^2 (Maxtek model No. 149211-2). The crystals were mounted in a Maxtek CHC-100 crystal holder and the measurement system consisted of a Maxtek PLO10 phase locked oscillator and a Hewlitt Packard 53132A universal counter, interfaced to a microcomputer.

4.53 Cleaning Crystals

Prior to the application of the polymer coating to the electrode area, the crystals were prepared using Pirannha etch solution (1:3 30% v/v H_2O_2: conc. H_2SO_4). The crystals were immersed in the solution for ten minutes, then rinsed with deionised water and ethanol and dried overnight.

4.6 Imprinted polymer films

In order to coat the quartz crystals with an MIP film a bulk MIP polymer was required which can then be coated onto the QCM device. Prior to the formation of the imprinted polymer nandrolone must first be converted to a polymerisable derivative, in this case the 4-vinylphenyl carbonate ester of nandrolone. As outlined above the ester functions as a covalently bound template monomer that was easily cleaved to yield a non-covalent recognition site. The MIP polymer film was produced via a four stage synthesis.

Step 1:

4-Vinyl phenol, Figure 5.4. was prepared as per Corson *et al.*,[31] A mixture of 16.2g.(0.10 mole) of *p*-acetoxystyrene, 13.8g.(0.25 mole) of potassium hydroxide and 140ml. of water was stirred at 0°C until homogeneous (2 hrs). The stirred cold solution was acidified to *p*H 8 to produce 12g. (100% yield) of 4-vinylphenol. The 4-vinylphenol product was identified by NMR.

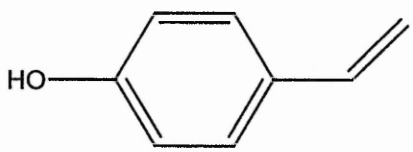

Figure 4.3: 4-Vinylphenol.

Step 2:

2.4g. (8.3mmol) of nandrolone in 30ml of dry tetrahydrofuran (THF) with butylated hydroxytoluene (BHT) (trace) was cooled on ice. Then 2.0ml of triethylamine (NET_3) (dried over KOH) was added dropwise to this cold solution. 9.60ml of phosgene (in toluene) was also added dropwise to reduce fuming. This solution was stirred at 0°C under nitrogen for 6 hours. The product of step 2 was nandrolone chloroformate, Figure 4.4.

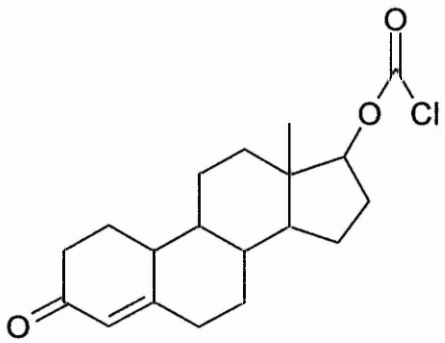

Figure 4.4: Nandrolone chloroformate.

Step 3:

A solution containing 1.05g (8.3mmol) of 4-vinylphenol in 20ml of dry THF with BHT (trace) and 1.0ml. of NET_3 (dried over KOH) was added dropwise to the nandrolone chloroformate prepared above in step two. The solution was stirred at room temperature overnight. The crude product was filtered and the solid discarded. The liquor was evaporated down with BHT. After evaporation the residue was dissolved in DCM and washed with water. The organic layer was collected and evaporated down to yield the product which is further cleaned by running through a silica column. 4-vinylphenyl carbonate ester of nandrolone was identified by NMR.

Step 4:

The monomer mixture with porogenic solvent was dispensed into a sample tube and the initiator added, the tube was then sealed and sonicated for 15 minutes to degas the polymerization solution. The polymerization was then performed in a water bath at 65°C for 24 hours. The polymer obtained was a brittle solid which was crushed and sieved to <38 μm particle size. The ground polymer was extracted with methanol in a soxhlet apparatus overnight and then dried under vacuum at 40°C. The polymer was

suspended in 1M sodium hydroxide in methanol and refluxed for 6 hours. The cooled solutions were added to an excess of dilute HCl. The products were filtered and washed with water, methanol and ether. Polymers were soxhlet extracted with methanol and then hexane and dried under vacuum at 40°C.

4.7 Coatings

Two methods were used to coat the QCMs. In the first technique 10mg of PVC powder was dissolved in 5ml of THF and 30mg of MIP particles were suspended in solution with thorough stirring. A QCM was fixed via vacuum to a laboratory spin coater and coated with 10µl of the pvc/polymer solution. the suspension was spread over the surface of the Au electrode by rotating the sensor at 600-900 rpm for a period of five minutes.

The second technique involved the polymer film being cast by dispensing 2 µl of the polymerisation solution directly onto the surface of the Cr/Au electrode of the QCM and then covered immediately with a 13 mm diameter microscope coverslip. Prior to use the coverslip was treated with Sigma cote. Polymerisation was initiated by UV radiation using a 125 W medium pressure mercury lamp (Photochemical reactors 3012) under an

inert atmosphere for 30 minutes. Subsequently the coverslip was removed and the quartz crystals were then hydrolysed as in step 4.

4.8 Evaluation of sensor response

As in chapters 2, 3, and later 5, the coated crystals were tested by placing them in the crystal holder connected to an oscillator. This holder was immersed in a beaker filled with ethanol, which was placed in a large volume of water to prevent rapid temperature-changes during the experiment. Voltage and frequency were recorded and the data was transferred to a computer using a Labview programme (National Instruments Corporation, Austin, Texas). After connecting together the crystal holder and oscillator and eliminating the influence of the cable between them by adjusting the oscillator, the frequency was left to stabilize.

Solutions containing known amounts of nandrolone were prepared in ethanol. The coated quartz crystals were placed into a beaker of ethanol until a stable response was obtained, then 6 ml of nandrolone solution was added to the stirred bulk ethanol solution via successive 1 ml aliquots. The frequency was recorded until a stable response was obtained. After each 6 ml addition of analyte the coated quartz crystal was soaked in the porogenic solvent for 10 minutes and the experiment was repeated.

As outlined previously the QCM device is affected by changes in ambient temperature which can result in a drift in resonant frequency. On the timescale of the experiment, the change in frequency caused by environmental conditions could be greater than that caused by the mass loading of the quartz crystal. In order to overcome this difficulty the frequencies of two quartz crystals immersed in the ethanol solution, one crystal coated with the MIP and one crystal coated with the non imprinted polymer, were measured simultaneously following the DQCM technique of Bruckenstein *et al.*,[32] The resultant difference in frequency between the two crystals can be used to assess the response of the crystal to mass loading of the analyte, as the non imprinted polymer displayed no change in resonant frequency with mass loading; all experiments were performed in this manner.

4.9 Response of sensors to mass loading

The change in resonant frequency of the MIP quartz crystal as a function of nandrolone concentration is shown in Figure 4.5.

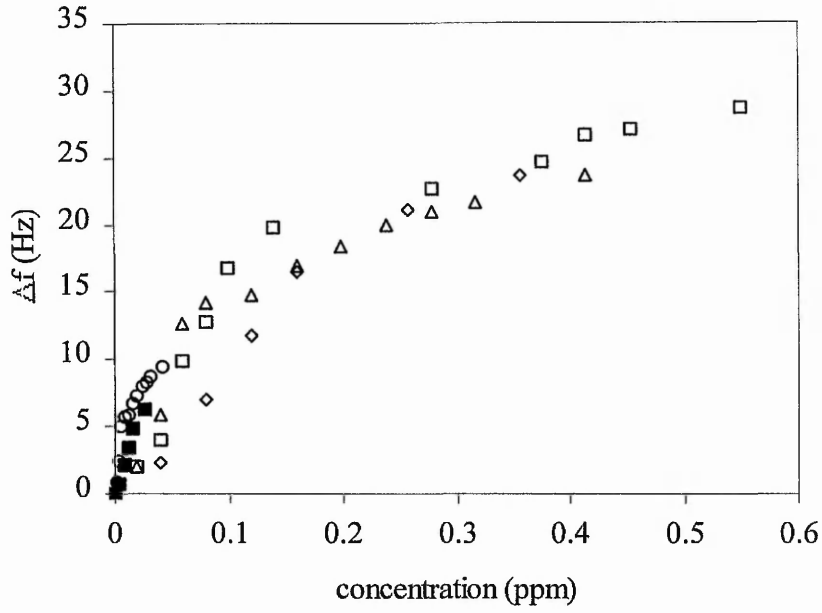

Figure 4.5: Frequency decrease as a function of nandrolone concentration. Coating 1 (solid squares), coating 2 (open circles), coating 3 (open triangles), coating 4 (open diamonds) and coating 5 (open squares).

There is an initial linear decrease in frequency corresponding to increase in nandrolone concentration up to about 0.2 ppm with a gradient in the range $S_{nandrolone} = -1178.7 \pm 69.2$ Hz ppm^{-1}, which reaches saturation at concentrations exceeding 0.2 ppm. Similar sorption isotherms have been observed by Haupt *et al.*,[24] for the binding of S-propranolol, Percival *et al.*,[33] for the binding of the monoterpene L-menthol and by Stanley *et al.*,[34] for the binding of the amino acid L-serine to a molecularly imprinted polymer. Such sorption isotherms are expected for polymers that contain immobilised binding sites, such as found in MIPs. The data presented in Figure 4.5 shows the

response for 5 different quartz crystals each with a MIP coating produced in the same way. The agreement suggests this methodology for coating the quartz crystals with MIP is not only reproducible between measurements but also between different batches of coatings.

Once again the affinity of the MIP polymers towards nandrolone can be evaluated using a one site Langmuir-type binding isotherm analysis.,[35] as discussed in chapters 2 and 3.

$$Kc\frac{\Delta f}{\Delta f_\infty}+\frac{\Delta f}{\Delta f_\infty}=Kc$$

Using the data shown in Figure 4.5, the calculated apparent association constant K = 123.2 ± 10.9 μM. The calculated apparent dissociation constant is similar to those found in MIPs.[33,34,36]

Three other steroids of interest in monitoring drug abuse in sport, testosterone, stanazolol and epitestosterone were examined in order to investigate the selectivity of the MIP, as shown in Figure 4.6. No change in resonant frequency was observed upon the addition of up to 2 ppm for all further steroids.

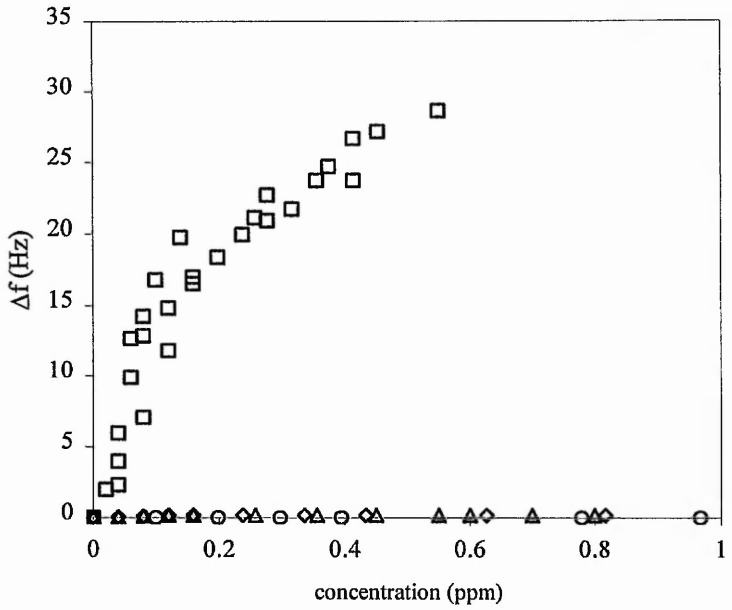

Figure 4.6: Frequency response as a function of concentration for nandrolone (open squares), testosterone (open diamonds), epitestosterone (open triangles) and stanozolol (open circles).

4.10 Conclusion

MIP coated quartz crystal sensors have been described which can selectively detect the steroid nandrolone in the liquid phase with a detectability of 6 ppb. The natural extension of this work is to enhance the sensitivity of the sensors to enable a low cost screening technique of biological samples to be produced. Firstly, it is may be possible to increase the concentration of binding sites in the MIP by increasing the ratio of the

functional monomer to template. Secondly, by increasing the mass sensitivity of the acoustic device. This may be achieved by increasing the resonant frequency of the sensor as the sensor response to mass loading is proportional to the square of the operating frequency. Above a fundamental frequency of 10 MHz, surface acoustic wave devices (SAWs) may be employed in place of the QCM that will extend the range of operating frequencies to over 1 GHz.[37,38] Such acoustic wave devices can be incorporated in a light weight and low cost oscillator circuit allowing an inexpensive screening technique to be developed. The non-covalently prepared MIP is also capable of binding nandrolone but with reduced efficiency.

.

4.11 References

1. IOC. Olympic movement Anti-Doping Code. *Lausanne*: IOC, **2000**.
2. H.H.D.Meyer, S.Hoffmann, *Food Addit. Contam.*, **1987**, 4, 149.
3. G.Degand, P.Schmitz, J.Maghuin-Rogister, *J. Chromatogr.*, **1989**, 489, 235.
4. R.J.Verbeke, *Chromatogr.*, **1979**, 177, 69.
5. L.A.Van Ginkel, H.Van Blitterswijk, P.W.Zoontjes, D.Van Den Bosch, R.W.Stephany, *J. Chromatogr.* **1988**, 445, 385.
6. H.F.de Brabander,P.Vanhee, S.van Hoye, R.Verbeke, *J. Planar Chromatogr.* **1989**, 2, 33.
7. Th. Reuvers, E. Perogordo, Alimentaria, E. **1986**, 170, 27.
8. E.Daeselerie, A.de Guesquierie, C. van Peteghem, *J. Chromatogr. Sci.*, **1992**, 30, 409.
9. A.Boenke, *Anal. Chim. Acta.*, **1993**, 275, 3.
10. B.Le Bizec, M-P.Montrade, F.Monteau, F.Andre, *Anal. Chim. Acta.*, **1993**, 275, 123.
11. G.van Vyncht, P.Gaspar, E.Depauw, G.Maghuin-Rogister, *J. Chromatogr.* B., **1996**, 686, 189.
12. Y.Galliard, G.J.Pepin, *Chromatogr.* A., **1997**, 763, 149.
13. Y. E. Charles, *Anabolic steroids in Sports and Exercise*, Dekker & Sons, US, **2000**.
14. T. Donohoe, N. Johnson, *Foul play*, T. J. Press, Padstow, UK, **1986**.
15. G. Wadlre, B. Hainline, *Drugs and the Athlete*, Davis, Philadelphia, **1989**.
16. C. D. Kochakian, *History of Anabolic-Androgenic Steroids*, G. C. Linn, US, **1990**.

17. C. D. Kochakian, *Historical review of Anabolic-Androgenic Steroids*, Springer-Verlag. Berlin, **1976**.

18. R. S. Sethi, *Biosens. Bioelectron.*, **1994**, 9, 243.

19. G. Wulff, A. Sarhan, *Angew. Chem. Int. Ed. Engl.*, **1972**, 11, 341.

20. G. Wulff, *Angew. Chem. Int. Ed. Engl.*, **1995**, 34, 1812.

21. F. L. Dickert, O. Hayden, *Trends Anal. Chem.*, **1999**, 18, 192.

22. K. Haupt, K. Mosbach, *Chem. Rev.*, **2000**, 100, 2495.

23. D. Kriz, O. Ramstrom, K. Mosbach, *Anal. Chem.*, **1997**, 69, 345.

24. K. Haupt, K. Noworyta, W. Kutner, *Anal. Commun.*, **1999**, 36, 391.

25. B. Sellergren, *Anal. Chem.*, **1994**, 66, 1578.

26. C. Liang, H. Peng, X. Bao, L. Nie, S. Yao, *Analyst*, **1999**, 124, 1781.

27. A. Kugimiya, T. Takeuchi, *Electroanalysis*, **1999**, 11, 1158.

28. K. J. Shea, E. A. Thompson, S. D. Pandey, P. S. Beauchamp, *J. Am. Chem. Soc.*, **1980**, 102, 3149.

29. B. R. Hart, D.J. Rush, K. J. Shea, *J. Am. Chem. Soc.*, **2000**, 122, 460.

30. M. J. Whitcombe, M. E. Rodriguez, P. Villar, E. N. Vulfson, *J. Am. Chem. Soc.*, **1995**, 117, 7105.

31. B. B. Corson, W. J. Heintzelman, L. H. Schwartzman, H.E. Tiefenthal, R. J. Lokken, J. E. Nickels, G. R. Atwood, F. J. Pavlik, *J. Org. Chem.*, **1958**, 23, 544.

32. S. Bruckenstein, M. Michalski, A. Fensore, Z. Li, Z, A. R. Hillman, *Anal. Chem.*, **1994**, 66, 1847.

33. C. J. Percival, S. Stanley, M. Galle, A. Braithwaite, M. I. Newton, G. McHale, W. Hayes, *Anal. Chem.*, **2001**, 73, 4225.

34. S. Stanley, C. J. Percival, T. Morel, A. Braithwaite, M. I. Newton, G. M^{c}Hale and W. Hayes, *Submitted to Sensors and Actuators B*, 2002.

35. E. Yilmaz, K. Mosbach, K. Haupt, *Anal. Commun.*, **1999**, 36, 167.

36. G. Vlatakis, L.I. Andersson, R. Müller, K. Mosbach, *Nature*, **1993**, 364, 645.

37. H. S. Ji, S. McNiven, K. Ikebukuro, I. Karube, *Anal. Chim. Acta.,* **1999**, 390, 93.

38. B. Jakoby, G. M. Ismail, M. P. Byfield, M. J. Vellekoop, *Sens. Actuators A.*, **1999**, 76, 93.

Chapter five

Sensor for polycyclic aromatic hydrocarbon detection

5.1 Abstract

A chemically coated piezoelectric sensor has been developed for the determination of PAHs in the liquid phase. An organic monolayer attached to the surface of a gold electrode of a quartz crystal microbalance (QCM) via a covalent thiol-gold link complete with an ionically bound recognition element has been produced. This study has employed the PAH derivative 9-anthracene carboxylic acid which once bound to the alkane thiol functions will function as the recognition element. Selective binding of anthracene via π-π-interaction has been observed as a frequency-shift subsequently quantified by piezoelectric microgravimetry with the QCM transducer. The lower limit of detection of the target analyte was 2 ppb with a linear response range of 0 – 50 ppb. The sensor was able to distinguish between different PAHs despite π-π-interaction being the sole communication between recognition element and analyte. The design and construction of a multi-purpose PAH sensor chip based upon a recognition group bound by either an ionic or covalent bond to the crystal coating is described. It is envisaged that these techniques could be employed to create recognition elements for different PAHs.

5.2 Introduction

Polycyclic aromatic hydrocarbons (PAHs) are a complex class of hydrocarbons resulting from the incomplete combustion of organic substances such as fossil fuels,[1] coal,[2,3] fuel oil,[4] gas,[5] refuse,[6] wood,[7] tobacco[8] and foodstuffs.[9] Additional sources include wood preservative plants, incinerators, asphalt used in road and roofing operations and aluminium plants.[10] Because of the many and varied sources of PAHs they are ubiquitous throughout our environment as evidenced by the inclusion of 16 PAHs in the U.S. Environmental Protection Agency's "Priority Polycyclic Aromatic Hydrocarbon Pollutants,[11] as shown in Figure 5.1.

PAHs are characterised by their planar fused ring structures consisting of between two and seven aromatic rings. The conjugated π electron systems of these aromatic compounds determines their physical and chemical properties. Naphthalene, for example, a two ringed compound, is the smallest member of the class and is found in the vapour phase in the atmosphere whilst PAHs consisting of three to five rings are semi volatile and are present in the air in both the vapour and particulate phases. The PAHs with five or more rings are commonly found as solids adsorbed onto particulate matter in the atmosphere.[11]

The widespread generation and subsequent release of PAHs into the environment means that they are found in air, water and soil throughout the world often as a complex mixture where they may exist for months or years.[5] There are three primary sinks for PAHs, plant uptake, photo-oxidation and biodegradation.

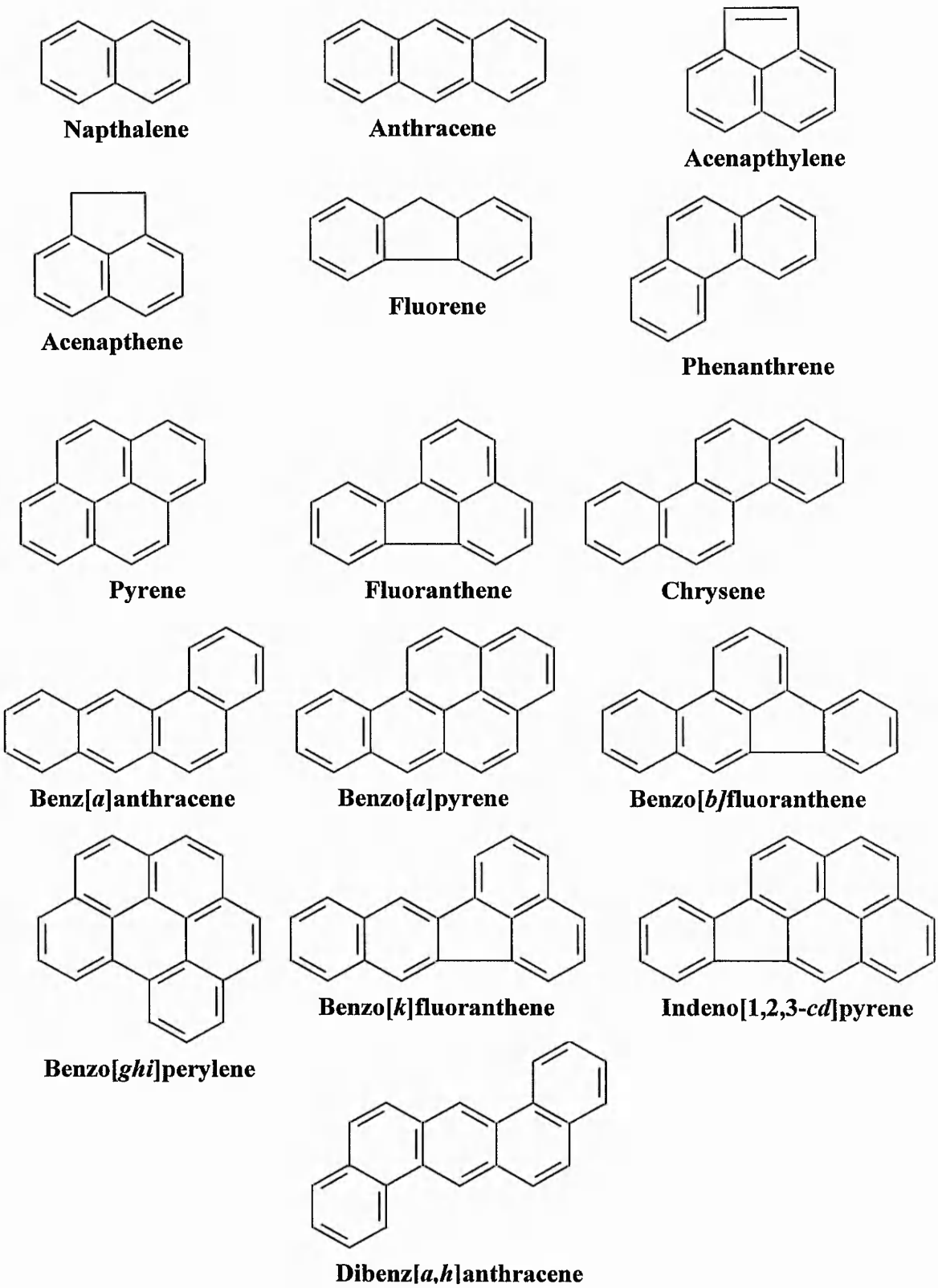

Figure 5.1: U.S. Environmental Protection Agency's "Priority PAH Pollutants".

The planar hydrophobic structure and high lipid solubility of PAHs makes their excretion from the body problematical. PAHs are able to intercalate with the structure of DNA and consequently disrupt the proper functioning of DNA potentially leading to cancer.[12] More often than not such damage is repaired, however if the mistake is not corrected the DNA can be misread resulting in defective proteins, which may ultimately lead to cancer. PAHs can also form adducts with DNA as a result of their oxidation within the liver. This combination of intercalation and chemical reactivity demonstrates why some PAHs are so carcinogenic. An example of possible PAH induced cancer is that of lung cancer, where PAHs are known to produce mutations in the p53 suppressor gene, which is present in about 60% of all lung cancer.[13] The possible health hazards associated with PAH exposure are numerous and include skin problems, immunodeficiency, reproductive difficulties and cancer.[14]

Whilst the effects of many PAHs on mammals is poorly understood a number are known or suspected carcinogens. The five ringed PAHs benzo(a)pyrene and dibenz(a)anthracene are known for their carcinogenicity. Benzo(a)pyrene is regarded as a key indicator compound of PAHs as it generally occurs in all mixtures where PAHs are present. The US-EPA has responded to the growing concern surrounding PAHs by establishing maximum contaminant levels (MCL's) for public drinking water to minimize the risk of adverse health effects. The MCL for total PAHs is 0.2 ppb.

In light of the obvious health effects associated with PAHs and their ever increasing use and emission into the environment there is a clear need to monitor these compounds. Ultimately the identification of marker compounds, such as benzo(a)pyrene and

dibenz(a)anthracene is sought to facilitate the assessment of the pollution potential problem and to model and calculate the flux of these polycyclic aromatic hydrocarbons. The development of analytical techniques for measuring the marker compounds simplifies the monitoring and analysis process.

Our increasing impact on the environment demands that we establish faster, cheaper and more accurate ways to monitor a wide variety of compounds. Screening for the presence of specific marker compounds in situ is cost effective and provides an immediate assessment of potential problems. Such an approach to monitoring and analysis can avoid expensive laboratory based analysis although these may be necessary for a full evaluation of pollutants present. Gravimetric sensors, as outlined previously, are well suited as transducer elements for chemical sensors, being portable, rapid and sensitive. For applications in chemical sensing, a recognition element is added to the acoustic wave device capable of selectively binding the analyte to the device surface. The response of these devices is then based on a decrease in their resonant frequency as mass is attached to the device or the recognition element.

The work presented in this chapter describes the development and assessment of such a recognition element selective for the PAH anthracene. An organic monolayer containing the recognition element is attached to the surface of a gold electrode on a quartz crystal microbalance (QCM) via a covalent thiol-gold bond. Two distinct strategies have been developed and evaluated, one involving the ionic attachment of the recognition element 9-anthracene carboxylic acid to the organic monolayer the other the covalent attachment.

5.3 Selective coatings

The QCM device, whilst very sensitive to mass changes, lacks selectivity. It is therefore necessary to create a coating on the surface of the QCM in order to develop a sensor that responds specifically to a single substance.

In order to produce a coating capable of selectively binding the target analyte possible modes of communication between it and the recognition element must be identified. With molecular imprinting this communication is frequently through hydrogen bonding, clearly not an option here. The analyte does, however, possess a planar fused aromatic ring structure. Examples exist in nature whereby compounds exhibiting aromaticity are able to interact via their π-electron systems, for example DNA.

This electronic interaction can occur when the π-bonds of an aromatic molecule undergo a spontaneous polarization, Figure 5.2. The spontaneous dipole that results induces a second dipole on another aromatic molecule so attracting one to the other.[15]

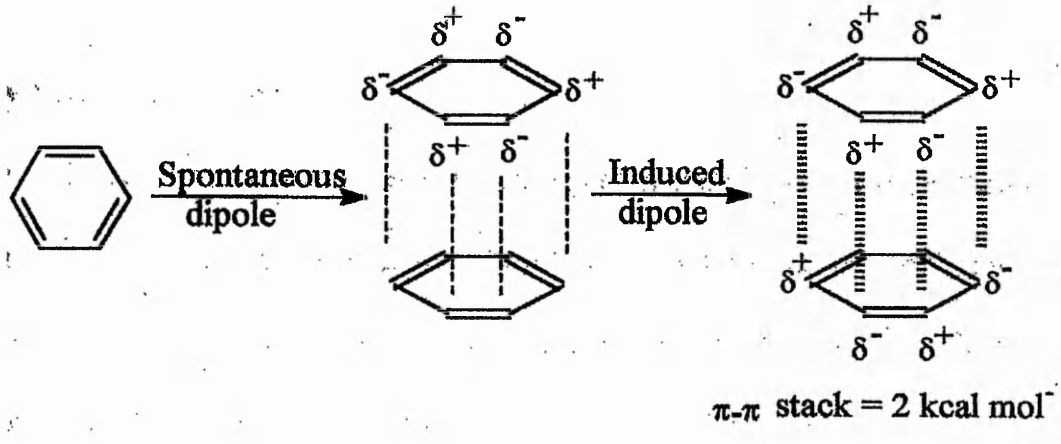

Figure 5.2: π-π Stacking interaction.[17]

This affinity of one aromatic system for another offers the potential for the interaction of the target PAH with a recognition element having complimentary aromaticity. The obvious choice for a recognition element would be the target PAH itself possessing as it does identical, and therefore complimentary aromaticity.

Recently Dickert *et al.*,[16] have shown that a molecularly imprinted polymer coated QCM utilising such Van der Waals interactions displayed an affinity towards a range of PAHs. Molecular imprinting is well established as a means of producing artificial recognition sites but requires extensive and time consuming developmental work in terms of assessing the stoichiometry of suitable functional monomers, crosslinkers and porogenic solvents.[17]

An alternative approach could involve the use of self-assembled monolayers (SAMs), which are essentially two dimensional molecular imprints, overcoming some of the shortfalls of the imprinting strategy.[18] The application of self assembled monolayers coupled with recognition elements capable of π-π interaction directly onto the surface of a QCM transducer offers a much simpler strategy for the production of a sensor selective for polyaromatic hydrocarbons.

Organic compounds can be readily chemisorbed onto the surface of a gold coated QCM via a metal-sulfur bond.[19] Immersion of a gold film into a solution of alkanethiols results in a stable tightly packed monolayer with a covalent bond between the sulfur and the gold,[20] equation 5.1.

$$RSH + Au \rightarrow RS\text{-}Au + \tfrac{1}{2} H_2 \qquad 5.1$$

where R is an alkane chain backbone.

The resultant alkanethiol monolayer is shown in Figure 5.3.

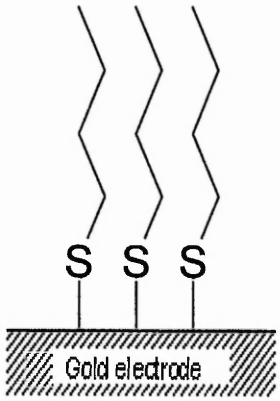

Figure 5.3: Thiol chemisorption onto a gold surface.

PAHs attached to the terminal ends of the alkane thiols could bind similar PAHs in solution around the QCM sensor via π-π interaction. Figure 5.4.

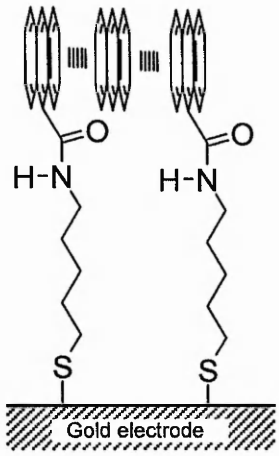

Figure 5.4: π-π-stacking interaction in coating on crystal

The additional mass thus bound in the organic layer on top of the QCM results in a mass increase and thus a subsequent decrease of the resonance frequency. This interaction is likely to occur with any PAH present in the solution but most favorably with PAH molecules that have an almost identical structure to the aromatic system attached to the organic molecules on the electrode. Thus the necessary selectivity is achieved.

For this coating to be effective in terms of its ability to interact with the target analyte via π-π stacking, there has to be enough space between different PAH-groups of the organic layer. This space is in part provided by existing irregularities of the gold electrode of the QCM. However, to ensure a high number of sites for PAH-PAH interaction shorter alkanethiols have been introduced as spacers in the coating-solution. Figure 5.5.

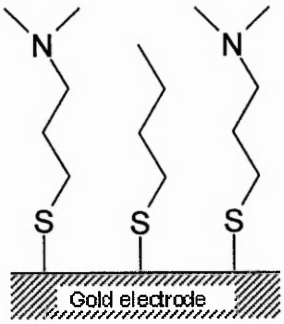

Figure 5.5: Different alkanethiols deposited on gold surface.

The use of two different alkanethiols with different tail groups is known to form a mixed monolayer when depositing from solution onto a gold surface rather than phase segregating into macroscopic domains.[21]

To produce an organic monolayer with a PAH recognition element bound to the terminal end, an ionic and a covalent bonding strategy was pursued. A carboxylic acid derivative of the corresponding PAH is necessary for the synthesis of both systems. In this project, 9-anthracenecarboxylic acid has been exclusively used. It is non-carcinogenic, can be easily obtained and is structurally closer to the larger carcinogenic PAHs than the carboxylic acid derivative of napthalene.

5.4 Experimental

5.41 Chemicals

3-Dimethylpropylchloride hydrochloride, potassium carbonate, potassium thioacetate, 1-butanethiol, 9-anthracenecarboxylic acid, thionyl chloride, 5-amino-1-pentanol, p-toluene-sulfonyl chloride, anthracene, naphthalene, benzo[a]pyrene and 1,2:5,6-

dibenzanthracene were purchased from Aldrich Chemicals (Dorset, UK). All the solvents were of analytical grade and all reagents were used as supplied.

5.42 Instrumentation

The quartz crystal microbalance was produced using unpolished AT-cut, 25 mm diameter, plano-plano quartz crystals with Cr/Au contacts, operating at a fundamental resonant frequency of 5 MHz and with an electrode area of approximately 133 mm^2 (Maxtek model No. 149211-2). The crystals were mounted in a Maxtek CHC-100 crystal holder and the measurement system consisted of a Maxtek PLO10 phased locked oscillator and a HP53132A universal counter interfaced to a microcomputer.

5.43 Cleaning Crystals

Before using the crystals, former coatings and contaminants were removed and the surface was prepared in the following manner: The crystals were scrubbed with tetrahydrofuran (THF) and then placed into Piranha etching solution (1:3 v/v 30% H_2O_2 : conc. H_2SO_4) for 10min. Afterwards they were rinsed with distilled water, then ethanol and dried.

5.5 Synthesis of ionically bound coating

Synthesis of the organic monolayer employing the ionically bound recognition element is given in Scheme 5.1.

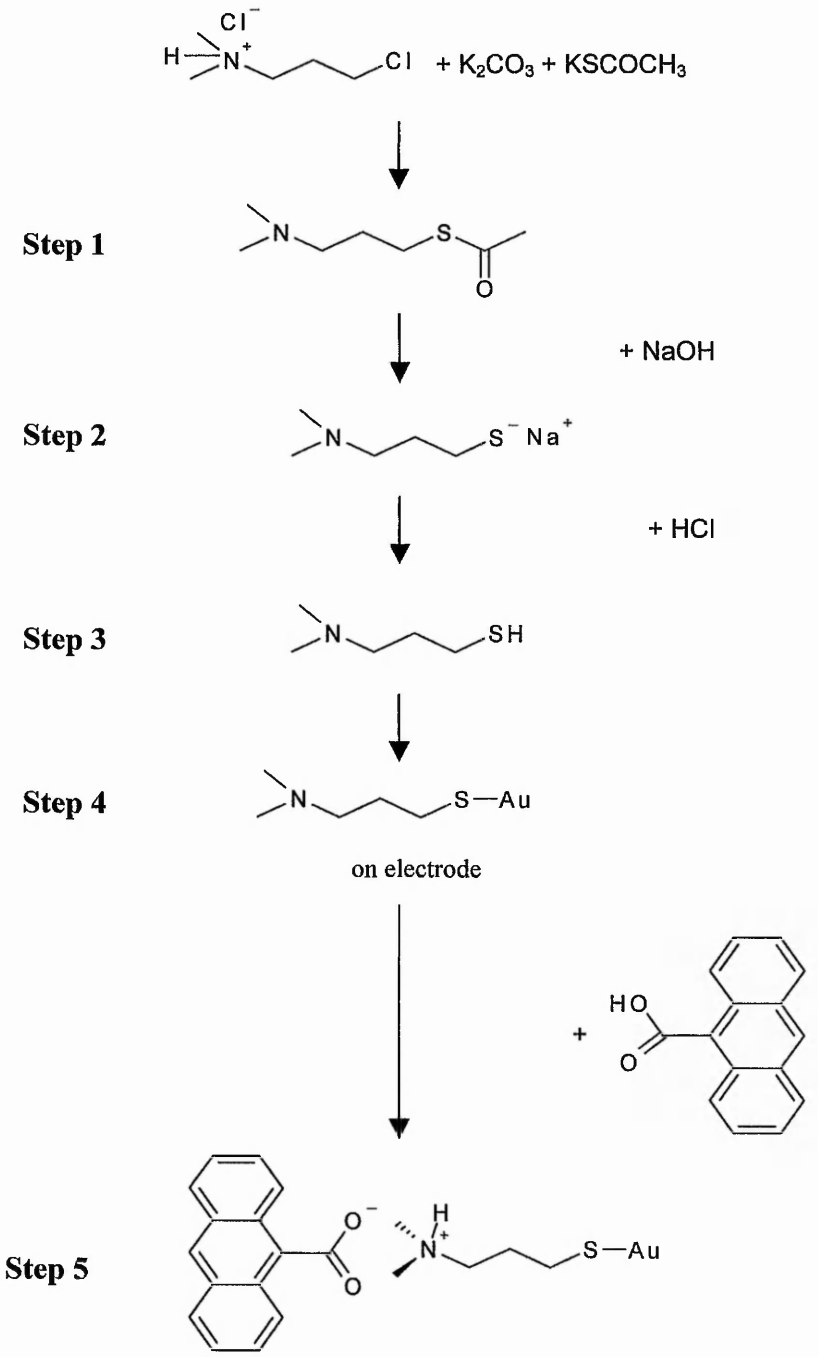

Scheme 5.1: Synthesis of ionic coating.

0.01 mol of 3-dimethylaminopropylchloride hydrochloride $(CH_3)_2N(CH_2)_3Cl{\cdot}HCl$ was stirred together with 0.01 mol potassium carbonate (K_2CO_3) in 20 mL of dried acetone under nitrogen for 30 minutes, liberating the base at the nitrogen-atom. 0.01 mol of potassium thioacetate ($KSCOCH_3$) was added, stirred for 2.5 hours and left overnight. The precipitate was filtered off and the liquor evaporated to yield $(CH_3)_2N(CH_2)_3SCOCH_3$ (dimethylaminopropylthioacetate) as the product of step1. Appendix 5.1.

The acetate group was replaced by a sodium ion in (step 2) by dissolving 0.3 g of dimethylaminopropylthioacetate in 15 ml 4-molar sodium hydroxide-methanol solution. The quartz crystals were then immersed into this solution to which was added 30 mL 2-M HCl and 0.5 molar equivalent of 1-butanethiol to dimethylaminopropylthioacetate. The acid neutralizes the hydroxide and the thiolate-ion is protonized forming a thiol-group (step 3) a covalent bond with the gold electrode on the crystal surface was then formed (step 4). Simultaneously, the butanethiol fixes on the gold electrode in the same manner, forming spacers between the aminothiols. The crystals were left in this solution for 4 hours.

The recognition element was attached by soaking the crystals in an equimolar solution of 9-anthracenecarboxylic acid and dimethylaminopropylthioacetate in 30 mL of ethanol for 1 hour. Reference crystals were prepared in the same way but without exposure to 9-anthracenecarboxylic acid. All crystals were subsequently removed from solution and washed with ethanol and stored under nitrogen until screened.

Anthracene carboxylate-ions form an ionic link with quarternary ammonium-ions at the end of the organic chains on the crystal (step 5). It was thus not possible to obtain an NMR-spectrum for the substance formed in this last step, supporting the hypothesis that an ionic product was formed.

Dimethylaminopropanethiol $(CH_3)_2N(CH_2)_3SH$ has been linked with 9-anthracene carboxylic acid through a proton-exchange (scheme 5.2), to produce an organic monolayer complete with an ionically bound PAH-recognition group.

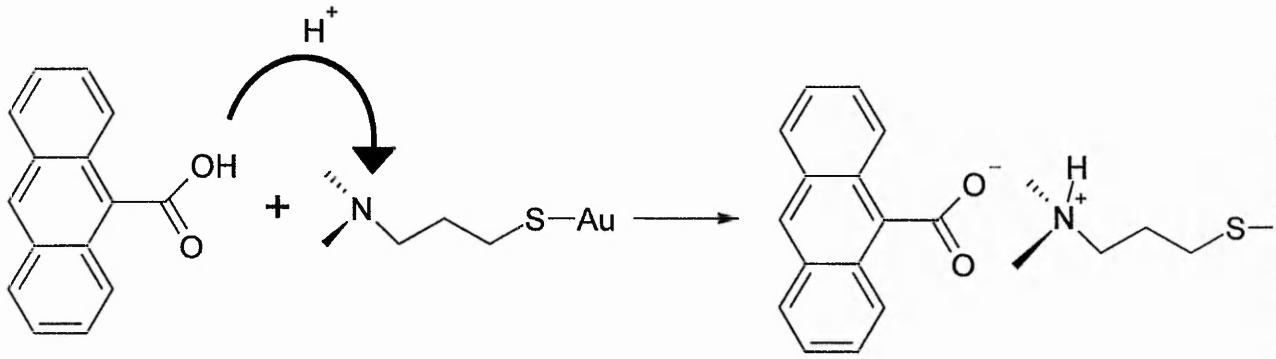

Scheme 5.2: Proton-exchange forming ionic adduct.

The ionic link between the recognition element and alkanethiol can be broken by treatment with a hydroxide-solution, subsequent immersion of the aminopropanethiol coated QCM in a solution containing a different PAH-carboxylic acid could it is envisaged, yield a QCM-sensor selective for the new PAH. Alternatively the same PAH-group that was originally employed as recognition element could be utilized in order to replenish the sensor for further use. This strategy offers a clear advantage over the covalent approach.

5.6 Covalent Coating

The covalent approach is represented schematically in scheme 5.3.

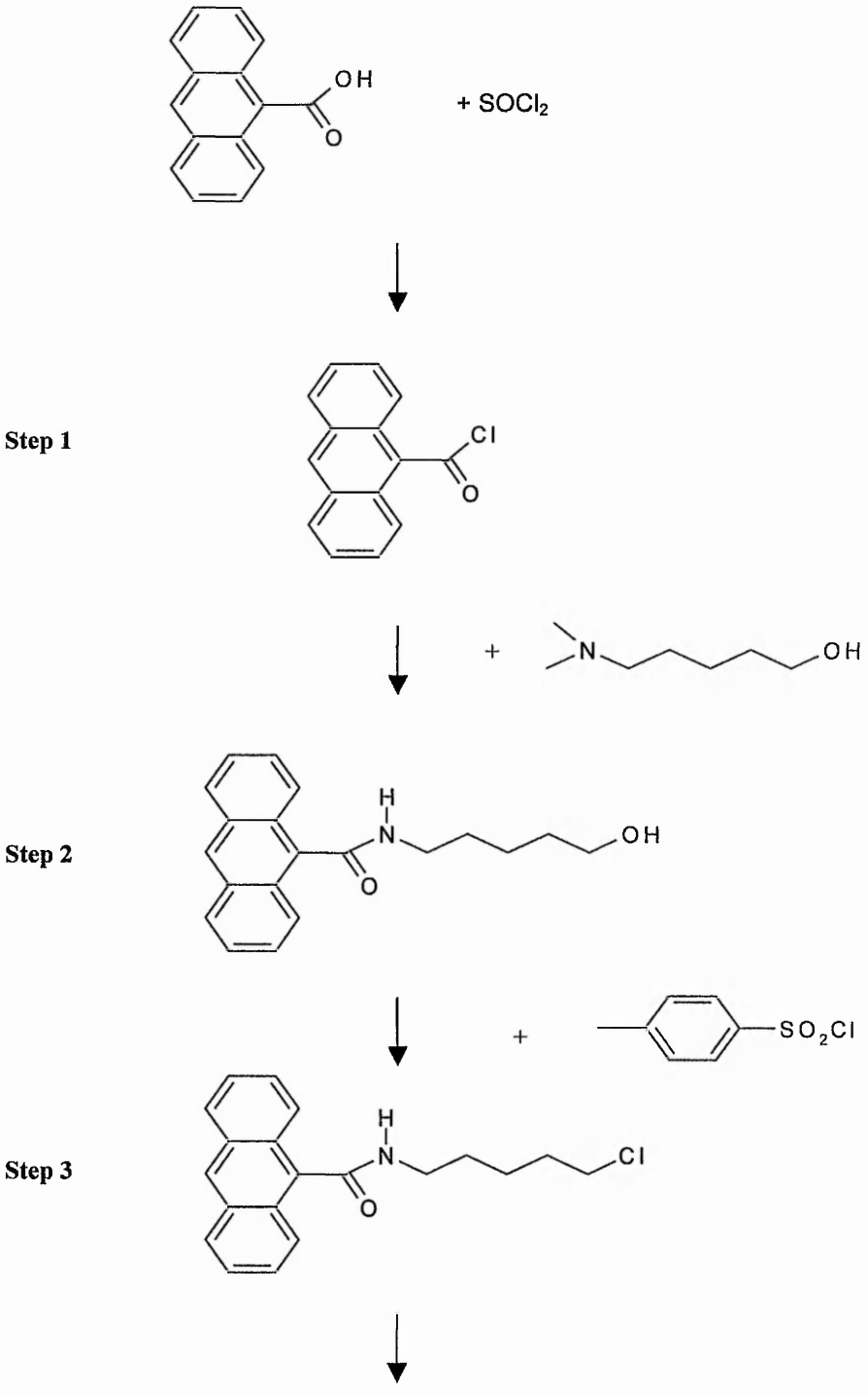

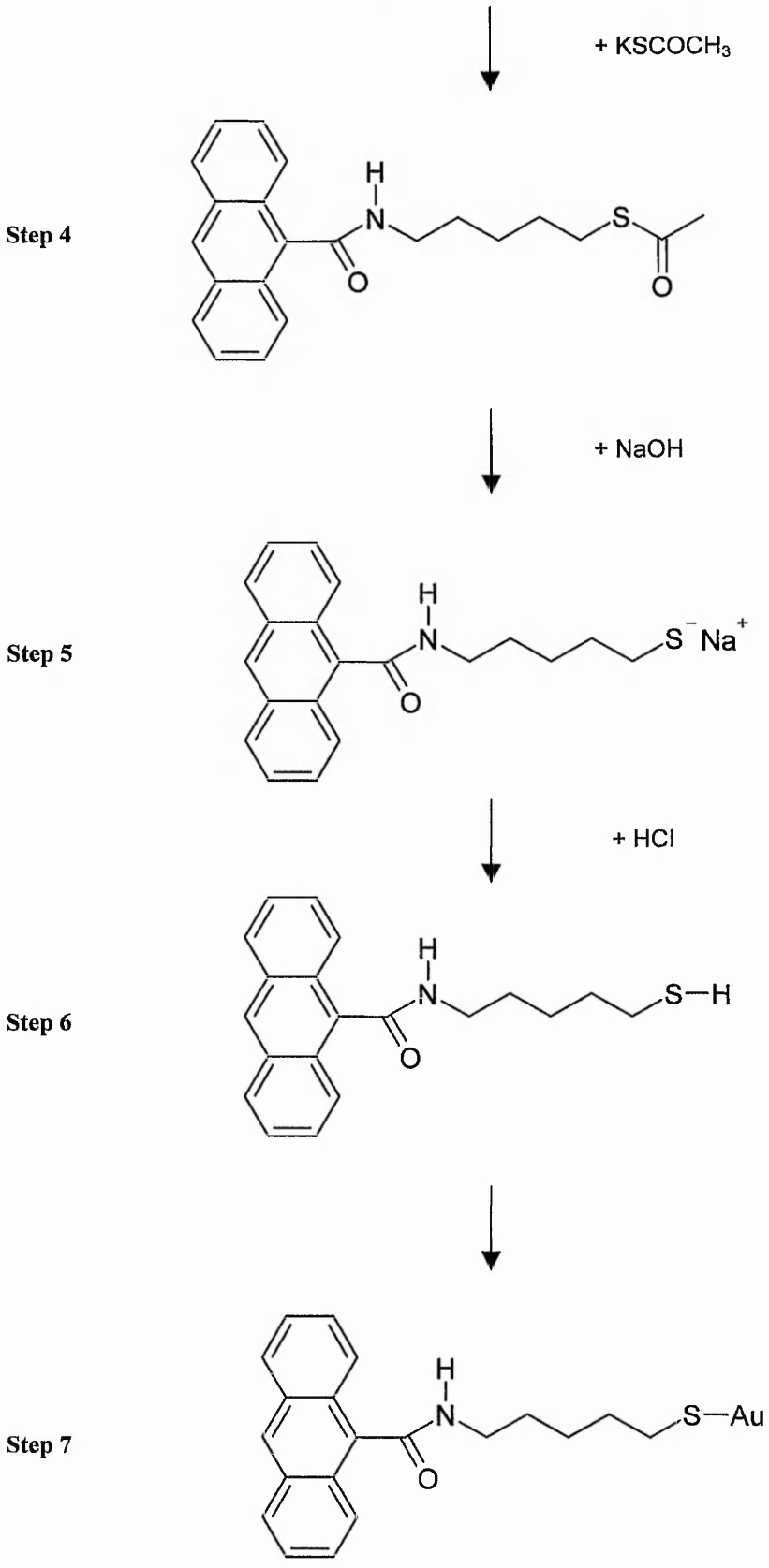

on electrode

Scheme 5.3: Synthesis of covalent coating.

Step 1, the hydroxyl-group was replaced by a chlorine-atom by heating 4 g of 9-anthracenecarboxylic acid with an excess of thionyl chloride $SOCl_2$ over a water bath at 43°C for 1 hour (Appendix 5.2, 5.3). The remaining thionyl chloride was then removed by rotary evaporation, the product being redissolved in 10 ml of ether.

5-amino-1-pentanol 2.5 times the molar equivalent of 9-anthracenecarboxylic used in step 1 was dissolved in 15 mL of ether. The two solutions were stored at 0°C until cooled and subsequently added together with stirring. The anthracene carbonylchloride and the amino alcohol react to form an amide as the product of step 2 (Appendix 5.4).

The ether was then evaporated off and the remaining solid washed first with distilled water, then with hot ethanol to remove remaining unreacted starting material. The product was then dissolved in pyridine and an equal molar amount of p-toluenesulfonyl chloride ($CH_3C_6H_4SO_2Cl$) added so that the hydroxyl-group might be replaced by a chlorine-atom (step 3).

The solution was swirled in a round bottomed flask to ensure mixture and left stoppered overnight during which a precipitate formed. The reaction mixture was then poured into 10 mL of distilled water at 0°C and stirred occasionally with a glass rod for ca. 40 min. The solid was filtered off and washed with H_2O, then with 2-molar HCl and again with H_2O. The solid was then recrystallized in a small volume of hot chloroform. 0.5 g of the product was then stirred together with a molar equivalent of potassium thioacetate $KSCOCH_3$ in dried acetone under nitrogen for 30 minutes. The terminal chlorine-atom was exchanged for the thioacetate-group to give the product of step 4 (Appendix 5.5).

Step 5, Acetone was evaporated off and the product dissolved in 15 mL of 4-molar NaOH-methanol-solution accompanied by stirring for 30 minutes.

The quartz crystals were then immersed into this solution to which was added 30 mL 2-molar HCl and half the molar equivalent of 1-butanethiol to the step 4 product used. As with the ionic coating, the acid would neutralize the hydroxide and the thiolate-ion would be protonized forming a thiol-group step 6. A covalent bond with the gold of the electrode on the crystal is then formed, step 7 and simultaneously, the butanethiol fixes on the gold electrode in the same manner, forming spacers in the coating monolayer. After 4 hours the sensor crystals were taken out, rinsed with ethanol, dried with nitrogen and kept under nitrogen.

The NMR-spectrum of the product of step 4 (Appendix 5.5) indicates, however, that the product of step 2 is still present at this stage. It therefore has to be assumed that either step 3 or step 4 of the synthesis were unsuccessful. Despite this fact the sensor coated according to the described synthesis showed a response to anthracene in a surrounding solution. The reason for this result may be that some of the product of step 2 has formed bonds with the gold surface of the electrode probably via the hydroxyl-group. If this assumption can be ascertained and the reaction modified in favour of the product bound to the gold, it may considerably shorten the process of coating a QCM with a monolayer of molecules.

5.7 Results and Discussion

5.71 Evaluation of sensor response for ionic coating

The coated crystals were tested by placing them in the crystal holder, outlined in Chapter 2, connected to an oscillator. The holder was immersed in a beaker filled with ethanol, which was placed in a large volume of water to prevent rapid temperature-changes during the experiment. Voltage and frequency were recorded and the data was transfered to a computer using a Labview progamme (National Instruments Corporation, Austin, Texas). After connecting the crystal holder and oscillator and eliminating the influence of the cable between them by adjusting the oscillator, the frequency was left to stabilize.

Solutions containing known amounts of the target analyte were prepared in ethanol. The coated quartz crystal was placed into a beaker of ethanol until a stable response was obtained, then 9 ml of the analyte solution was added to the stirred bulk ethanol solution via successive additions of 0.1mL to 1.5mL aliquots. The frequency was recorded until a stable response was obtained. After each 9 ml addition of analyte the coated quartz crystal was washed repeatedly with ethanol for 10 minutes and the experiment was repeated.

These injections each caused a downward shift in the measured resonance-frequency of the crystal following a step pattern, Figure 5.6, indicating a mass-increase on the surface. Figure 5.6 also shows the effect of different temperatures of the medium

surrounding the crystal and the injected solution, represented by the peaks that follow each addition. The response time after each addition until the temperature effects had worn off and an equilibirium between bound and free PAHs had developed was approximately 40 s. The noise level was very low (ca. 0.4Hz) so that even small changes in resonance frequency were detectable.

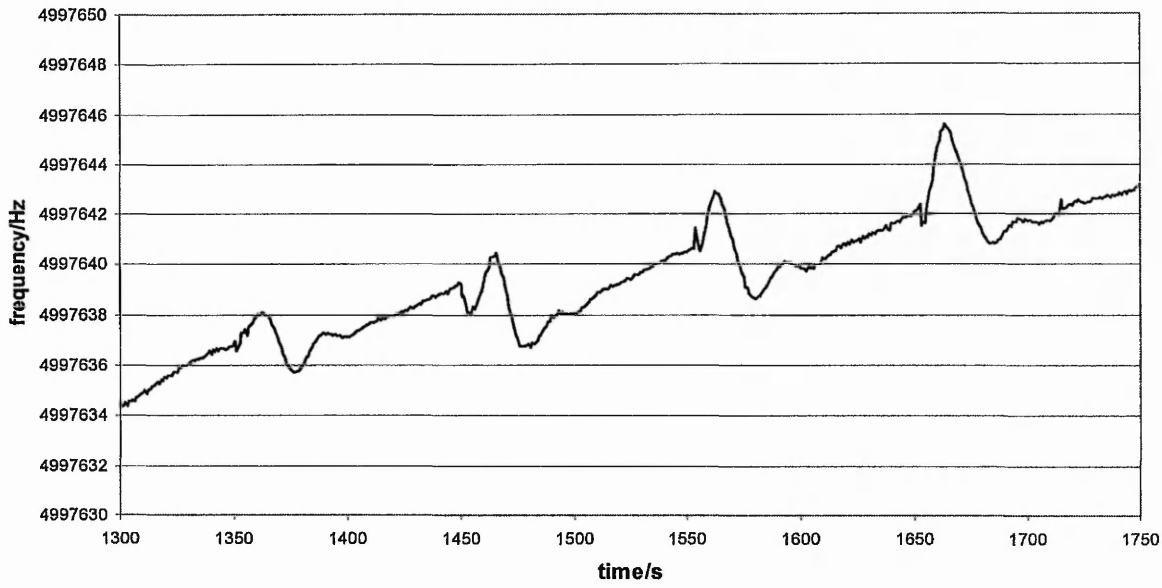

Figure 5.6: Ionic coating screened with sequential additions of anthracene-solution.

During the synthesis of the PAH appended organic monolayer, reference crystals were prepared in exactly the same manner but without the ionically bound recognition element.

This reference crystal was screened in the same way as the others, Figure 5.7.

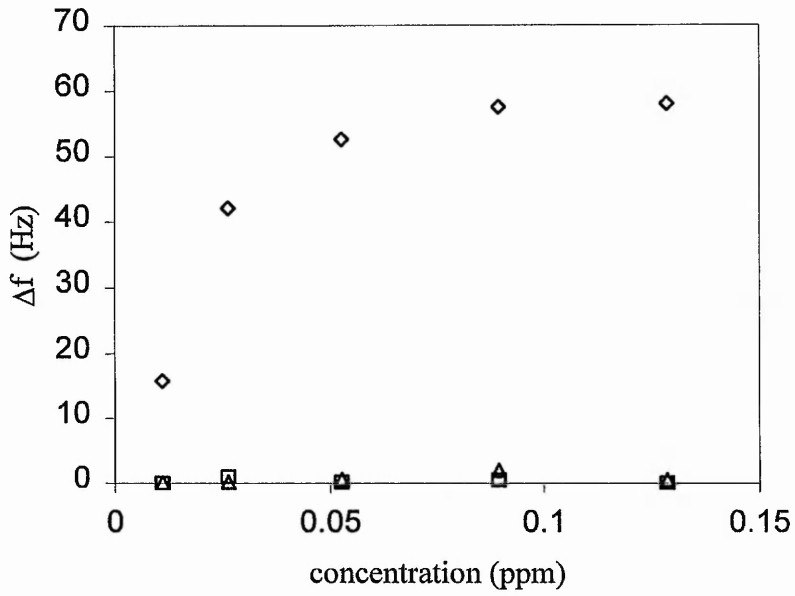

Figure 5.7: Response of PAH sensor (diamonds) and reference (squares and triangles) crystals.

During the screening of coated crystals the change in resonance frequency caused by environmental conditions was sometimes greater than that caused by mass loading on the surface of the sensor device. In order to address this difficulty the frequencies of two quartz crystals immersed in the ethanol solution, one crystal with the ionically appended PAH coating and one reference crystal were measured simultaneously following the DQCM technique of Bruckenstein *et al.*,[22] The resultant difference in frequency between the two crystals can be used to assess the response of the crystal to mass loading of the analyte, as the non PAH coating displayed no change in resonant frequency with mass loading all experiments were performed in this manner.

5.72 Response of sensors to mass loading

Figure 5.8. shows typical frequency-shifts against the respective concentration of anthracene in the test-solution. The concentration is calculated by taking into account the change in volume of the solution in the beaker with each addition.

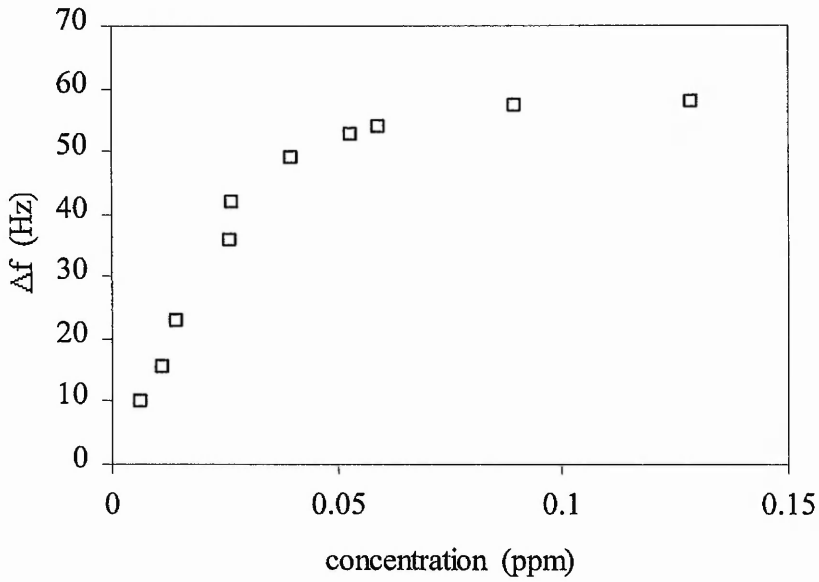

Figure 5.8: Frequency shift against PAH-concentration for ionic coating.

There is an initial linear decrease in frequency corresponding to an increase in the anthracene concentration up to about 15 ppb with a gradient to this point in the range $S_{anthracene}$= -2.047±0.042 Hz ppm^{-1}. Saturation is reached at concentrations exceeding 20ppm. Similar sorption isotherms have been observed by Percival *et al.*,[23] and Haupt *et al.*,[24] for the binding of analytes to a polymer with a finite number of interaction sites. Between screenings the crystals were thoroughly rinsed with ethanol. This cleaning protocol appears to have been only partially successfully. Subsequent test runs with one

crystal showed in general a greatly reduced frequency-shift, as evidenced in Figure 5.9. The number of available analyte interaction sites therefore is reduced with many of them either blocked or removed by the cleaning process.

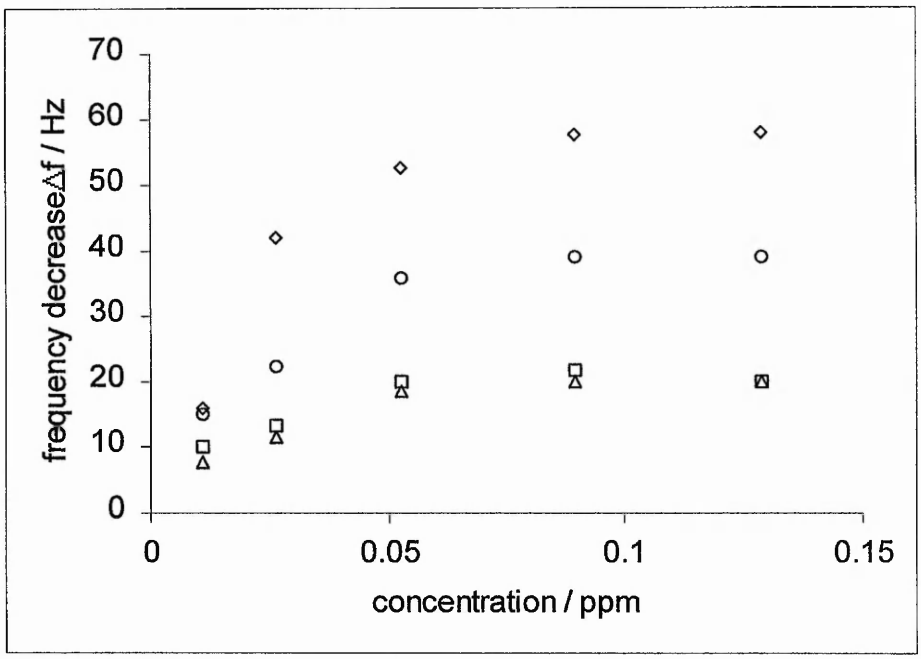

Figure 5.9: Subsequent test runs with one crystal run 1 (diamonds); run 2 (squares); run 3 (triangles) and after replenishing coating (circles).

The ionic link that holds the PAH element in place can be readily cleaved and replaced by another recognition element. To examine this, coated crystals that had already been screened were placed first into a 4-molar sodium hydroxide solution for 1hour. The crystals were then left in 9-anthracenecarboxylic acid-ethanol solution overnight in order to replenish the coating. Figure 5.9. also shows a comparison between the fresh coating and the replenished coating. The measured frequency-shift was still clearly below its original value. Thus it is evident that under the experimental conditions used it

is not possible to recover 100% of the analyte interaction sites. All the subsequent analysis were performed on fresh coatings.

The data presented in Figure 5.10 shows the response for 18 different quartz crystals each with a PAH coating prepared in the same way. This close agreement suggests that the methodology employed for coating the quartz crystals is reproducible between different coatings.

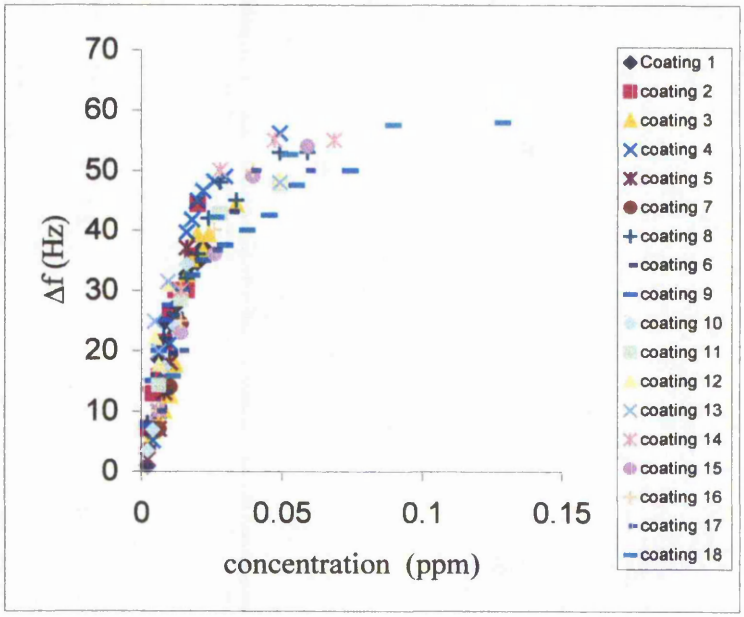

Figure 5.10: Replicate screenings with different devices.

5.73 Selectivity

To examine the selectivity of the coated QCM sensors, crystals coated with the anthracene recognition element were challenged with solutions containing different PAHs, as shown in Figure 5.11. All curves show linear behaviour upto 20 ppb, with saturation evident at concentrations exceeding 20 ppm, the gradients of which are presented in Table 5.1.

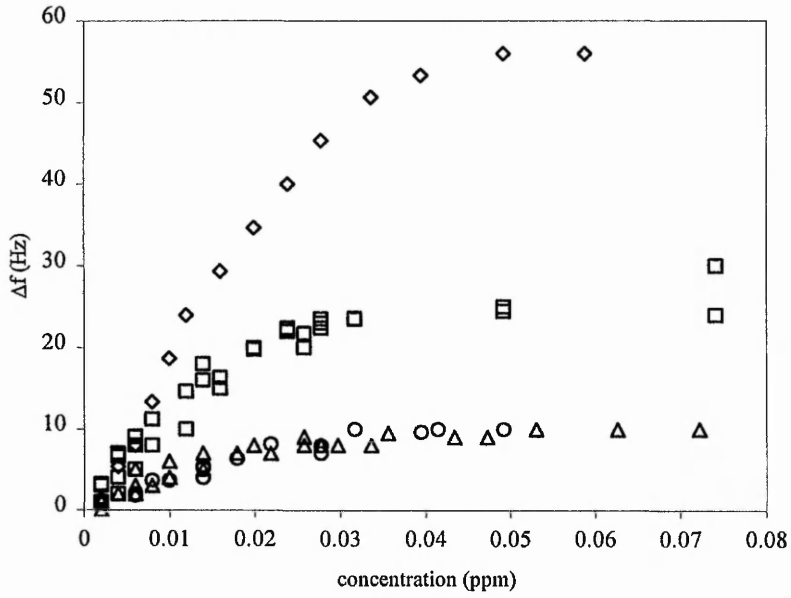

Figure 5.11 The range of PAH analogues that the selectivity of the ionic coated quartz crystals were tested towards Anthracene (diamonds); Naphthalene (squares); 1,2:5,6-Dibenz-anthracene (triangles) and Benzo[a]pyrene (circles).

The affinity of the ionically PAH appended organic coatings towards PAHs can be evaluated using one site Langmuir-type binding isotherm analysis.[25]

$$Kc\frac{\Delta f}{\Delta f_\infty}+\frac{\Delta f}{\Delta f_\infty}=Kc$$

Where K is the apparent dissociation constant, c is the free analyte concentration at equilibrium Δf is the frequency change and Δf∞ is the frequency corresponding to complete coverage. Although this does not reflect the real situation in the coating it allows for a comparison of binding between coatings. Using the data in Figure 10 the apparent dissociation constants K were estimated and given in Table 1.

Constant	Anthracene	Napthalene	Benzo[a]pyrene	1,2:5,6-Dibenz-anthracene]
$S_{initial}$ **/ppb^{-1}**	-2.047±0.042	-0.988±0.048	-0.327±0.019	-0.437±0.024
K / ppm^{-1}	60.16	51.94	47.22	31.26

Table 5.1: A summary of the experimentally evaluated apparent dissociation constants and initial slopes.

Anthracene shows the largest apparent dissociation constant, which suggests that the anthracene recognition groups attract anthracene more readily than other PAHs. The reason for this behaviour is assumed to be the nearly identical π-electron systems of the dissolved molecules and the coating. Napthalene has a smaller value of apparent

dissociation constant than anthracene. This infers that either, Napthalene has a lower molecular mass than anthracene and the same number of naphthalene-molecules with a lower relative molecular mass results in a smaller additional mass in the coating and thus a smaller frequency-shift, or alternatively, the anthracene-groups of the coating show a lower affinity to the somewhat different π-electron system of the naphthalene molecules. The predominance of one effect over the other is not apparent from the naphthalene and anthracene frequency shifts. However, trials of the sensor with benzo[a]pyrene and 1,2:5,6-dibenzanthracene suggest that the lower frequency shift of the anthracene sensor to that observed for naphthalene is in fact a result of the lower affinity of the sensor to naphthalene. Both benzo[a]pyrene and 1,2:5,6-dibenzanthracene are five membered PAHs and consequently possess higher masses than the target analyte, however they show decidedly lower affinities for the sensor as evidenced by their low apparent dissociation constants. This very much suggests that the anthracene recognition element selectively binds the target analyte anthracene in preference to other PAHs. The coating has less affinity for the larger PAHs and this effect overrides the influence of their comparatively larger molecular weight. This indicates that the coating displays a degree of selectivity resulting from π-electron geometry.

5.74 Evaluation of sensor response for covalent coating

Crystals with a covalent coating were screened in an identical manner to those possessing an ionic coating. However, as the crystals with covalent coating became saturated with analyte at distinctly lower concentrations than the ones with ionic coating, a solution of only 0.3 ppm PAH was used in all subsequent screenings. The injections resulted in downward shifts of the resonance frequency caused by the bonding of PAHs to the coating. Thus a step pattern resulted from subsequent injections of PAH-solution, Figure 5.12. With observed response times of ca. 40 s and very low noise levels of ca. 0.4 Hz these variables were similar to those encountered during the screening of the QCM's prepared with the ionic coating.

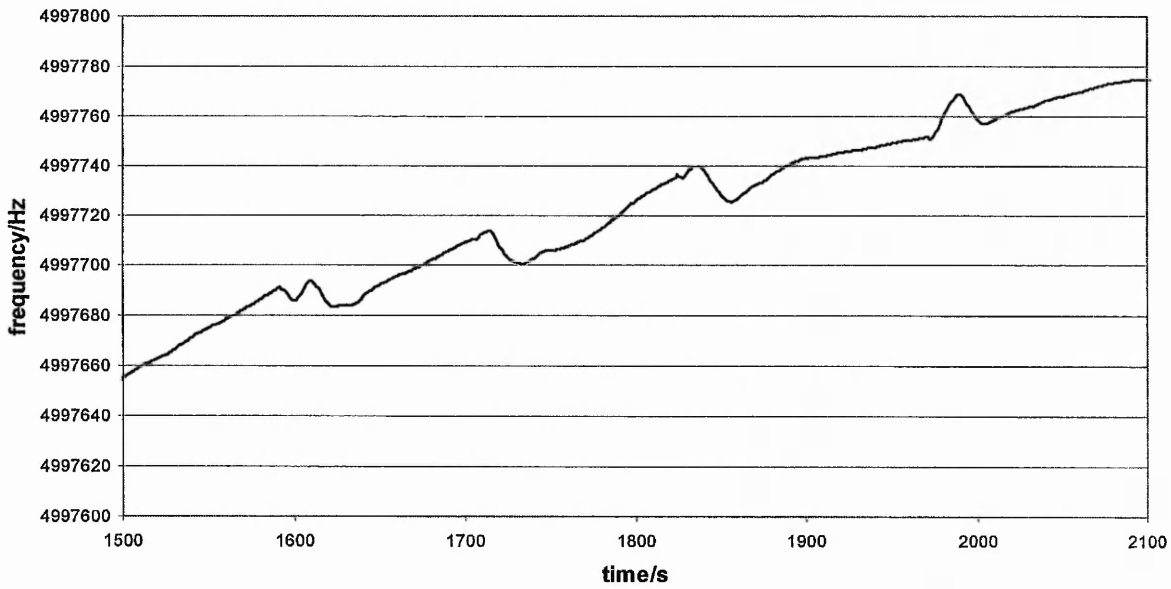

Figure 5.12: Covalent coating screened with successive anthracene-solutions.

5.75 Observed Frequency-shifts

In Figure 5.13. the frequency-shifts against concentration of PAHs in the solution is shown. As with the ionic coating, two parts can be distinguished. In the first part, the graph is linear, the frequency-shift is directly proportional to the concentration of the solution. In the second part, saturation takes place as more and more interaction sites are blocked with PAHs until no more frequency-shift could be observed.

The monitored limit of detection was ca. 0.6 ppb, a linear relationship between concentration and frequency-shift occurred up to ca. 20 ppm. Saturation could be observed at ca. 5 ppb indicating that a decisively smaller number of interaction sites were present on crystals with the covalent coating than on the ones with ionic coating. The reason for this is assumed to be that the bond between the coating molecules and the gold surface is not based on a thiol-group as with the ionic coating but on a hydroxyl-group. A reaction of a hydroxyl-group with gold is less favourable than with a thiol-group. It can therefore be assumed that less coating molecules and thus less interaction sites are present on crystals prepared with the described covalent coating.

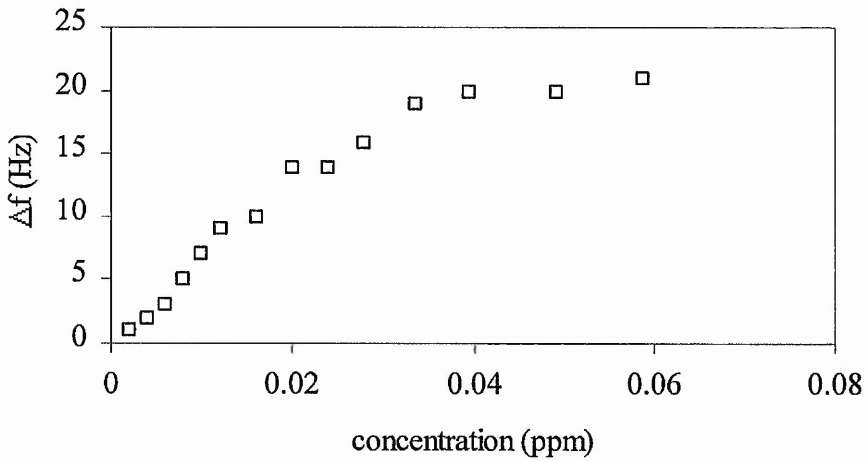

Figure 5.13: Frequency-shift against anthracene-concentration for covalent coating.

As in the case of the ionic coating the frequency-shift at the point of saturation varied between different crystals in the range 4 ppb.

Subsequent tests with the same crystal that was washed with ethanol in between measurements showed a greatly reduced response to exposure to PAH's. Soaking a crystal in the non-polar solvent cyclohexane for 1hour gave a slight improvement in comparison to the preceding test of this sensor. This maybe as a result of the higher solubility of 9-anthracene carboxylic acid in cyclohexane as opposed to ethanol.
These results for the covalent coatings need to be verified by further studies, beyond this research programme.

5.8. Conclusion and Future Work

It is clear that quartz crystal sensors coated with a monolayer of aminothiols with an ionically bound anthracene-group can be used to selectively detect the PAH anthracene in the liquid phase with a typical detectability of 2 ppb.There are several possibilities to further improve the sensitivity:

Firstly, it may be possible to increase the number of interaction sites on the QCM. To achieve this the synthesis of the coating may be improved to give a higher yield. For instance, the effect of different amounts of the spacer 1-butanethiol may also be examined in order to achieve an optimal accessibility of the interaction sites.
Secondly the mass sensitivity of the acoustic device can be improved. This may be achieved by increasing the resonance frequency of the sensor as the sensor response to

mass loading is proportional to the square of the operating frequency. The upper limit for quartz crystal microbalances operating at the fundamental frequency is around 10MHz; the higher the frequency the thinner the crystal. Alternatively, surface acoustic wave devices (SAWs) may be employed that will extend the range of operating frequencies to over 1GHz.[26]

The covalent coating has been less successful with an achieved detectability of 0.6ppb. Consideration must be given to the creation of an alkane thiol with a covalently bound recognition element. Further work should include a study of linearity by analysing solutions in the range 1-4 ppb.

Future work to be considered would be to look at strategies for the effective cleavage of the ionically bound PAH recognition element and subsequent replenishment with the same or different PAH receptor, for instance benzo[a]pyrene, which, as key marker compound for the whole range of PAHs is of topical interest. A sensor using a naphthalene-group may be able to detect the insecticide napthylacetic acid that is closely related to naphthalene and preliminary studies to this end have shown promise. Finally techniques to achieve results with greater reproducibility may be examined.

Ultimately a sensor for the evaluation of PAHs in the liquid phase whilst useful should not the ultimate goal as the larger potentially more toxic PAHs are usually bound to particulates in the atmosphere. A potentially more useful sensor for the real time determination of atmospheric particulates by an acoustic wave device is currently under development and it is envisaged that particulates bound to the acoustic wave device

could be subjected to analysis by mass spectrometry for instance possibly by the application of a MALDI source directly onto the sensor.

5.9 References

1. R.P. Wayne, *Chemistry of the Atmospheres*, 3rd ed., Oxford University Press, Oxford, **2000**.
2. T. Vo-Dinh, P.R. Martinez, *Anal. Chim. Acta.*, **1981**,125, 13.
3. J. L. Mumford, C. T. Helmes, X. Lee, J. Seidenberg, S. Nesnow, *Carcinogenesis,* **1990**, 11, 397.
4. B. A. Benner Jr., G. E. Gordon, S. A. Wise, *Environ. Sci. Technol.*, **1989**, 23, 1269.
5. B. J. Finlayson-Pitts, J. M. Pitts, *Chemistry of the Upper and Lower Atmosphere*, 1st ed., Academic Press, New York, **1999**.
6. W. M. G. Lee, Y. S. Yuan, J. C. Chen, *J. Environ. Sci. Health*, **1993**, A28, 1017.
7. I. Alfheim, T, Ramdahl, *Environ. Mutagen.*, **1984**, 6, 121.
8. L. A. Gundel, K. R. R. Mahanama, J. M. Daisey, *Environ. Sci. Technol.*, **1995**, 29, 1607.
9. N. T. Crosby, D. C. Hunt, L. A. Philip, I. Patel, *Analyst*, **1981**, 106, 135.
10. T. Vo-Dinh, *Chemical Analysis of Poly Aromatic Hydrocarbons*, 1st ed., John Wiley and Sons, New York, **1989**.
11. C. E. Junge, *Adv. Environ. Sci. Technol.*, **1977**, 8, 7.
12. D. J. Hoffman, B. A. Rattner, G. A. Burton Jr.; J. Cairns Jr., *Handbook of Ecotoxicology*, Lewis Publishers, London, **1995**.
13. J. C. Chuang, S. A. Wise, S. Cao, J. Mumford, *Environ. Sci. and Technol.*, **1992**, 26, 999.

14. L. E. Smith, M. F. Denissenko, W. P. Bennet, H. Li, S. Amin, M. Tang, G. P. Pfeifer, *J. Natl. Cancer Inst.*, **2000**, 92, 803.

15. J. Israelachvili, *Intermolecular & Surface Forces*, 2nd Edition, Academic Press, **1992**.

16. F. L. Dickert, M. Tortschanoff, W. E. Bulst, G. Fischerauer, *Anal. Chem.*, **1999**, 71, 4559.

17. T. Takeuchi, J. Matsui, *Acta. Polym.*, **1996**, 47, 471.

18. S. A. Piletsky, E. V. Piletskaya, T. A. Sergeyeva, T. L. Panasyuk, A. V. El'skaya, *Sens. Actuators B.*, **1999**, 60, 216.

19. K. Uosaki, *Electrochemistry*, **1999**, 12, 1105.

20. R. G. Nuzzo, D. L. Allara, *J. Am. Soc.*, **1983**, 105,4481.

21. C. Bain, G. M. Whitesides, *J. Am. Soc.*, **1998**, 110, 6560.

22. S. Bruckenstein, M. Michalski, A. Fensore, Z. Li, Z, A. R. Hillman, *Anal. Chem.*, **1994**, 66, 1847.

23. C. J. Percival, S. Stanley, M. Galle, A. Braithwaite, M. I. Newton, G. McHale, W. Hayes, *Anal. Chem.*, **2001**, 73, 4225.

24. K. Haupt, K. Noworyta, W. Kutner, *Anal. Commun.*, **1999**, 36, 391.

25. E. Yilmaz, K. Mosbach, K. Haupt, *Anal. Commun.*, **1999**, 36, 167.

26. B. Jakoby, G. M. Ismail, M. P. Byfield, M. J. Vellekoop, *Sens. Actuators A.*, **1999**, 76, 93.

Appendix: ^{13}C-NMR-spectra

Appendix 1:

Figure 5.14: Product of step 1 of synthesis of ionic coating

The three peaks at ca. 77 ppm correspond to the solvent chloroform. The highest peak at ca. 43 ppm is assumed to correspond to the methyl-groups attached to the amino-group because they are virtually identical in starting material and product. The peak at ca. 195 ppm is assumed to correspond to the carbonyl group, the other seven peaks to the other carbon atoms in the starting product 3-dimethylampinopropylchloride (three CH_2-groups) and the step 1 product (three CH_2-groups, one CH_3-group). It can therefore be assumed that only a part of the starting substance converts to the product and that a part remains unchanged.

Figure 5.15: 9-Anthracenecarboxylic acid

Apart from the solvents and the reference peak at ca. 0 ppm the spectrum show the carbonyl group at ca. 169 ppm. The fourteen carbon-atoms with eight different electronic environments of the anthracene-group are assumed to correspond to the cluster of peaks around 125ppm. Seven individual peaks are distinguishable.

Figure 5.16: Product of step 1 of synthesis of covalent coating

Little difference can be seen between the NMR-spectra of 9-anthracenecarboxylic acid and the product of step 1. This may be because the replacement of the hydroxyl-group by the chlorine-atom has only little effect on the electronic environment of the carbon-atoms.

Figure 5.17: Product of step 2 of synthesis of covalent coating

This spectrum shows a group of peaks associated with the anthracene-group and a peak associated with the carbonyl group. Their positions are slightly different, when compared to figure 5.16, with ca. 127 ppm and 170 ppm respectively. The CH_2-group next to the hydroxyl-group shows a peak at ca. 61 ppm, the other four CH_2-groups can be associated with peaks between 23 ppm and 40 ppm, one of them hidden at the site of the peaks of the solvent DMSO at ca. 40 ppm. Each peak is accompanied by a second smaller one, which indicates that a different substance is present. This probably is unreacted 5-amino-1-pentanol and 9-anthracenecarbonylchloride of step 1.

Figure 5.18: Product of step 4 of synthesis of covalent coating

This spectrum is very similar to the one of the product of step 2 (Figure 5.17), only the accompanying second peaks are missing, because the rest of unreacted substance has been cleared away during steps 3 and 4. No peaks associated with the acetate-group could be identified. It therefore has to be assumed that the product of step 2 is still present and has not reacted to step 4.

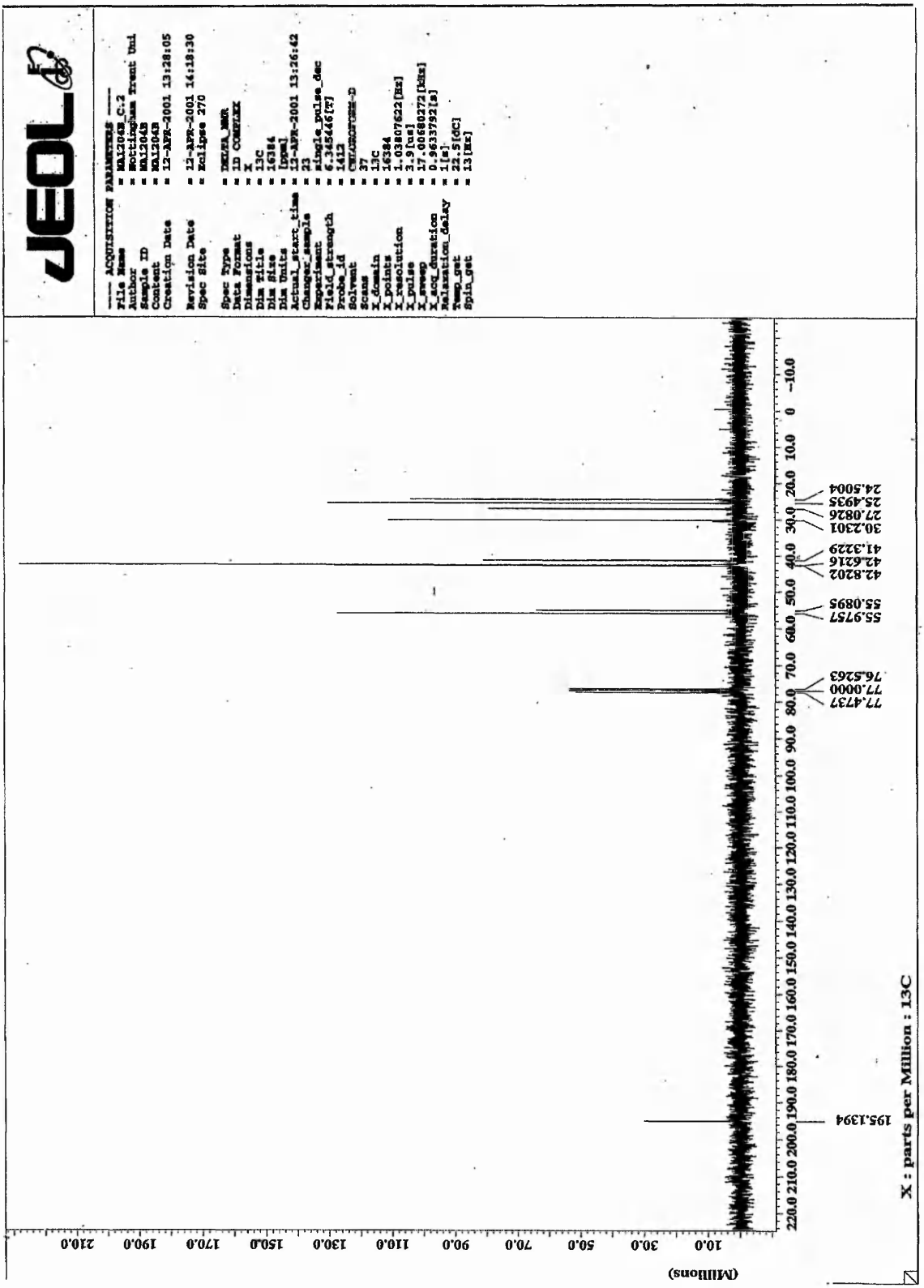

Figure 5.14: Product of step 1 of synthesis of ionic coating

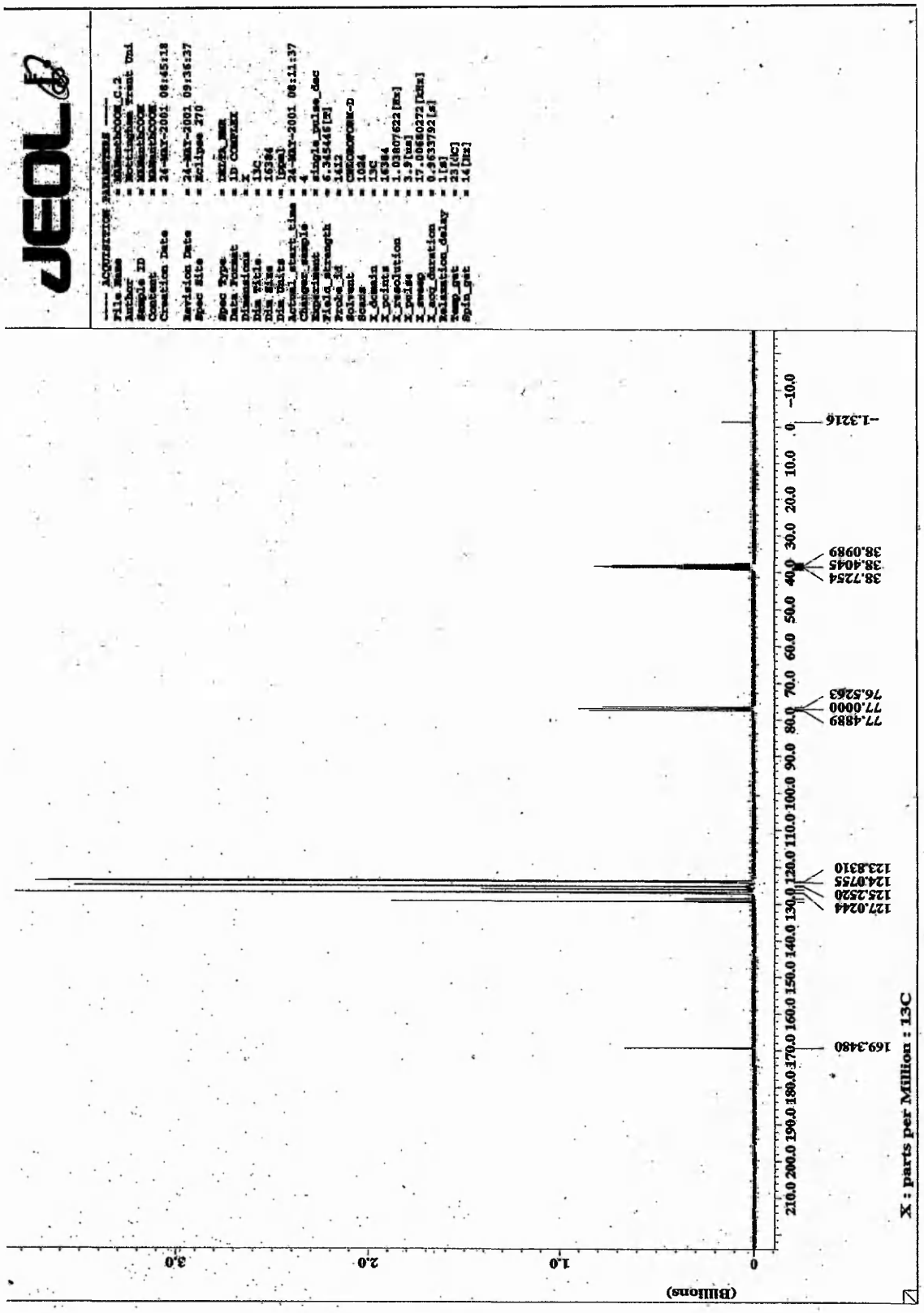

Figure 5.15: 9-Anthracenecarboxylic acid

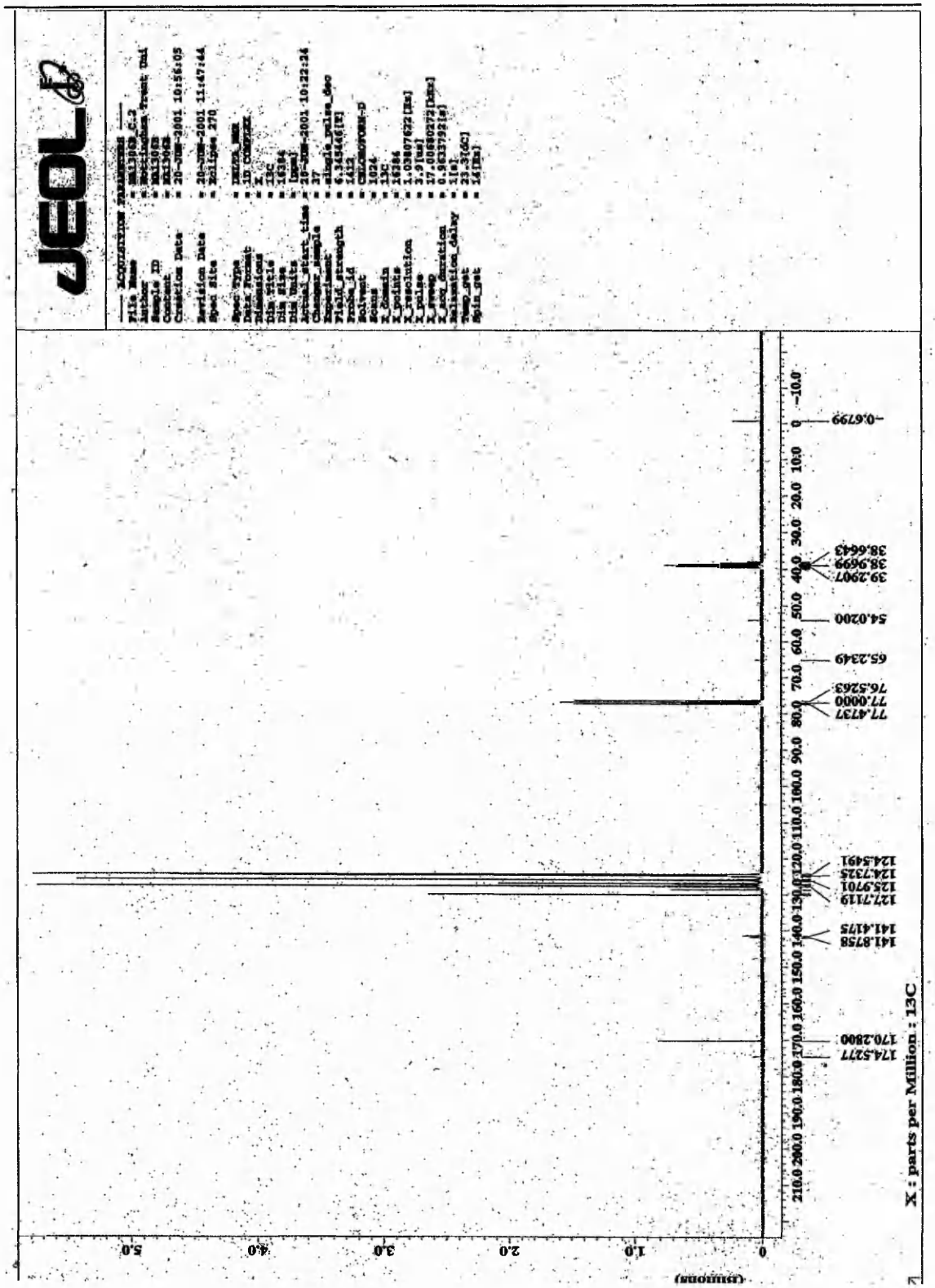

Figure 5.16: Product of step 1 of synthesis of covalent coating

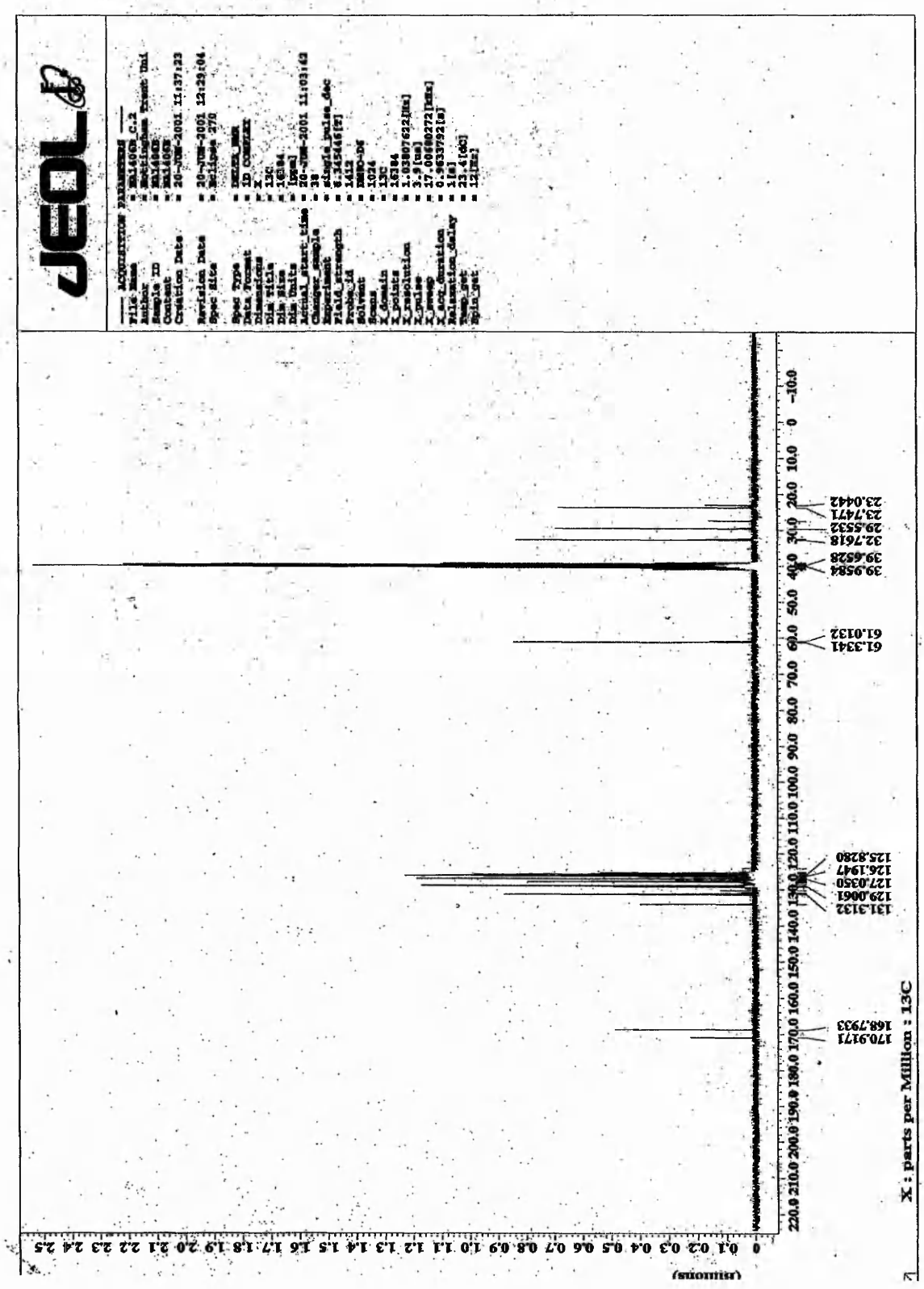

Figure 5.17: Product of step 2 of synthesis of covalent coating

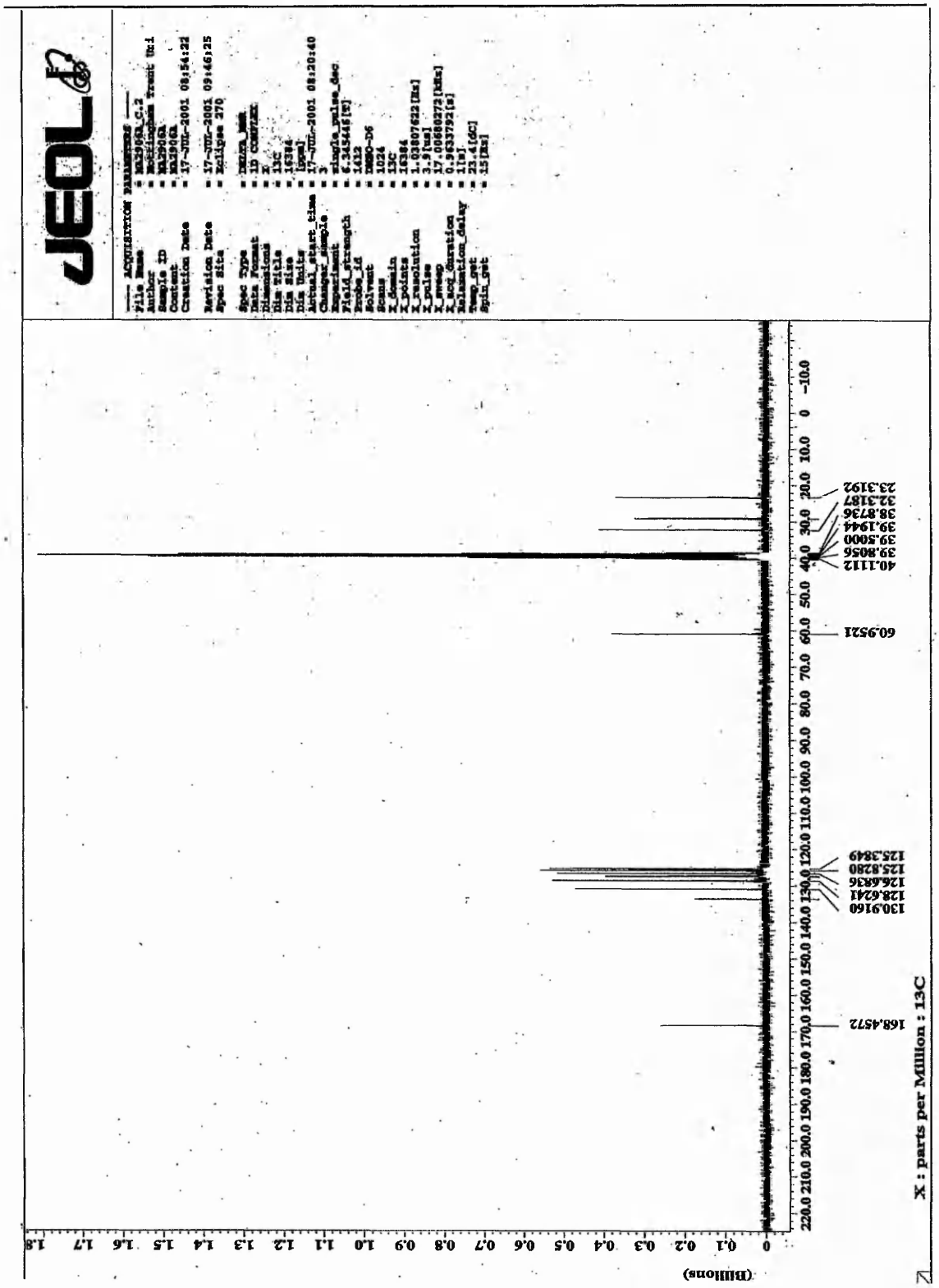

Figure 5.18: Product of step 4 of synthesis of covalent coating

Chapter six

Conclusions and future work

6.0 Conclusions and future work

The focus of this PhD thesis has been the development of recognition elements for sensors. The recognition elements have each been applied to QCMs functioning as sensor transducers. Three different approaches have been utilized to develop recognition elements, namely non-covalent imprinting, covalent imprinting and affinity type phase. In all cases the selectivity of the recognition element was has been quantified by piezoelectric microgravimetry by monitoring frequency changes as a function of analyte concentration.

6.1 Molecular imprinting

6.1.1 Non –Covalent Imprinting

Non-covalent imprinting for the production of recognition elements for the monoterpene L-menthol and the amino acid L-serine has been investigated. Ideally a sensor should respond only to the target analyte, this is not the case with the non-covalently prepared recognition elements. However the sensors do respond differently when challenged with analytes analogous to the template molecule.

In the case of L-menthol the MIP-QCM displayed no change in resonant frequency upon the addition of up to 2 ppm for all terpenes that did not contain an OH moiety. The inability for the MIP-QCM to detect limonene, menthone and citronellal is demonstrative of the role of the functional monomer in analyte rebinding; non-covalent

interactions between the carbonyl groups or double bonds of the analyte and the functional monomer (MAA) do not occur. However, the MIP-QCM exhibits a lower response towards D-menthol as a function of concentration. The enantiomeric selectivity coefficient of the MIP used in this work was 3.6. The ability of the recognition element to bind the target analyte over its enantiomeric isomer D-menthol is particularly interesting in view of the fact that the selectivity of the binding site is as a consequence of a single functional group-functional moiety interaction, the first reported enantioselective artificial receptor of this kind.

The non covalent approach was also used to produce a MIP-QCM for the detection of L-serine. As in the case of L-menthol the recognition element responded differently towards D-serine owing to the enantioselectivity of the binding sites. The observed enantiomeric selectivity coefficient of 4.8 compares interestingly with the 3.6 observed for L-menthol and is considered to be a function of the number of sites available for non-covalent interaction. This is further supported by the finding of Haupt *et al.*,[1] who produced an MIP capable of the enantiomeric discrimination of R and S propranolol, with an enantiomeric selectivity coefficient of 5.0. The L-menthol sensor has been reported in "*Analytical Chemistry*", appendix 6.1. The L-serine sensor has been submitted for "*Sensors and Actuators*", B., appendix 6.2.

6.12 Covalent Imprinting

Literature indicates that covalent imprinting produces a homogeneous population of binding sites within the imprinted polymer. In part this stability of the 'covalent

complex' is responsible for the high binding affinities (in comparison to non covalent MIPs) associated with covalently imprinted polymers with in excess of 75% of print sites being re-occupied.[2] Thus, covalent imprinting should produce a more selective recognition element. In order to assess this hypothesis a covalent MIP recognition element was developed for the detection of the steroid nandrolone.

Whilst responding preferentially to the target analyte the non-covalent MIP-QCM sensors also responded to analogous compounds. In contrast the covalently prepared MIP-QCM responded only to the target analyte. This result seems to suggest that covalent imprinting produces recognition sites that exhibit greater selectivity than that of the non-covalent approach. However, a direct comparison of the non-covalent and covalent approaches is complicated by the differences in the mode of attachment of MIP to QCM. The nandrolone sensor has been reported in "*The Analyst*", appendix 6.3.

6.2 Affinity phase

Molecular imprinting has been shown to be a powerful technique for producing selective recognition elements for sensors. Suitable target analytes must, however, possess functional groups capable of interacting non-covalently with the functional monomers. This requirement limits the general applicability of imprinting. In order to extend the capabilities of the use of QCMs for the detection of key analytes further techniques for the production of recognition elements need to be investigated. A third method based upon an affinity type phase, has been examined.

An organic monolayer attached to the surface of a gold electrode of a quartz crystal microbalance (QCM) via a covalent thiol-gold link complete with an ionically bound recognition element selective for anthrancene was produced. This study has employed the PAH derivative 9-anthracene carboxylic acid to function as the recognition element. Binding of anthracene via π-π-interaction has been observed as a frequency-shift in the QCM. The relative response of the sensor altered for different PAHs despite π-π-interaction being the sole communication between recognition element and analyte. Analogous to the imprinting approach the coated sensor should, ideally only respond to the target analyte. However the sensors do respond differently when challenged with analytes analogous to the template molecule. It can be seen that both the MIP described by Dickert *et al.*,[3] and our ionic coating display an affinity towards PAHs and that both approaches display some selectivity in terms of size and shape of PAH. The PAH work has been submitted for publication in Analytical Chemistry, appendix 6.4.

6.3 Future Work

The natural extension of this work would be to increase the sensitivity of the sensors to enable the detection of "realistic" concentrations likely to encountered in natural matrices, for example, urine.

6.3.1 Detection of Gas Phase Analytes

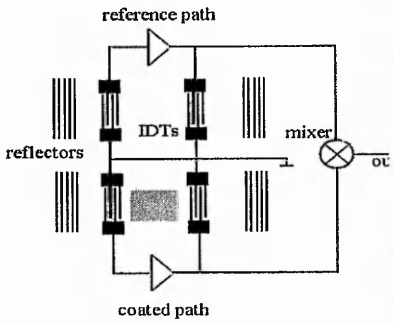

Since the first report by Suerbrey in 1959[4] of the relationship between frequency shift in a quartz resonator and the mass of substance deposited on the surface, the use of acoustic wave oscillators for sensing has become routine. The sensitivity to mass loading of acoustic wave resonators increases with the square of the resonant frequency. SAWs were first reported for sensing applications by Wohltjen and Dessy in 1979[5], expanding their ideas to cover most modern aspects of SAW sensors in 1984[6]. For quartz SAW delay line oscillators they reported that a frequency change Δf is obtained from an increase in mass per unit area (in grams), $\Delta m/A$, of $\Delta f = - 1.3 \times 10^6 f_o^2 (\Delta m/A)$, where f_o is the resonant frequency of the device. Hence, for a 97 MHz device of area 1 cm^2 this corresponds to a minimum detectable mass change of 80 pg. The incorporation of a surface coating that is specific to a particular gas species allows SAW devices to be used for a wide range of gas sensing applications. Problems of temperature drift are often compensated for by employing a second uncoated device along side the sensing device and the difference in oscillation frequency is then used as the measured parameter; a schematic diagram is shown in figure 6.1.

The effectiveness of SAW devices for field based atmospheric applications has been demonstrated by Ostanin *et al.*,[7] who have used the mass sensing principle to determine the dew point variation with altitude. In this work, the substrate temperature of a SAW device was varied until a large change in resonance was detected due to condensation of

water vapour on the substrate. Key advantages of the SAW approach were its low cost, low thermal mass, lightweight and low power consumption which were ideal for instrument deployment in a weather balloon.

The work presented in this thesis has shown that QCMs, coated with recognition elements, operating at 5 MHz, can be used to selectively detect the terpenes and PAHs in the liquid phase. It could be easily envisaged to extend this work to include the coating of SAW device for the detection of gas phase hydrocarbons.

6.3.2 Detection of Liquid Analytes

In Rayleigh-SAW devices, the surface normal component of oscillation leads to large attenuation in *aqueous* environments. However, other modes, such as, shear horizontally polarised surface acoustic waves (SH-SAWs), surface transverse waves (STWs), acoustic plate modes (APM)s and Love waves have only in-plane components of surface oscillation. Such modes are also excited using lithographically fabricated IDT's. In these modes, the motion of the liquid entrained by the oscillation is damped and decays within a penetration depth, δ, of the interface; in water for a 150 MHz oscillation $\delta \sim 40$ nm. At its simplest level, the frequency response of the acoustic shear wave oscillation measures the interfacial mass within the penetration depth. This concept provides a powerful technique for monitoring *solid-liquid* interfacial changes with applications including *in-situ* monitoring of electrochemically induced changes in films and chemical and biological sensing. Most recently, it has been realised that acoustic wave devices can respond to the viscoelastic properties of (acoustically thick)

films and that quantitative information on a polymer's high frequency shear moduli can be extracted.

Most polymer materials have a similar acoustic velocity and are suitable candidates for use as Love wave guiding layers. The optimum layer thickness to give maximum mass sensitivity depends on the frequency of operation with a typical value of 1 μm for operation at 100 MHz.

The technique that has been employed for producing the MIP films in this thesis has been to cast them by dispensing the polymerisation solution directly onto the surface of the substrate and then covering immediately with a microscope coverslip. Whilst this technique produces reproducible film properties, it does not allow accurate determination of final film thickness. A range of techniques could be investigated for producing controlled thickness of the MIP layers and in particular the modification of the viscosity of the polymer to allow deposition by spin coating; these will then be assessed for optimum Love wave guiding thickness. The implementation of a SAW, rather than a QCM, should provide a significantly increased sensitivity allowing the detection of key biological analytes in, for example, urine.

6.4 References

1. K. Haupt, K. Noworyta, W. Kutner, *Anal. Commun.*, **1999**, 36, 391.
2. B.Sellergren, *Anal. Chem.* 1994, **66**, 1578.
3. K. Haupt, K. Noworyta, W. Kutner, *Anal. Commun.*, **1999**, 36, 391.
4. B.Sellergren, *Anal. Chem.* 1994, **66**, 1578.
5. F. L. Dickert, O. Hayden, *Trends Anal. Chem.*, **1999**, 18, 192.
6. G. Z. Sauerbrey, *Zeitschrift Fur Physik* **155**, 206 (1959).
7. H. Wohltjen. K. Dessy, *Anal Chem.*, **51**, 1458 (1979).
8. H. Wohltjen, *Sensors and Actuators*, **5**, 307 (1984).
9. J. Ostanin, R. L. Jones, R. A. Cox, A surface acoustic wave frost-point hygrometer for measurements of stratospheric water vapour, Technical presentation. **2000.**

Appendix

Appendix 6.91

Anal. Chem. **2001**, *73*, 4225–4228

Molecular-Imprinted, Polymer-Coated Quartz Crystal Microbalances for the Detection of Terpenes

C. J. Percival,*,† S. Stanley,† M. Galle,† A. Braithwaite,† M. I. Newton,† G. McHale,† and W. Hayes‡

Department of Chemistry and Physics, The Nottingham Trent University, Nottingham NG11 8NS, U.K., and Department of Chemistry, University of Reading, Whiteknights, Reading RG6 6AD, U.K.

A piezoelectric sensor coated with an artificial biomimetic recognition element has been developed for the determination of L-menthol in the liquid phase. A highly specific noncovalently imprinted polymer (MIP) was cast in situ on to the surface of a gold-coated quartz crystal microbalance (QCM) electrode as a thin permeable film. Selective rebinding of the target analyte was observed as a frequency shift quantified by piezoelectric microgravimetry with the QCM. The detectability of L-menthol was 200 ppb with a response range of 0−1.0 ppm. The response of the MIP-QCM to a range of monoterpenes was investigated with the sensor binding menthol in favor of analogous compounds. The sensor was able to distinguish between the D- and L-enantiomers of menthol owing to the enantioselectivity of the imprinted sites. To our knowledge, this is the first report describing enantiomeric resolution within an MIP utilizing a single monomer-functional moiety interaction. It is envisaged that this technique could be employed to determine the concentration of terpenes in the atmosphere.

It is well known that HO_x (the sum of OH and HO_2) plays an important role in the formation of tropospheric ozone. Recently, Wennberg et al.,[1] noted that the levels of HO_x in the upper troposphere are greater than previously modeled using just the oxidation of CH_4. The presence of non-methane hydrocarbons (e.g., C_2H_6) and other oxygenated species (e.g., $CH_3C(O)CH_3$) in the upper troposphere is now believed to significantly augment the rate of formation of CH_3O_2, which can lead to an autocatalytic formation of HO_x.[1] There is an obvious need to measure oxygenated species in the atmosphere as a function of altitude. In this respect, terpenes represent a significant natural source of oxygenated hydrocarbons in the Earth's atmosphere that needs to be quantified.[2]

Generally, atmospheric hydrocarbons (such as terpenes) are collected and preconcentrated on a chromatographic-type stationary phase prior to analysis by, for example, ATD-GC/MS[3] in order to separate and identify the components of the sample. An alternative approach involves identifying key marker compounds that might be used to assess the pollution potential problem to model and calculate the flux of these terpenes. The development of analytical techniques for measuring the marker compounds would therefore greatly simplify the monitoring and analysis process, obviating the need for sample preconcentration and chromatographic separation. Such a technique involves the use of chemical sensors such as thickness shear mode devices coated with a recognition element.

Gravimetric sensors, such as the quartz crystal microbalance (QCM), are well suited as transducer elements for chemical sensors, being portable, rapid, and sensitive. For applications in chemical sensing, a recognition element is added to the acoustic wave device capable of selectively binding the analyte to the device surface. The response of these devices is then based on a decrease in their resonant frequency as mass is attached to the device or the recognition element.

The search for highly selective, low-cost, stable, and facile chemical sensors for a huge array of environmental industrial analytes has attracted increasing interest in recent years with greater and greater specificity being sought. Molecular recognition is a highly efficient and essential feature of biological systems in nature and as such has found application in biosensors.[4] Natural biological recognition systems, while highly selective, are of limited use, however, as a result of poor chemical and thermal stability, limited assay range, lifespan, and expense. The use of artificial recognition materials has been proposed as a means of addressing some of the limitations inherent in biosensors. One of the most promising examples of artificially generated recognition materials is the molecularly imprinted polymer (MIP). MIPs are highly cross-linked polymers which are inherently stable and capable of high selectivities approaching that of their natural counterparts. MIPs have become well established as a means of producing biomimetic recognition sites since first reported over 25 years ago[5,6] with the selectivity and binding affinities of MIP

* Corresponding author: (e-mail) carl.percival@ntu.ac.uk.
† The Nottingham Trent University.
‡ University of Reading.

(1) Wennberg, P. O.; Hanisco, T. F.; Jaegle, L.; Jacob, D. J.; Hintsa, E. J.; Lazendorf, E. J.; Anderson, J. G.; Gao, R.-S.; Keim, E. R.; Donnelly, S. G.; Del Negro, L. A.; Fahey, D. W.; Mckeen, S. A.; Salawitch, R. J.; Webster, C. R.; May, R. D.; Herman, R. L.; Proffitt, M. H.; Margitan, J. J.; Atlas, E. L.; Schauffler, S. M.; Flocke, F.; McElroy C. T.; Bui, T. P. *Science* **1999**, *279*, 49–53.
(2) Wayne, R. P. *Chemistry of Atmospheres*, 3rd ed.; Oxford University Press: Oxford, U.K., 2000; pp 349–360.
(3) Allen, M. R.; Braithwaite, A.; Hills, C. C. *Environ. Sci. Technol.* **1997**, *31*, 1054–1061.
(4) Sethi, R. S. *Biosens. Bioelectron.* **1994**, *9*, 3, 243–264.
(5) Wulff, G.; Sarhan, A. *Angew. Chem., Int. Ed. Engl.* **1972**, *11*, 341.

10.1021/ac0155198 CCC: $20.00
Published on Web 08/01/2001

being comparable to antibody–antigen interactions. Two distinct imprinting strategies have evolved: (i) covalent and (ii) noncovalent template polymerizations. Covalent imprinting involves the conversion of the template (or an analogue) into a polymerizable derivative that is then copolymerized with a suitable cross-linker to afford a resin that covalently incorporates the template. Covalent interactions between the template and the functional monomer have the advantage that the binding groups remain precisely oriented during elevated temperatures that are often a feature of the polymerization process. The stability of the covalent bond produces a homogeneous population of binding sites within the imprinted polymer. In part, this stability of the "covalent complex" is responsible for the high binding affinities (in comparison to noncovalent MIPs) associated with covalently imprinted polymers with in excess of 75% of print sites being reoccupied.[7] Covalent imprinting has been widely used to produce MIPs that are selective for a range of analytes including, caffeine in human urine and serum,[8] the plant hormone indoleacetic acid,[9] macromolecules,[10] the chiral benzodiazepine,[11] and the steroid cholesterol.[12] In contrast, noncovalent imprinting, which we have employed in our study, involves the self-assembly of suitable functional monomers around the template molecule. Following addition of a cross-linker, this assembly is then "fixed" by polymerization. Subsequent removal of the noncovalently bound template reveals vacant recognition sites that are specific to the target analyte in terms of their spatial and electronic environment. Noncovalent imprinting has inherent advantages over the covalent strategy as a consequence of the rapid and reversible nature of noncovalent interaction between the polymer and the template. Noncovalent imprinting has been reported with MIPs selective for many analytes including, (*R*)- and (*S*)-propanolol,[13] the odorant methylisoborneol,[14] steroids,[15] carboxylic acids,[16] nucleotide bases,[17] enantiomeric resolution of amino acids,[18,19] dyes,[20] and PAHs.[21]

Acoustic wave microsensors have been gaining widespread recognition as sensors for a wide range of analytes with an excellent review recently published.[22] The QCM is one such device and is ideally suited to the evaluation of molecular recognition by the measurement of in situ mass changes on the surface of the recognition material allowing rapid screening of a range of polymer systems without the need for prior calibration. MIPs as recognition elements for sensors are increasingly of interest[23,24] and MIP-QCM have started to appear in the literature; work in this area has been recently reviewed.[25] Initially these studies concentrated on analyte rebinding in gaseous media; however, recently, an MIP-QCM sensor has been reported for the detection of the chiral β-blocking drug (*S*)-propanolol in the liquid phase.[13] In this work, a piezoelectric sensor coated with a noncovalently imprinted recognition element for the monoterpene L-menthol is presented.

EXPERIMENTAL SECTION

Reagents. All terpenes and the functional monomer methacrylic acid (MAA) were purchased from Lancaster synthesis. The cross-linkers ethylene glycol dimethacrylate (EDMA) and trimethylolpropane trimethacrylate (TRIM) were supplied by Aldrich Chemicals. The initiator 2,2′-azobis(2-methylpropionitrile) was supplied by Acros Chemicals. All the solvents were of analytical grade and all reagents were used as supplied.

Quartz Crystal Microbalance. The quartz crystal microbalance was produced using unpolished AT-cut, 25-mm-diameter, plano–plano quartz crystals with Cr/Au contacts, operating at a fundamental resonant frequency of 5 MHz and with an electrode area of ~133 mm^2 (Maxtek model 149211-2). The crystals were mounted in a Maxtek CHC-100 crystal holder, and the measurement system consisted of a Maxtek PLO10 phased locked oscillator and a HP53132A universal counter interfaced to a microcomputer.

Prior to the application of the polymer coating to the electrode area, the crystals were prepared using Pirannha etch solution (1:3 30% v/v H_2O_2/concentrated H_2SO_4). The crystals were immersed in Pirannha etch solution for 10 min, then rinsed with deionized water and ethanol, and dried overnight.

Imprinted Polymer Films. Copolymers of poly(EDMA-*co*-MAA) were used for the preparation of the molecular imprinted polymers. In a typical MIP synthesis, the polymerization mixture consisted of L-menthol (1.5 mmol), methacrylic acid (6.0 mmmol), EDMA (10–40 mmmol), and chloroform (74 mmol) with AIBN (0.19 mmol) as the polymerization initiator. The polymerization mixture was degassed by sonication for 5 min and then cooled on ice for 5 min prior to use. The quartz crystals were coated with polymer using the sandwich casting method described by Kugimiya and Takeuchi.[9] The polymer film was cast by dispensing 2 μL of the polymerization solution directly onto the surface of the Cr/Au electrode and then covered immediately with a 13-mm-diameter microscope coverslip. Prior to use, the cover slip was treated with Sigma Cote (Sigma, St. Louis, MO) to reduce the adhesion of the MIP to the cover slip. Polymerization was initiated by UV light radiation using a 125-W medium-pressure mercury lamp (Photochemical reactors 3012) under an inert atmosphere for 30 min. Control samples of nonimprinted polymers were synthesized in a similar manner, without the addition of the L-menthol template to the polymerization solution. The quartz crystals were washed for 10 min in ethanol and dried prior to use.

(6) . Wulff, G. *Angew. Chem., Int. Ed. Engl.* **1995**, *34*, 1812–1832.
(7) Sellergren, B. *Anal. Chem.* **1994**, *66*, 1578–1582.
(8) Liang, C.; Peng, H.; Bao, X.; Nie, L.; Yao, S. *Analyst* **1999**, *124*, 1781–1785.
(9) Kugimiya, A.; Takeuchi, T. *Electroanalysis* **1999**, *11*, 1158–1160.
(10) Shea, K. J.; Thompson, E. A.; Pandey, S. D.; Beauchamp, P. S. *J. Am. Chem. Soc.* **1980**, *102*, 3149–3155.
(11) Hart, B. R.; Rush, D. J.; Shea, K. J. *J. Am. Chem. Soc.* **2000**, *122*, 460–465.
(12) Whitcombe, M. J.; Rodriguez, M. E.; Villar, P.; Vulfson, E. N. *J. Am. Chem. Soc.* **1995**, *117*, 7105–7111.
(13) Haupt, K.; Noworyta, K.; Kutner, W. *Anal. Commun.* **1999**, *36*, 391–393.
(14) Ji, H. S.; McNiven, S.; Ikebukuro, K.; Karube, I. *Anal. Chim. Acta* **1999**, *390*, 93–100.
(15) Ramstrom, O.; Ye, L.; Krook, M.; Mosbach, K. *Anal. Commun.* **1998**, *35*, 9–11.
(16) Ramstrom, O.; Andersson, L. I.; Mosbach, K. *J. Org. Chem.* **1993**, *58*, 7562–7564.
(17) Spivak, D. A.; Shea, K. J. *Macromoleculues* **1998**, *31*, 2160–2165.
(18) Andersson, L. I.; Mosbach, K. *J. Chromatogr.* **1990**, *516*, 313–322.
(19) Andersson, L. I.; O'Shanessy, D. J.; Mosbach, K. *J. Chromatogr.* **1990**, *513*, 167–179.
(20) Glad, M.; Norrlow, O.; Sellergren, B.; Seigbahn, N.; Mosbach, K. *J. Chromatogr.* **1985**, *347*, 11–23.
(21) Dickert, F. L.; Tortschanoff, M.; Bulst, W. E.; Fischerauer, G. *Anal. Chem.* **1999**, *71*, 4559–4563.
(22) Grate, J. W. *Chem. Rev.* **2000**, *100*, 2627–2648.
(23) Dickert, F. L.; Hayden, O. *Trends Anal. Chem.* **1999**, *18*, 192–199.
(24) Haupt, K.; Mosbach, K. *Chem. Rev.* **2000**, *100*, 2495–2504.
(25) Kriz, D.; Ramstrom, O.; Mosbach, K. *Anal. Chem.* **1997**, *69*, 345A–349A.

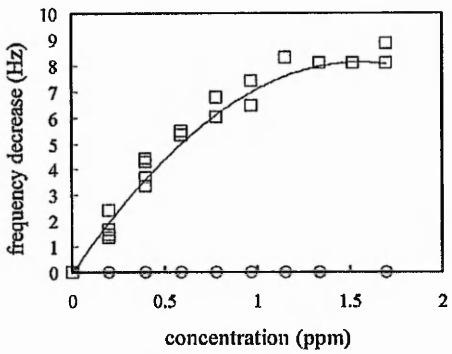

Figure 1. Response of the QCM sensors to L-menthol for the MIP coated (squares) and nonimprinted polymer coated (circles). Using five repeat runs and the MIP film thickness was 2 μm.

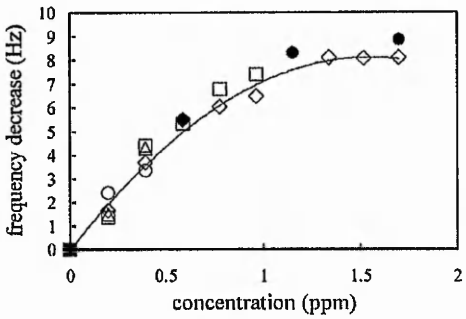

Figure 2. Resonant frequency change of the QCM with L-menthol TRIM cross-linked MIP coating 1 (diamonds); EDMA cross-linked MIP coating NUMBER 1 run 1 (squares); EDMA cross-linked MIP coating 1 run 2 (circles); EDMA cross-linked MIP coating 2 (solid circles), and TRIM cross-linked MIP coating 2 (triangles).

Evaluation of Sensor Response. Solutions containing known amounts of the analyte were prepared in ethanol. The coated quartz crystals were placed into a beaker of ethanol until a stable response was obtained, and then 9 mL of analyte solution was added to the stirred bulk ethanol solution via successive 1-mL aliquots. The frequency was recorded until a stable response was obtained. After each 9-mL addition of analyte, the coated quartz crystal was soaked in the porogenic solvent for 10 min and the experiment was repeated.

RESULTS AND DISCUSSION

Effect of Cross-Linker. The effect of cross-linker concentration in the MIP was investigated by variation of the amount of cross linker employed in the polymerization mixture. Cross-linker concentrations were varied from 10 to 40 mmol (from 55 to 83%) and of these, the 40-mmol cross-linked copolymer proved unsuccessful. On each attempt, the 40-mmol cross-linked MIP displayed considerable contraction and separated from the electrode. Yilmaz et al.[26] reported similar results and suggested that high cross-linker concentrations can lead to a rigid polymer film with significantly reduced adherence to the electrode surface. The 10- and 20-mmol cross-linked EDMA copolymer displayed no change in resonant frequency upon the addition of up to 2 ppm L-menthol. However, the lack of frequency shift of the lower concentrations of cross-linker indicates that the increased flexibility of the polymer results in the relaxation of the imprinted sites so that no response is observed. The 30-mmol cross-linked EDMA copolymer displayed a repeatable shift in resonant frequency on addition of L-menthol, which is shown in Figure 1 (squares). The 30-mmol copolymer is rigid enough to selectively rebind the template, yet retains suitable adherence to the electrode.

In light of the studies upon the effect of cross-linker concentration, control experiments were performed to assess the response of quartz crystals coated with the nonimprinted "blank" 30-mmol cross-linked EDMA polymer toward L-menthol. These data are also shown in Figure 1 (circles), and it can be seen that no change in resonant frequency was observed upon addition of up to 2 ppm of analyte. This result indicates that binding of the analyte to the "blank" was insignificant.

It can be seen from Figure 1 that, although the data for the imprinted polymer-coated quartz crystals falls on a repeatable curve, some scatter in the data is observed. This may be attributed to the drift in resonant frequency that is caused by changes in the environmental conditions such as temperature. On the time scale of the experiment, the change in frequency caused by environmental conditions could be greater than that caused by the mass loading of the quartz crystal. To overcome this difficulty, the frequencies of two quartz crystals immersed in the ethanol solution, one crystal coated with the MIP and one crystal coated with the nonimprinted polymer, were measured simultaneously following the DQCM technique of Bruckenstein et al.[27] The resultant difference in frequency between the two crystals can be used to assess the response of the crystal to mass loading of the analyte, as the nonimprinted polymer displayed no change in resonant frequency with mass loading; all further experiments were performed in this manner.

Response of the Sensors to Mass Loading of L-Menthol. The change in resonant frequency of the MIP quartz crystal as a function of L-menthol concentration is shown in Figure 2. There is an initial linear decrease in frequency corresponding to increase in menthol concentration up to ~0.8 ppm with a gradient in the range $S_1 = -8.9 \pm 0.6$ Hz ppm^{-1}, which reaches saturation at concentrations exceeding 1.1 ppm. Similar sorption isotherms have been observed by Haupt et al.[13] for the binding of (*S*)-propanolol to a molecularly imprinted polymer and such sorption isotherms are expected for polymers that contain immobilized binding sites, such as found in MIPs. The data presented in Figure 2 show the response for five different quartz crystals each with a MIP coating produced in the same way. The agreement suggests that our methodology for coating the quartz crystals with MIP is reproducible not only between runs but also between different coatings.

The affinity of the MIP polymers toward L-menthol can be evaluated using a one-site Langmuir-type binding isotherm anaylsis.[26]

$$Kc\frac{\Delta f}{\Delta f_\infty} + \frac{\Delta f}{\Delta f_\infty} = Kc$$

where K is the apparent dissociation constant, c is the free analyte

(26) Yilmaz, E.; Mosbach, K.; Haupt, K. *Anal. Commun.* **1999**, *36*, 167–170.

(27) Bruckenstein, S.; Michalski, M.; Fensore, A.; Li, Z.; Hillman, A. R. *Anal. Chem.* **1994**, *66*, 1847–1852.

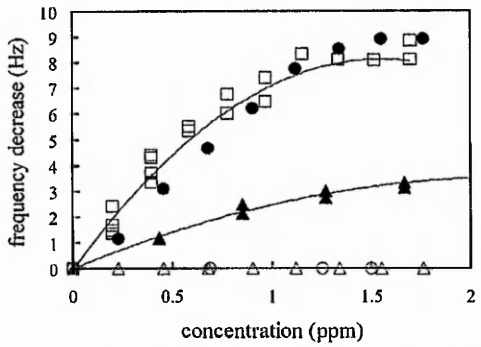

Figure 3. Range of monoterpene analogues that the selectivity of the MIP-coated quartz crystals were tested toward L-menthol (squares), D-menthol (solid triangles), citronellol (solid circles), citronellal (triangles), and menthone (circles).

concentration at equilibrium, Δf is the frequency change, and Δf_∞ is the frequency corresponding to complete coverage. Although this does not reflect the real situation in the polymer, it allows for a comparison of binding between polymers. Using the data shown in Figure 2, the calculated apparent dissociation $K = 4.5 \pm 0.5$ μM. The calculated apparent dissociation constants are similar to those found in MIPs.[28]

Selectivity of Sensors. A number of other terpenes (limonene, menthone, citronellol, citronellal, D-menthol) were examined in order to investigate the selectivity of the MIP. No change in resonant frequency was observed upon the addition of up to 2 ppm for all terpenes that did not contain an OH moiety, as shown in Figure 3. The inability of the MIP-QCM to detect limonene, menthone, and citronellal is demonstrative of the role of the functional monomer in analyte rebinding; noncovalent interactions between the carbonyl groups or double bonds of the analyte and the functional monomer (MAA) do not occur.

The MIP used also responds to D-menthol as shown in Figure 3 (solid triangles). Analogous to L-menthol, there is an initial linear decrease in frequency corresponding to increase an increase in D-menthol concentration up to ~0.8 ppm with a gradient in the range $S_2 = -2.4 \pm 0.2$ Hz ppm^{-1}. The enantioselectivity of the MIP coating can be assessed by evaluating the ratio of the initial linear change in frequency of L-menthol (squares) to D-menthol (solid triangles) S_1/S_2. Hence, the enantiomeric selectivity coefficient of the MIP used in this work was 3.6. Haupt et al.[13] also reported enantiomeric discrimination between (*R*)- and (*S*)-propanolol using a noncovalent imprint of (*S*)-propanolol with an enantiomeric selectivity coefficient of 5. The lower selectivity coefficient of our MIP is considered to be a function of the number of sites available for noncovalent interaction in menthol compared with propanolol. The lower selectivity of our MIP compared with that of (*S*)-propanolol is explained by the reduced number of binding sites within the menthol MIP. The L-menthol MIP has one point of interaction with the OH functional group. The imprinting process produces a cavity that is selective in terms of size and shape as well as complimentary functionality. Therefore, a lower response of the quartz crystal toward D-menthol was observed as a result of the incorrect spatial orientation of the receptor sites for the OH group of D-menthol within the cavities. This is further supported by the observed change of resonant frequency for citronellol, shown by the solid circles in Figure 3. Citronellol shares the same functional group as menthol, but the overall size of the molecule is smaller and exhibits similar binding characteristics within the cavity. As a result, the changes in resonant frequency of the MIP quartz crystal as a function of citronellol concentration are similar to that of L-menthol. The response of the imprinted sensors to the template, D-menthol, and citronellol but not to limonene, menthone, or citronellal demonstrates the molecular imprint effect. However, the enantioselectivity of the polymer matrix as a consequence of trapped menthol cannot be excluded. The importance of both the functional monomer in analyte rebinding and the observed shape selectivity support enantioselectivity of the binding site as the most probable reason for the observed chiral discrimination.

CONCLUSION

In this article, we have shown that MIP-coated quartz crystal sensors can be used to selectively detect the monoterpene menthol in the liquid phase with a sensitivity of 200 ppb. The natural extension of this work is to enhance the sensitivity of the sensors to enable the gas-phase detection of terpenes; this may be achieved in two ways. First, it is may be possible to increase the concentration of binding sites in the MIP by increasing the ratio of the functional monomer to template and, second, by increasing the mass sensitivity of the acoustic device. This may be achieved by increasing the resonant frequency of the sensor as the sensor response to mass loading is proportional to the square of the operating frequency. The upper limit for quartz crystal microbalances operating at the fundamental frequency is ~10 MHz; the higher the frequency, the thinner the crystal. Alternatively, surface acoustic wave devices may be employed that will extend the range of operating frequencies to over 1 GHz.[14,29] The implementation of these enhancements should provide an increased sensitivity, allowing the detection of atmospheric levels of gaseous terpenes.

ACKNOWLEDGMENT

The authors gratefully acknowledge the financial support of The Royal Society research grant 574006.G503/21268/SM.

Received for review May 11, 2001. Accepted July 3, 2001.

AC0155198

(28) Vlatakis, G.; Andersson, L. I.; Müller, R.; Mosbach, K. *Nature* **1993**, *364*, 645–647.

(29) Jakoby, B.; Ismail, G. M.; Byfield, M. P.; Vellekoop, M. J. *Sens. Actuators A* **1999**, *76*, 93–97.

Appendix 6.92

Enantioselective detection of L- Serine

S. Stanley[a], C. J. Percival[a*], T. Morel[a], A. Braithwaite[a], M. I. Newton[a], G. McHale[a] and W. Hayes[b]

[a] Department of Chemistry and Physics, The Nottingham Trent University, Clifton Lane, Nottingham NG11 8NS, UK

[b] Department of Chemistry, University of Reading, Whiteknights, Reading RG6 6AD, UK

corresponding author: e-mail carl.percival@ntu.ac.uk

telephone +44 115 8483522

fax +44 115 8486636

Abstract

An acoustic wave sensor coated with an artificial biomimetic recognition element has been developed to selectively detect the amino acid L-serine. A highly specific non-covalently imprinted polymer was cast on one electrode of a quartz crystal microbalance (QCM) as a thin permeable film. Selective rebinding of the L-serine was observed as a frequency shift in the QCM with a detection limit of 2 ppb and for concentrations up to 0.4 ppm. The sensor binding is shown to be capable of discrimination between L- and D-stereoisomers of serine as a result of the enantioselectivity of the imprinted binding sites.

Keywords: L-serine; molecular imprinted polymers (MIP); enantioselectivity; Quartz crystal microbalance (QCM); acoustic wave

1. Introduction

The synthesis of enantiomerically pure organic compounds presents a major challenge to industry. The pharmacological and biological activities of chiral organic compounds is well known to be dependent upon their specific stereochemistry. Thus there is a clear need for sensors capable of enantiomeric discrimination. In peptide and protein synthesis enantiomerically pure compounds are essential and in the case of naturally occurring peptidic species, the majority of the amino acids building blocks possess the L-configuration. In asymmetric synthesis, racemic mixtures starting materials must be resolved prior to use or one enantiomer may be consumed in a preferential manner *via* enantioselective synthesis. Both of these approaches require significant methodological development, either involving the preparation of diastereoisomers that can then be separated by tedious fractional crystallization or the construction of highly selective chiral auxiliaries. An alternative approach to such traditional methods of chiral discrimination is the use of molecular imprinted polymers (MIP) [1]. Chiral recognition sites within MIP can be synthesised in a relatively direct manner and therefore the potential exists to remove enantiomers in a quantitative fashion from a racemic mixture. In addition to the difficulties in separating enantiomers, conventional identification of chiral substrates has involved expensive and time consuming derivatisation methods or optical studies such as circular dichroism. The development of an analytical technique for the real time analysis and quantification of one enantiomeric species in a racemic mixture would greatly simplify the monitoring and analysis process obviating the need for sample preconcentration and chromatographic separation.

MIPs have become well established as a means of producing biomimetic recognition sites since first reported over 25 years ago [2,3] with the selectivity and binding affinities of MIP being comparable to antibody-antigen interactions. Two distinct imprinting strategies have evolved: covalent and non-covalent template polymerisations. Covalent imprinting involves the conversion of the template (or an analogue) into a polymerisable derivative that is then copolymerised with a suitable cross-linker to afford a resin that covalently incorporates the template. Covalent interactions between the template and the functional monomer have the advantage that the binding groups remain precisely orientated during elevated temperatures that are often a feature of the polymerisation process. The stability of the covalent bond produces a homogeneous population of binding sites within the imprinted polymer. In part this stability of the 'covalent complex' is responsible for the high binding affinities (in comparison to non covalent MIP) associated with covalently imprinted polymers with in excess of 75% of print sites being re-occupied [4]. Covalent imprinting has been widely used to produce MIPs that are selective for a range of analytes including caffeine in human urine and serum [5,6], the plant hormone indole acetic acid [7], macromolecules [8], benzodiazepine [9] and the steroid cholesterol [10]. In contrast, the conceptually simpler non-covalent approach involves the self-assembly of suitable functional monomers around the template molecule. Following addition of a cross-linker this assembly is then 'fixed' by polymerisation. Subsequent removal of the non-covalently bound template reveals vacant recognition sites that are specific to the target analyte in terms of their spatial and electronic environment. Non-covalent imprinting has inherent advantages over the covalent strategy as a consequence of the rapid and reversible nature of non-

covalent interaction between the polymer and the template. Non-covalent imprinting has been reported with MIPs selective for many analytes including, R- and S-propranolol [11], the odorant methylisoborneol [12], steroids [13], carboxylic acids [14], nucleotide bases [15], enantiomeric resolution of amino acids [16,17], dyes [18] and PAHs [19]. In this work a piezoelectric sensor coated with a non-covalently imprinted recognition element for the amino acid L-Serine is presented. The enantioselectivity of the imprinted binding sites is investigated for discrimination between L- and D-stereoisomers of serine.

2. Experimental

2.1 Reagents

All amino acids and the functional monomer methacrylic acid (MAA) were purchased from Lancaster Synthesis. The cross-linker, ethylene glycol dimethacrylate (EDMA) was supplied by Aldrich Chemicals. The initiator 2,2'-Azobis(2-methylpropionitrile) was supplied by Acros Chemicals. All the solvents were of analytical grade and all reagents were used as supplied.

2.2 Quartz Crystal Microbalance

The quartz crystal microbalance consisted of a Maxtek PLO10 phased locked oscillator and an Agilent HP53132A universal counter interfaced to a microcomputer. The quartz crystals used were unpolished AT-cut, 25 mm diameter, with Cr/Au contacts, operating at a fundamental resonant frequency of 5 MHz. The electrode area was approximately 133 mm^2 (Maxtek model No. 149211-2) and the crystals were mounted in a Maxtek CHC-100 crystal holder. Prior to the application of the polymer coating to the electrode area, the

crystals were prepared using Pirannha etch solution (1:3 30% v/v H_2O_2: conc. H_2SO_4). The crystals were immersed in Pirannha etch solution for ten minutes, then rinsed with deionised water and ethanol and dried overnight.

2.3 Imprinted polymer films

Co-polymers of poly (EDMA-co-MAA) were used for the preparation of the molecular imprinted polymers. In a typical MIP synthesis, the polymerisation mixture consisted of L-Serine (1.5 mmol), methacrylic acid (6.0 mmol), EDMA (30 mmol), 90:10 cyclohexanol:dodecanol (74 mmol) with AIBN (0.19 mmol) as the polymerisation initiator. The polymerisation mixture was degassed by sonication for 5 minutes and then cooled on ice for 5 minutes prior to use. The quartz crystals were coated as described by Kugimiya and Takeuchi [7]. With a polymer film being cast by dispensing 2 µl of the polymerisation solution directly onto the surface of the Cr/Au electrode and then covered immediately with a 13 mm diameter microscope coverslip. Prior to use the coverslip was treated with Sigma cote (Sigma, St. Louis, MO) to reduce the adhesion of the MIP to the coverslip. Polymerisation was initiated by UV light radiation using a 125 W medium pressure mercury lamp (Photochemical Reactors 3012) under an inert atmosphere for 30 minutes. Control samples of non-imprinted polymers were synthesized in a similar manner, without the addition of the L-Serine template to the polymerisation solution. The quartz crystals were washed for 10 minutes in ethanol and dried prior to use.

2.4 Cross linker

Previously reported work evaluating the effect of cross linker concentration in the MIP was employed to select the optimum imprinting conditions [20]. Cross linker concentrations were varied from 10 and 40 mmol (from 55 to 83 %) and of these, the 10, 20 and 40 mmol cross linked co-polymers proved unsuccessful. The 30 mmol cross-linked EDMA co-polymer displayed a repeatable shift in resonant frequency on addition of L-Serine and was rigid enough to selectively rebind the template whilst adhering to the QCM. The 40 mmol cross-linked MIP displayed considerable contraction and separated from the electrode. These findings were in agreement with previously reported results [21] and suggest that high cross linker concentrations can lead to a rigid polymer film with significantly reduced adherence to the electrode surface. As a result 30 mmol cross-linked polymers were used throughout this study.

2.5 Evaluation of sensor response

Solutions containing known amounts of the analyte were prepared in 90:10 cyclohexanol:dodecanol. The coated quartz crystals were placed into a beaker of water until a stable response was obtained, then 6 ml of analyte solution was added to the stirred bulk ethanol solution via successive 1 ml aliquots. The frequency was recorded until a stable response was obtained. After each 6 ml addition of analyte the coated quartz crystal was soaked in the porogenic solvent for 10 minutes and the experiment was repeated. Control experiments were performed to assess the response of quartz crystals coated with non-imprinted 'blank' polymers; no detectable change in resonant frequency

was observed upon the addition of up to 2 ppm of analyte. On the timescale of the experiment, the change in frequency caused by environmental conditions could be greater than that caused by the mass loading of the quartz crystal. In order to overcome this difficulty the frequencies of two quartz crystals immersed in the ethanol solution, one crystal coated with the MIP and one crystal coated with the non imprinted polymer, were measured simultaneously following the DQCM technique of Bruckenstein *et al.* [22]. The resultant difference in frequency between the two crystals can be used to assess the response of the crystal to mass loading of the analyte, as the non-imprinted polymer displayed no change in resonant frequency with mass loading; all further experiments were performed in this manner.

3. Results and Discussion

The change in resonant frequency of the MIP quartz crystal as a function of L-Serine concentration is shown in Figure 1. There is a linear decrease in frequency corresponding to increase in L-Serine concentration up to about 0.2ppm with a gradient in the range S_1 = 482 ± 16 Hz ppm^{-1}, which reaches saturation at concentrations exceeding 0.5 ppm. These sorption isotherms are expected for polymers that contain immobilised binding sites, such as those found within MIP and are consistent with those reported by Haupt *et al.* [11] for the binding of S-propanolol. The data presented in Figure 1 shows the response for 4 different quartz crystals each with a MIP coating produced in the same way. The agreement suggests that our methodology for coating the quartz crystals with MIP is not only reproducible between runs but also between different coatings. The affinity of the MIP polymers towards L-Serine can be evaluated using a one site Langmuir-type binding

isotherm analysis [23] $Kc(\Delta f/\Delta f_\infty)+(\Delta f/\Delta f_\infty)=Kc$ where K is the apparent dissociation constant, c is the free analyte concentration at equilibrium Δf is the frequency change and Δf_∞ is the frequency corresponding to complete coverage. Although this does not reflect the real situation in the polymer it allows for a comparison of binding between polymers. Using the data shown in Figure 1, the calculated apparent dissociation, K was 35.45 μM. The calculated apparent dissociation constant is similar to those previously reported for MIPs [24].

The MIP used also responded to D-Serine as shown by the + symbols in Figure 1. Analogous to L-Serine, there is an initial linear decrease in frequency corresponding to increase an in D-Serine concentration up to about 0.4 ppm with a gradient in the range S_2= 99.71 ± 7.10 Hz ppm^{-1}. The enantioselectivity of the MIP coating can be assessed by evaluating the ratio of the initial linear change in frequency of L-Serine to D-Serine S_1/S_2. Hence, the enantiomeric selectivity coefficient of the MIP used in this work was 4.8. Recently our laboratory [20] has reported enantiomeric discrimination between L- and D-menthol using a non-covalent imprint of L-menthol with an enantiomeric selectivity coefficient of 3.6. The increased selectivity coefficient of the L-serine MIP is considered to be a function of the number of sites available for non-covalent interaction in L-serine compared to that of L-menthol. Haupt *et al.* [11] have also reported report enantiomeric discrimination between R- and S-propranolol using a non-covalent imprint of S-propranolol with an the enantiomeric selectivity coefficient of 5. Both L-serine and S-propranolol have three possible sites of interaction and show similar enatioselectivity, whereas L-Menthol has only one possible site for interaction and shows a much smaller enantioselectivity. The imprinting process produces a cavity that is selective in terms of

size and shape as well as complimentary functionality. Therefore, a lower response of the quartz crystal towards D-Serine was observed as a result of the incorrect spatial orientation of the receptor sites for the amine, alcohol and carboxylic acid residues of D-Serine within the cavities.

4. Conclusion

In this work we have demonstrated that an MIP coated quartz crystal sensor can be used to detect the amino acid L-Serine in the liquid phase up to 0.4 ppm and with a sensitivity of 2 ppb. The enantioselectivity of the MIP coating has also been investigated for L-Serine and D-Serine giving an enantiomeric selectivity coefficient of 4.8. Further enhancement of the sensitivity of the sensors would enable the chiral discrimination of ever-smaller quantities of chiral actives. This may be achieved by increasing the concentration of binding sites in the MIP by increasing the ratio of the functional monomer to template or alternatively by increasing the mass sensitivity of the acoustic device; the latter by increasing the resonant frequency of the sensor. The upper limit for quartz crystal microbalances operating at the fundamental frequency is around 10 MHz, however, surface acoustic wave devices (SAWs) may be employed that would extend the range of operating frequency by more than an order of magnitude [12,25].

References

[1] K. Haupt, Molecularly imprinted polymers in analytical chemistry, *Analyst* **126** (2001) 747-756.

[2] G. Wulff and A. Sarhan, Use of polymers with enzyme-analogous structures for the resolution of racemates, *Angew. Chem. Int. Ed. Engl.*, **11** (1972) 341-346.

[3] G. Wulff, Molecular Imprinting in Cross-Linked Materials with the Aid of Molecular Templates - A Way towards Artificial Antibodies *Angew. Chem. Int. Ed. Engl.*, **34** (1995) 1812-1832.

[4] B. Sellergren, Direct Drug Determination by Selective Sample Enrichment on an Imprinted Polymer, *Anal. Chem.*, **66** (1994) 1578-1582.

[5] G. Wulff, A. Sarhan and K. Zabrocki, Enzyme-Analogue Built Polymers and Their Use for the Resolution of Racemates, *Tetrahedron Lett.*, **44** (1973) 4329-4332.

[6] C. Liang; H. Peng, X. Bao, L. Nie and S. Yao, Study of a Molecular Imprinting Polymer Coated BAW Bio-Mimic Sensor and Its Application to the Determination of Caffeine in Human Serum and Urine, *Analyst,* **124** (1999) 1781-1785.

[7] A. Kugimiya and T. Takeuchi, Molecularly Imprinted Polymer-Coated Quartz Crystal Microbalance for Detection of Biological Hormone, *Electroanalysis*, **11** (1999) 1158-1160.

[8] K. J. Shea; E. A. Thompson, S.D. Pandey and P. S. Beauchamp, Template Synthesis of Macromolecules. Synthesis and Chemistry of Functionalized Macroporous Polydivinylbenzene, *J. Am. Chem. Soc.* **102** (1980) 3149-3155.

[9] B. R. Hart, D. J. Rush and K. J. Shea, Discrimination Between Enantiomers of Structurally Related Molecules: Separation of Benzodiazepines by Molecularly Imprinted Polymers. *J. Am. Chem. Soc.* **122** (2000) 460-465.

[10] M. J. Whitcombe, M. E. Rodriguez, P. Villar and E. N. Vulfson, A new method for the introduction of recognition site functionality into polymers prepared by molecular

imprinting: Synthesis and characterization of polymeric receptors for cholesterol, *J. Am. Chem. Soc.*, **117** (1995) 7105-7111.

[11] K. Haupt, K. Noworyta and W. Kutner, Imprinted Polymer-Based Enantioselective Acoustic Sensor Using a Quartz Crystal Microbalance, *Anal. Commun.*, **36** (1999) 391-393.

[12] H. S. Ji, S. McNiven, K. Ikebukuro and I. Karube, Selective Piezoelectric Odor Sensing Using Molecularly Imprinted Polymers, *Anal. Chim. Acta*, **390** (1999) 93-100.

[13] O. Ramstrom, L. Ye, M. Krook and K. Mosbach, Screening of a Combinatorial Steroid Library Using Molecularly Imprinted Polymers. *Anal. Commun.*, **35** (1998) 9-11

[14] O. Ramstrom, L.I. Andersson, and K. Mosbach, Recognition Sites Incorporating Both Pyridinyl and Carboxy Functionalities Prepared by Molecular Imprinting, *J. Org. Chem.*, **58** (1993) 7562-7564

[15] D. A. Spivak and K. J. Shea, Binding of Nucleotide Bases by Imprinted Polymers, *Macromoleculues*, **31** (1998) 2160-2165.

[16] L. Andersson and K. Mosbach, Enantiomeric resolution of amino acid derivatives on molecularly imprinted polymers as monitored by potentiometric measurements, *J. Chromatogr.* **516** (1990) 313-322.

[17] L. I. Andersson, D. J. O'Shanessy and K. Mosbach, Molecular recognition in synthetic polymers: preparation of chiral stationary phases by molecular imprinting of amino acid amides, *J. Chromatogr.*, **513** (1990) 167-179.

[18] M. Glad, O. Norrlow, B. Sellergren, N. Seigbahn and K. Mosbach, Use of Silane Monomers for Molecular Imprinting and Enzyme Entrapment in Polysiloxane-coated Porous Silica, *J. Chromatogr.* **347** (1985) 11-23.

[19] F. L. Dickert, M. Tortschanoff, W. E. Bulst and G. Fischerauer, Molecularly Imprinted Sensor Layers for the Detection of Polycyclic Aromatic Hydrocarbons in Water, *Anal. Chem.*, **71** (1999) 4559-4563.

[20] C. J. Percival, S. Stanley, M. Galle, A. Braithwaite, M. I. Newton, G. M^{c}Hale and W. Hayes, Molecular-imprinted, polymer-coated quartz crystal microbalances for the detection of terpenes, *Anal. Chem.*, **73** (2001) 4225-4228.

[21] E. Yilmaz, K. Mosbach and K. Haupt, Influence of Functional and Cross-Linking Monomers and the Amount of Template on the Performance of Molecularly Imprinted Polymers in Binding Assays, *Anal. Commun.*, **36** (1999) 167-170.

[22] S. Bruckenstein, M. Michalski, A. Fensore, Z. Li and A. R. Hillman, Dual quartz-crystal microbalance oscillator circuit – minimizing effects due to liquid viscosity, density and temperature, *Anal. Chem.*, 1994, **66**, 1847-1852.

[23] D. Kriz, O. Ramstrom and K. Mosbach, Molecular imprinting - New possibilities for sensor technology, *Anal. Chem.*, 1997, **69**, 345A-349A.

[24] G. Vlatakis, L.I. Andersson, R. Müller and K. Mosbach, Drug Assay Using Antibody Mimics Made by Molecular Imprinting, *Nature* **364** (1993) 645-647.

[25] B. Jakoby, G. M. Ismail, M. P. Byfield and M. J. Vellekoop, A Novel Molecularly Imprinted Thin Film Applied to a Love Wave Gas Sensor, *Sens. Actuators* A, **76**, (1999) 93-97.

Acknowledgements

The authors gratefully acknowledge the financial support of The Royal Society research grant 574006.G503/21268/SM.

Figure 1

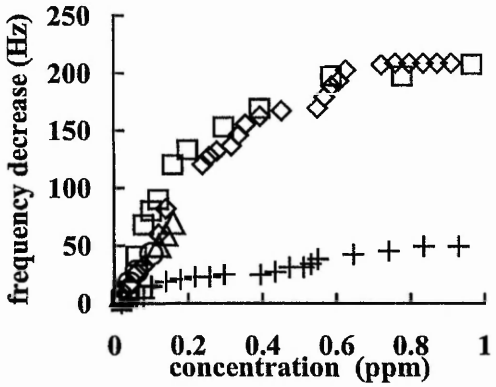

Figure Caption

Figure 1

The resonant frequency change of the QCM as a function of concentration for L-serine (different coatings shown as squares, diamonds, circles and triangles) and D-serine (+).

Appendix 6.93

Molecular imprinted polymer coated QCM for the detection of nandrolone

C.J.Percival[a], S.Stanley[a], A.Braithwaite[a], M.I.Newton*[a] and G.McHale[a]

[a]*Department of Chemistry and Physics, The Nottingham Trent University, Clifton Lane, Nottingham NG11 8NS, UK Fax: 44 115 8486636; Tel: 44 115 8483365; E-mail: Michael.Newton@ntu.ac.uk*

An acoustic wave sensor coated with an artificial biomimetic recognition element has been developed to selectively screen for nandrolone in the liquid phase. A highly specific covalently imprinted polymer (MIP) was spin coated on to one electrode of a quartz crystal microbalance (QCM) as a thin permeable film. Selective rebinding of the nandralone was observed as a frequency shift in the QCM for concentrations up to 0.2 ppm with the sensor binding shown to favour nandrolone over analogous compounds.

Introduction

One of the most widely abused classes of banned drugs in sports is anabolic steroids (e.g. nandrolone). Anabolic steroids, which are related in structure and activity to the male hormone testosterone, are used by competitors to improve muscle strength and accelerate recovery times from exercise and so to extend their training effectiveness. The abuse of anabolic steroids in human and equine sports has led to a strict ban of anabolic steroids by national and international sports federations and by the Medical commission of the International Olympic Committee (IOC). Urine analysis is recommended for the detection of all banned drugs on the current IOC list[1]. A wide variety of methods for the detection of anabolic steroids in urine have been described. Immunoassay techniques can provide an effective means of screening numerous sample[2,3] since they are rapid and inexpensive. However, these techniques have limited specificity and can give false positive results. Several TLC and HPTLC methods have been proposed[4-7] but these methods have low sensitivity and the sample preparation is laborious. GC-MS has been proved to be a suitable technique for the detection of anabolic steroids[8-12]. In general however, GC-MS based procedures require expensive equipment and involve lengthy sample extraction and subsequent derivatisation.

Molecular recognition is a highly efficient and essential feature of biological systems in nature and as such has found application in biosensors[13]. Natural biological recognition systems, whilst highly selective, are of limited use, however, as a result of poor chemical and thermal stability, limited assay range, lifespan and expense. The use of artificial recognition materials has been proposed as a means of addressing some of the limitations inherent in biosensors. One of the most promising examples of artificially generated recognition materials are the molecularly imprinted polymers (MIP). MIPs are highly cross-linked polymers, which are inherently stable and capable of high selectivities approaching that of their natural counterparts. MIPs have become well established as a means of producing biomimetic recognition sites since first reported over 25 years ago[14,15] with the selectivity and binding affinities of MIP being comparable to antibody-antigen interactions. Two distinct imprinting strategies have evolved: i) covalent and ii) non-covalent template polymerisations. Covalent imprinting involves the conversion of the template (or an analogue) into a polymerisable derivative that is then copolymerised with a suitable cross-linker to afford a resin that covalently incorporates the template. Covalent interactions between the template and the functional monomer have the advantage that the binding groups remain precisely orientated during elevated temperatures that are often a feature of the polymerisation process. The stability of the covalent bond produces a homogeneous population of binding sites within the imprinted polymer. In part this stability of the 'covalent complex' is responsible for the high binding affinities (in comparison to non covalent MIPs) associated with covalently imprinted polymers with in excess of 75% of print sites being re-occupied[16]. Covalent imprinting has been widely used to produce MIPs that are selective for a range of analytes including, caffeine in human urine and serum[17], the plant hormone indole acetic acid[18], macromolecules[19], the chiral benzodiazepine[20] and the steroid cholesterol[21], which has formed the basis of our approach. In contrast, non-covalent imprinting involves the self-assembly of suitable functional monomers around the template molecule. Following addition of a cross-linker this assembly is then 'fixed' by polymerisation. Subsequent removal of the non-covalently bound template reveals vacant recognition sites that are specific to the target analyte in terms of their spatial and electronic environment. Non-covalent imprinting has inherent advantages over the covalent strategy as a consequence of the rapid and reversible nature of non-covalent interaction between the polymer and the template. Non-covalent imprinting has been reported with MIPs selective for many analytes including, R- and S-propranolol[22], the odorant methylisoborneol[23], steroids[24], carboxylic acids[25], nucleotide bases[26], enantiomeric resolution of amino acids[27,28], dyes[29] and PAHs[30]. In this work we present an alternative technique for the selective direct detection of nandrolone in liquids using a covalently imprinted recognition element for potential use as a screening device.

Experimental

Reagents

All steroids and the functional monomer methacrylic acid (MAA) were purchased from Lancaster synthesis. The ethylene glycol dimethacrylate (EDMA), Phosgene and 4-Acetoxystyrene were supplied by Aldrich chemicals. The initiator 2,2'-Azobis(2-methylpropionitrile) (AIBN) was supplied by Acros chemicals. All the solvents were of analytical grade and all reagents were used as supplied.

Quartz Crystal Microbalance

The quartz crystal microbalance consisted of a Maxtek PLO10 phased locked oscillator and an Agilent HP53132A universal counter interfaced to a microcomputer. The quartz crystals used were unpolished AT-cut, 25 mm diameter, with Cr/Au contacts, operating at a fundamental resonant frequency of 5 MHz. The electrode area was approximately 133 mm^2 (Maxtek model No. 149211-2) and the crystals were mounted in a Maxtek CHC-100 crystal holder. Prior to the application of the polymer coating to the electrode area, the crystals were prepared using Pirannha etch solution (1:3 30% v/v H_2O_2: conc. H_2SO_4). The crystals were immersed in Piranha etch solution for ten minutes, then rinsed with deionised water and ethanol and dried overnight.

Molecular Imprinted Polymer Synthesis

Prior to the formation of the imprinted polymer, nandrolone was first converted to a polymerisable derivative, in this case the 4-vinylphenyl carbonate ester of nandrolone. The ester functions as a covalently bound template monomer that is easily cleaved to

yield a non-covalent recognition site. The MIP film was produced via a four stage synthesis:

1 Preparation of 4-vinylphenol: 4vinyl phenol was prepared as per Corson *et al.*[31] A mixture of 16.2g.(0.10 mole) of *p* - acetoxystyrene, 13.8g.(0.25 mole) of potassium hydroxide and 140ml. of water was stirred at 0°C until homogeneous (2 hrs). The stirred cold solution was acidified to *p*H 8 to produce 12g. (100% yield) of 4-vinylphenol and the 4-vinylphenol product was identified by NMR.

2.*Preparation of nandraolone chloroformate*: 2.4g. (8.3mmol) of nandrolone in 30ml of dry THF with BHT (trace) was cooled on ice. Then 2.0ml of NET_3 (dried over KOH) was added dropwise to this cold solution. 9.60ml of phosgene dropwise to reduce fuming. This solution was stirred at 0°C under nitrogen for 6 hours.

3. *Preparation of nandrolone (4-vinyl)phenyl carbonate*: A solution containing 1.05g (8.3mmol) of 4-vinylphenol in 20ml of dry THF with BHT (trace) and 1.0ml.of NET_3 (dried over KOH) was added dropwise to the nandrolone chloroformate prepared in step two. The solution was stirred at room temperature overnight. The crude product was filtered and the solid discarded. The liquor was evaporated down with BHT. After evaporation,the residue was dissolved in DCM and washed with water. The organic layer was collected and evaporated down to yield product which was further cleaned by running through a silica column; the product 4-vinylphenyl carbonate ester of nandrolone was identified by NMR.

4. MIP synthesis: The monomer mixture consisting of the product 4-vinylphenyl carbonate ester of nandrolone (1.5 mmol), Methacrylic acid (6.0 mmmol), EDMA (30 mmmol) and the porogenic solvent (9:1) hexane:tolune (74 mmol), were dispensed into a sample tube and the initiator AIBN (0.19 mmol) added the tube was the sealed and sonicated for 15minutes. The polymerisation was then performed in a water bath at 65°C for 24 hours. The polymer was obtained as a brittle solid which, is crushed and sieved to <38μm. The ground polymer was extracted with methanol in a soxhlet apparatus overnight and then dried under vacuum at 40°C.

The polymer was suspended in 1M sodium hydroxide in methanol and heated to refluxed for 6 hours. The cooled solutions are added to an excess of dilute HCl. The products are filtered and washed with water, methanol and ether. Polymers were soxhlet extracted with methanol and then hexane and dried under vacuum at 40°C. The films were then spin coated on to the crystals using the following technique: 10mg.of PVC powder was dissolved in 5ml of THF and 30mg of MIP particles were suspended in solution with thorough stirring. A QCM was fixed via vacuum to a laboratory spin coater and coated with 10μl of the pvc/polymer solution and the suspension spread over the surface of the Au electrode by rotating at 600-900 rpm for a period of five minutes.

Evaluation of sensor response

Solutions containing known amounts of the analyte were prepared in ethanol. The coated quartz crystals were placed into a beaker of ethanol until a stable response was obtained then, 6 ml of analyte solution were added to the stirred bulk ethanol solution via successive 1 ml aliquots. The frequency was recorded until a stable response was obtained. After each 6 ml addition of analyte the coated quartz crystal was soaked in the porogenic solvent for 10 minutes and the experiment was repeated. It is known that QCM are affected by changes in ambient temperature which cause a drift in resonant frequency. On the timescale of the experiment, the change in frequency caused by environmental conditions could be greater than that caused by the mass loading of the quartz crystal. In order to overcome this difficulty the frequencies of two quartz crystals immersed in the ethanol solution, one crystal coated with the MIP and one crystal coated with the non imprinted polymer, were measured simultaneously following the DQCM technique of Bruckenstein et. al.[32]. The resultant difference in frequency between the two crystals can be used to assess the response of the crystal to mass loading of the analyte as the non imprinted polymer displayed no change in resonant frequency with mass loading; all experiments were performed in this manner.

Results and Discussion

In figure 1 we show the change in resonant frequency of the QCM as a function of nandrolone concentration for two different coatings produced using an identical procedure. There is an initial linear decrease in frequency corresponding to increase in nandrolone concentration up to about 0.1 ppm with a gradient of -164 ± 10 Hz ppm^{-1}, which reaches saturation at concentrations exceeding 0.2 ppm. Similar sorption isotherms have been observed by Haupt et al.[22] for the binding of S-propranolol to a molecularly imprinted polymer and such sorption isotherms are expected for polymers that contain immobilised binding sites, such as found in MIPs. After the first cycle of exposures the response of the MIP degrades and gives a lower frequency change for the same analyte concentrations however, it can be seen that the response of fresh coatings is relativly reproducible. The affinity of the MIP towards nandrolone can be evaluated using a simple one site Langmuir-type binding isotherm anylsis[33] $Kc(\Delta f/\Delta f_\infty)+(\Delta f/\Delta f_\infty)=Kc$ where K is the binding coefficient, c is the free analyte concentration at equilibrium Δf is the frequency change and Δf_∞ is the frequency corresponding to complete coverage. Although this does not reflect the real situation in the polymer it allows for a comparison of binding between polymers. Using the data shown, the calculated binding coefficient $K = 123.2 \pm 10.9\ \mu M^{-1}$ which is similar to those found in other MIPs[34]. In figure 1 we also show the response of the QCM to testosterone and epitestosterone; no significant change in resonant frequency was observed upon the addition of these steroids up to a concentration 2 ppm.

Whilst the stability of the MIP to repeated exposures of nandralone does not demonstrate reproducibility, we have shown that fresh MIP coated quartz crystal sensors does offer reasonable reproducibly. The natural extension of this work is to enhance the sensitivity of the sensors to enable a low cost screening technique of biological samples to be produced. This

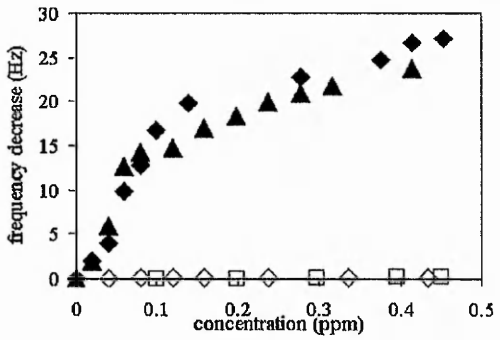

Fig1. Frequency decrease as a function of concentration for nandralone (solid triangles, solid diamonds), testosterone (open diamonds) and epitestostorone (open squares).

may be achieved firstly by increasing the concentration of binding sites in the MIP and secondly, by increasing the mass sensitivity of the acoustic device. The latter involves increasing the QCM resonant frequency; the upper limit for quartz crystal microbalances operating at the fundamental frequency being around 10 MHz. Alternatively, shear horizontal surface acoustic wave devices (SH-SAW) may be employed that will extend the range of operating frequencies by more than an order of magnitude[23,35]. Such acoustic wave devices may be incorporated

in lightweight and low cost oscillator circuit allowing an inexpensive screening technique to be developed.

References

1. IOC. Olympic movement Anti-Doping Code. *Lausanne*: IOC, 2000.
2. H.H.D.Meyer and S.Hoffmann, *Food Addit. Contam.* 1987, **4**, 149.
3. G.Degand, P.Schmitz, J.Maghuin-Rogister *J. Chromatogr.* 1989, **489**, 235.
4. R.J.Verbeke, *Chromatogr.* 1979, **177**, 69.
5. L.A.Van Ginkel, H.Van Blitterswijk, P.w.Zoontjes, D.Van Den Bosch, and R.W.Stephany, *J. Chromatogr.* 1988, **445**, 385.
6. H.F.de Brabander,P.Vanhee, S.van Hoye, and R.Verbeke, *J. Planar Chromatogr.* 1989, **2**, 33.
7. Th.Reuvers, Perogordo,E.Alimentaria, E. 1986, **170**, 27.
8. E.Daeselerie, A.de Guesquierie and C. van Peteghem, *J. Chromatogr. Sci.* 1992, **30**, 409.
9. A.Boenke, *Anal. Chim. Acta.* 1993, **275**, 3.
10. B.Le Bizec, M-P.Montrade, F.Monteau and F.Andre, *Anal. Chim. Acta.* 1993, 275, 123.
11. G.van Vyncht, P.Gaspar, E.Depauw and G.Maghuin-Rogister, *J. Chromatogr.* B. 1996, **686**, 189.
12. Y.Galliard and G.J.Pepin, *Chromatogr.* A. 1997, **763**, 149.
13. R.S.Sethi, *Biosens. Bioelectron.* 1994, **9**, 243
14. G.Wulff and A.Sarhan, *Angew. Chem. Int. Ed. Engl.* 1972, **11**, 341.
15. G.Wulff, *Angew. Chem. Int. Ed. Engl.* 1995, **34**, 1812
16. B.Sellergren, *Anal. Chem.* 1994, **66**, 1578
17. C.Liang, H.Peng, X.Bao, L.Nie and S.Yao, *Analyst* 1999, **124**, 1781
18. A.Kugimiya and T.Takeuchi, *Electroanalysis* 1999, **11**, 1158
19. K.J.Shea, E.A.Thompson, S.D.Pandey and P.S.Beauchamp, *J. Am. Chem. Soc.* 1980, **102**, 3149
20. B.R.Hart, D.J.Rush and K.J. Shea, *J. Am. Chem. Soc.* 2000, **122**, 460
21. M.J.Whitcombe, M.E.Rodriguez, P.Villar and E.N.Vulfson, *J. Am. Chem. Soc.* 1995, **117**, 7105
22. K.Haupt, K.Noworyta and W.Kutner, *Anal. Commun.* 1999, **36**, 391
23. H.S.Ji, S.McNiven, K.Ikebukuro and I.Karube, *Anal. Chim. Acta* 1999, **390**, 93
24. O.Ramstrom, L.Ye, M. Krook and K. Mosbach, *Anal. Commun.* 1998, **35**, 9
25. O.Ramstrom, L.I.Andersson and K.Mosbach, *J. Org. Chem.* 1993, **58**, 7562
26. D.A.Spivak, K.J. Shea, *Macromoleculues* 1998, **31**, 2160
27. L.I.Andersson and K. Mosbach, *J.Chromatogr.* 1990, **516**, 313
28. L.I.Andersson, D.J. O'Shanessy and K. Mosbach, *J. Chromatogr.* 1990, **513**, 167
29. M.Glad, O.Norrlow, B.Sellergren, N.Siegbahn and K. Mosbach, *J. Chromatogr.* 1985, **347**, 11
30. F.L.Dickert, M.Tortschanoff, W.E.Bulst and G. Fischerauer, *Anal. Chem.* 1999, **71**, 4559
31. B.B.Corson, W.J.Heintzelman, L.H.Schwartzman, H.E.Tiefenthal, R.J. Lokken, J.E. Nickels, G.R.Atwood and F. Pavlik, J. J. Org. Chem. 1958, **23**, 544
32. S.Bruckenstein, M. Michalski, A.Fensore, Z. Li and A.R.Hillman, *Anal. Chem.* 1994, 66, 1847-1852.
33. E.Yilmaz, K. Mosbach and K. Haupt, *Anal. Commun.* 1999, **36**, 167,
34. G.Vlatakis, L.I.Andersson, R. Müller and K. Mosbach, *Nature* 1993, **364**, 645
35. B.Jakoby, G.M.Ismail, M.P.Byfield and M.J.Vellekoop, *Sens. Actuators A* 1999, **76**, 93

Appendix 6.94

Anal. Chem. **2003,** *75,* 1573−1577

Detection of Polycyclic Aromatic Hydrocarbons Using Quartz Crystal Microbalances

S. Stanley,[†] C. J. Percival,*[,†] M. Auer,[†] A. Braithwaite,[†] M. I. Newton,[†] G. McHale,[†] and W. Hayes[‡]

Department of Chemistry and Physics, The Nottingham Trent University, Nottingham NG11 8NS, U.K., and Department of Chemistry, University of Reading, Whiteknights, Reading RG6 6AD, U.K.

A chemically coated piezoelectric sensor has been developed for the determination of PAHs in the liquid phase. An organic monolayer attached to the surface of a gold electrode of a quartz crystal microbalance (QCM) via a covalent thiol−gold link complete with an ionically bound recognition element has been produced. This study has employed the PAH derivative 9-anthracene carboxylic acid which, once bound to the alkane thiol, functions as the recognition element. Binding of anthracene via $\pi-\pi$ interaction has been observed as a frequency shift in the QCM with a detectability of the target analyte of 2 ppb and a response range of 0−50 ppb. The relative response of the sensor altered for different PAHs despite $\pi-\pi$ interaction being the sole communication between recognition element and analyte. It is envisaged that such a sensor could be employed in the identification of key marker compounds and, as such, give an indication of total PAH flux in the environment.

Polycyclic aromatic hydrocarbons (PAHs) are a complex class of hydrocarbons resulting from the incomplete combustion of organic substances, such as fossil fuels[1], coal,[2,3] fuel oil,[4] gas,[5] refuse,[6] wood,[7] tobacco,[8] and foodstuffs.[9] Additional sources include wood preservative plants, incinerators, asphalt road and roofing operations, and aluminum plants.[10] The widespread generation and subsequent release of PAHs into the environment means that they are found in air, water, and soil throughout the world, often as a complex mixture that may exist for months or years.[5]

PAHs are characterized by their fused-ring structures consisting of between two and seven aromatic rings. The conjugated π electron systems of these aromatic compounds determines their physical and chemical properties. Naphthalene, for instance, a two-ringed compound, is the smallest member of the class and is found in the vapor phase in the atmosphere, while PAHs consisting of three to five rings are present in the air in both the vapor and particulate phases. The PAHs with five or more rings are commonly found as solids adsorbed onto particulate matter in the atmosphere.[11]

The flat hydrophobic shape and high lipid solubility of PAHs makes their excretion from the body difficult. The PAH is then able to intercalate with the structure of DNA and, consequently, disrupt the proper functioning of DNA.[12] More often than not, such damage is repaired; however, if the mistake is not repaired, the DNA can be misread, resulting in defective proteins, which may ultimately lead to cancer.[12] The possible health hazards associated with PAH exposure are numerous and include skin problems, immunodeficiency, reproductive difficulties and cancer.[13]

Although the effects of many PAHs on mammals is poorly understood, a number are known or suspected carcinogens. The five-ringed PAHs benzo[*a*]pyrene and dibenz[*a*]anthracene are known for their carcinogenicity. Benzo[*a*]pyrene itself is regarded as a key indicator compound of PAHs because it occurs in all mixtures where PAHs are present. The U.S. EPA has established maximum contaminant levels (MCLs) for public drinking water to minimize the risk of adverse health effects. The MCL for total PAHs is 0.2 ppb. In light of the obvious health effects associated with PAHs and their ever increasing use and emission, there is a clear need to monitor these compounds.

Our increasing impact on the environment demands that we establish faster, cheaper and more accurate ways to analyze a wide variety of compounds. Gravimetric sensors, such as the quartz crystal microbalance (QCM), are well suited as transducer elements for chemical sensors, being portable, rapid, and sensitive. For applications in chemical sensing, a recognition element is added to the acoustic wave device capable of selectively binding the analyte to the device surface. The response of these devices

* Corresponding author. E-mail: carl.percival@ntu.ac.uk.
† The Nottingham Trent University.
‡ University of Reading.

(1) Wayne, R. P. *Chemistry of the Atmospheres,* 3rd ed.; Oxford University Press: Oxford, 2000.
(2) Vo-Dinh, T.; Martinez, P. R. *Anal. Chim. Acta* **1981**, *125*, 13−19.
(3) Mumford, J. L.; Helmes, C. T.; Lee, X.; Seidenberg, J.; Nesnow, S. *Carcinogenesis* **1990**, *11*, 397−403.
(4) Benner, B. A., Jr.; Gordon, G. E.; Wise, S. A. *Environ. Sci. Technol.* **1989**, *23*, 1269−1278.
(5) Finlayson-Pitts, B. J.; Pitts, J. M. *Chemistry of the Upper and Lower Atmosphere,* 1st ed.; Academic Press: New York, 1999.
(6) Lee, W. M. G.; Yuan, Y. S.; Chen, J. C. *J. Environ. Sci. Health* **1993**, *A28*, 1017−1035.
(7) Alfheim, I.; Ramdahl, T. *Environ. Mutagen.* **1984**, *6*, 121−130.
(8) Gundel, L. A.; Mahanama, K. R. R.; Daisey, J. M. *Environ. Sci. Technol.* **1995**, *29*, 1607−1614.
(9) Crosby, N. T.; Hunt, D. C.; Philip, L. A.; Patel, I. *Analyst* **1981**, *106*, 135−145.
(10) Vo-Dinh, T. *Chemical Analysis of Poly Aromatic Hydrocarbons,* 1st ed.; John Wiley and Sons: New York, 1989.
(11) Junge, C. E. *Adv. Environ. Sci. Technol.* **1977**, *8*, 7−26.
(12) Hoffman, D. J.; Rattner, B. A.; Burton, G. A. Jr.; Cairns, J. Jr. *Handbook of Ecotoxicology,* Lewis Publishers: London, 1995.
(13) Smith, L. E.; Denissenko, M. F.; Bennet, W. P.; Li, H.; Amin, S.; Tang, M.; Pfeifer, G. P. *J. Natl. Cancer Inst.* **2000**, *92*, 803−811.

10.1021/ac0257546 CCC: $25.00
Published on Web 02/25/2003

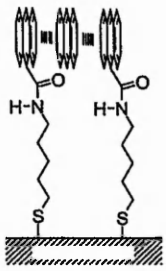

Figure 1. Schematic diagram of the $\pi-\pi$-stacking interaction in coating on crystal surface.

is then based on a decrease in their resonance frequency as mass is attached to the device or the recognition element.

Recently, Dickert et al.[14] showed that a molecularly imprinted polymer-coated QCM displays affinity toward a range of PAHs. In this work, an alternative approach was used that relies upon the formation of an alkanethiol monolayer upon the surface of the transducer to which is attached the recognition element. It is possible to form a mixed monolayer of two alkanethiols with different tail groups when depositing from a solution onto a surface rather than phase segregating into macroscopic domains.

To achieve a specific adsorption of PAHs onto the organic monolayer, PAH acid analogues were attached to the other end of alkanethiol, as indicated in Figure 1. The appended PAH groups form a $\pi-\pi$ stacking array. Other PAHs from a surrounding PAH solution bind to the PAH thiol layer via $\pi-\pi$ interaction between the π-electron systems of aromatic multirings. This electronic interaction, characteristic of aromatic systems, can occur when the π bonds of an aromatic molecule undergo spontaneous polarization. The spontaneous dipole that results induces a second dipole on another aromatic molecule and they are attracted to each other,[15] with the additional mass bound in the organic layer detected by the QCM. This interaction is likely to occur with any PAH in the solution, but most favorably with PAH-molecules that have a structure that is identical to the aromatic system employed as recognition element. Thus, the necessary selectivity is achieved for this coating to be effective in terms of its ability to interact with the target analyte via a $\pi-\pi$ stacking array.

In this work, a piezoelectric sensor with a preferential selectivity for the PAH anthracene is presented. An organic monolayer containing the recognition element is attached to the surface of a gold electrode of a quartz crystal microbalance (QCM) via a covalent thiol–gold bond.

EXPERIMENTAL SECTION

Reagents. 3-Dimethylaminopropyl chloride hydrochloride, potassium carbonate, anthracene, potassium thioacetate, 1-butanethiol, 9-anthracene carboxylic acid, naphthalene, benzo[*a*]pyrene and 1,2:5,6-dibenzanthracene were purchased from Aldrich Chemicals (Dorset, U.K.). All the solvents were of analytical grade and all reagents were used as supplied.

Quartz Crystal Microbalance. The quartz crystal microbalance was produced using unpolished AT-cut, 25-mm-diameter, plano–plano quartz crystals with Cr/Au contacts, operating at a fundamental resonance frequency of 5 MHz and with an electrode area of ~133 mm² (Maxtek model no. 149211-2). The crystals were mounted in a Maxtek CHC-100 crystal holder, and the measurement system consisted of a Maxtek PLO10 phased-locked oscillator and an Agilent HP53132A universal counter interfaced to a microcomputer.

Prior to the application of the polymer coating to the electrode area, the crystals were prepared using pirannha etch solution (1:3 30% v/v H_2O_2/conc H_2SO_4). The crystals were immersed in Pirannha etch solution for 10 minutes, then rinsed with deionized water and ethanol and dried overnight.

Scheme 1. Outline of the Synthesis of the Ionic Coating

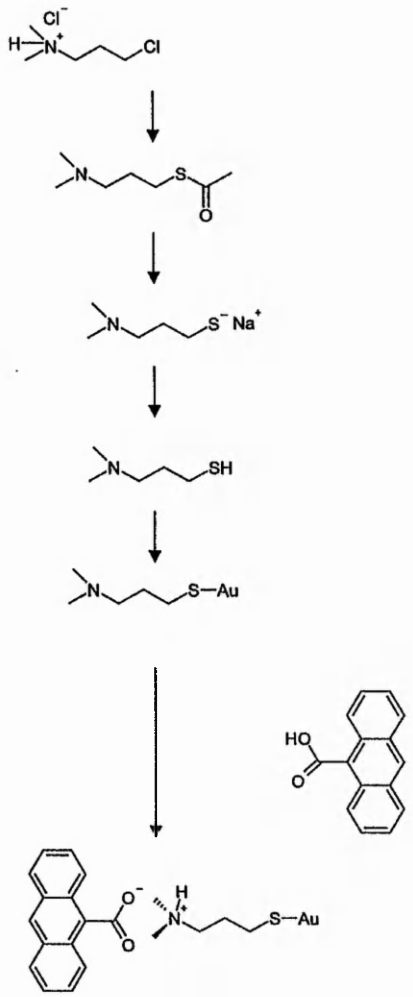

Ionic PAH Coating. The synthesis of the ionic coating is summarized in Scheme 1. A 0.01-mol portion of 3-dimethylaminopropyl chloride hydrochloride $(CH_3)_2N(CH_2)_3Cl{\cdot}HCl$ was stirred together with 0.01 mol potassium carbonate (K_2CO_3) in 20 mL of dried acetone under nitrogen for ~0.5 h. Subsequently, 0.01 mol of potassium thioacetate ($KSCOCH_3$) was added, stirred for ~2.5 h, and left overnight to form a precipitate. The solution was filtered

(14) Dickert, F. L.; Besenböck, M.; Tortschanoff, M. *Adv. Mater.* **1998**, *10*, 149.
(15) Israelachvili, J. *Intermolecular and Surface Forces*, 2nd ed.; Academic Press: New York, 1992.

off and evaporated, yielding a precipitate as the product of step 1, which was identified by NMR spectroscopy.

The acetate group was replaced by a sodium ion in step 2 by dissolving 0.3 g (~2 mmol) of diethylaminopropylthioactetate in 15 mL of 4 M sodium hydroxide–methanol solution. This solution was mixed with 30 mL of 2 M HCl and half the molar amount of 1-butanethiol in a glass beaker containing a quartz crystal. The acid neutralizes the hydroxide, and the thiolate ion is protonized, forming a thiol group (step 3) that subsequently forms a covalent bond with the gold of the electrode on the crystal surface (step 4). Simultaneously, the butanethiol fixes on the gold electrode in the same manner, forming spacers between the aminothiols. The crystals were left in this solution for ~4 h, then they were taken out of the solution. To ionically attach an anthracene molecule, the quartz crystals were placed directly into a solution of the same molar amount of 9-anthracenecarboxylic acid as aminothiol in ~30 mL of ethanol for ~1 h. Anthracenecarboxylate ions are assumed to form an ionic link with quarternary ammonium ions on top of the organic chains on the crystal (step 5). The crystals were rinsed with ethanol after having been taken out of the solution, then dried with and kept under nitrogen until they were screened.

Reference crystals were made by covalently binding the mixture of butanethiol and aminothiols to the quartz crystals. This is achieved by following the outlined synthesis and finishing at step 4. At this point, control samples (blank crystals) were washed with ethanol and dried under nitrogen.

Evaluation of Sensor Response. Solutions containing known amounts of the analyte were prepared in ethanol. The coated quartz crystals were placed into a beaker of ethanol until a stable response was obtained, then 9 mL of analyte solution was added to the stirred bulk ethanol solution via successive 1 mL aliquots. The frequency was recorded until a stable response was obtained. After each 9-mL addition of analyte, the coated quartz crystal was soaked in the porogenic solvent for 10 min, and the experiment was repeated.

A drift in resonance frequency of the QCM may be observed, which is caused by changes in the environmental conditions, such as temperature. On the time scale of the experiment, the change in frequency caused by environmental conditions could be greater than that caused by the mass loading of the quartz crystal. To overcome this difficulty, the frequencies of two quartz crystals immersed in the ethanol solution, one crystal with the ionic coating and one crystal with no attached PAH group coating were measured simultaneously following the DQCM technique of Bruckenstein et al.[16] The resultant difference in frequency between the two crystals can be used to assess the response of the crystal to mass loading of the analyte, because the crystal with no PAH coating displayed no detectable change in resonance frequency with mass loading; all experiments were performed in this manner.

RESULTS AND DISCUSSION

Response of the Sensors to Mass Loading of Anthracene. The change in resonance frequency of the coated quartz crystal as a function of anthracene concentration is shown in Figure 2. There is an initial linear decrease in frequency corresponding to an increase in anthracene concentration up to ~15 ppb, with a gradient in the range $S_{anthracene} = -2.047 \pm 0.042$ Hz ppb^{-1}, which reaches saturation at concentrations exceeding 20 ppb. Similar sorption isotherms have been observed for the binding of analytes to a polymer with a finite number of interaction sites.[17]

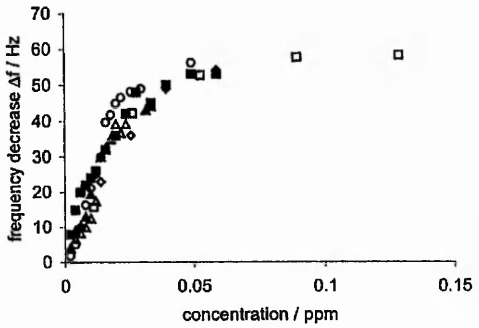

Figure 2. Resonance frequency change of the QCM with the ionic coating: coating 1 (◊), coating 2 (□), coating 3 (△), coating 4 (○), coating 5 (♦), and coating 6 (■).

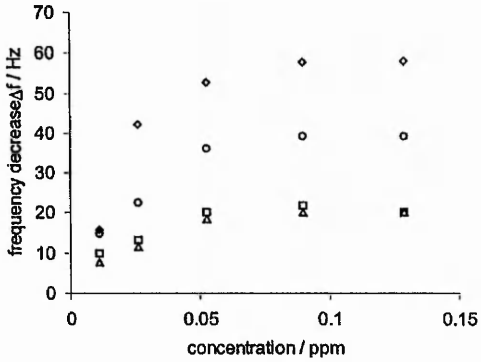

Figure 3. Resonance frequency change of the QCM with the ionic coating: run 1 (◊), run 2 (□), run 3 (△), and after replenishing coating (○).

The data presented in Figure 2 shows the response for six different quartz crystals, each with a PAH coating produced in the same way. The agreement suggests that our methodology for coating the quartz crystals is reproducible between different coatings.

Between screenings, the crystal was thoroughly rinsed with ethanol. This cleaning method, however, seems to have been only partly successful. Subsequent test runs with one crystal showed in general a greatly reduced frequency shift, as shown in Figure 3. This implies that the number of analyte interaction sites therefore has been reduced, many of them remaining blocked after the initial screening.

The ionic link that holds the aromatic groups in place can be broken, and another analyte interaction site can be attached. To examine this, coated crystals that had already been screened were placed first into a NaOH solution, then into a 9-anthracenecarboxylic acid–ethanol solution. Applying 4 M NaOH for ~1 h and 9-anthracenecarboxylic acid overnight was performed in order to replenish the coating. Figure 3 also shows a comparison between the fresh coating and the replenished coating. It can be seen that

(16) Bruckenstein, S.; Michalski, M.; Fensore, A.; Li, Z.; Hillman, A. R. *Anal. Chem.* **1994**, *66*, 1847–1852.

(17) Percival, C. J.; Stanley, S.; Galle, M.; Braithwaite, A.; Newton, M. I.; McHale, G.; Hayes, W. *Anal. Chem.* **2001**, *73*, 4225–4228.

Table 1. Summary of the Experimentally Evaluated Apparent Dissociation Constants and Initial Slopes

constant	anthracene	naphthalene	benzo[*a*]pyrene	1,2:5,6-dibenzanthracene
$S_{initial}$/ppb^{-1}	−2.047 ± 0.042	−0.988 ± 0.048	0.327 ± 0.019	0.437 ± 0.024
K, ppm^{-1}	60.16	51.94	47.22	31.26

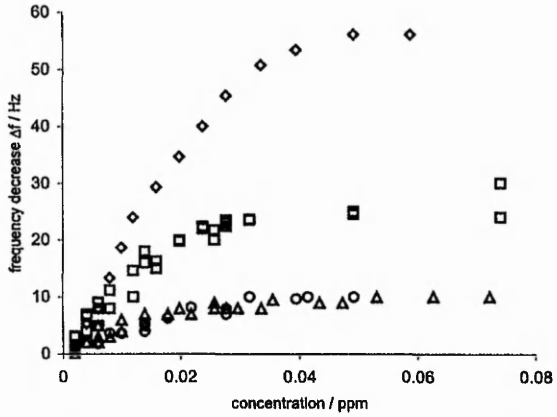

Figure 4. Range of monoterpene analogues that the selectivity of the ionic coated quartz crystals were tested toward: anthracene (◊), naphthalene (□), 1,2:5,6-dibenzanthracene (△), and benzo[*a*]pyrene (○).

the measured frequency shift was still clearly below its original value. Therefore, it can be seen that under the experimental conditions used, it is not possible to recover 100% of the analyte interaction sites. All subsequent analysis is performed on fresh coatings.

Selectivity. To examine the selectivity of the created sensor, crystals with the same coating with anthracene as a functional group were screened with different PAHs, as shown in Figure 4. All curves show linear behavior until the concentration reaches ~15−20 ppb, which reaches saturation at concentrations exceeding 20 ppb, the gradients of which are given in Table 1.

The affinity of the PAH ionic coatings toward PAHs can be evaluated using a one-site Langmuir-type binding isotherm anayl-sis,[18]

$$Kc\frac{\Delta f}{\Delta f_\infty} + \frac{\Delta f}{\Delta f_\infty} = Kc$$

where K is the apparent dissociation constant, c is the free analyte concentration at equilibrium, Δf is the frequency change, and Δf_∞ is the frequency corresponding to complete coverage. Although this does not reflect the real situation in the polymer, it allows for a comparison of binding between polymers. Using the data shown in Figure 4, the apparent dissociation constants K were estimated and are given in Table 1.

Anthracene shows the largest apparent dissociation constant, which indicates that the anthracene groups of the coating attract the anthracene molecules in the solution well. The reason for this behavior is assumed to be the nearly identical π-electron systems of the dissolved molecules and the coating.

Naphthalene has a smaller value of apparent dissociation constant than anthracene. This implies that either naphthalene has a lower molecular mass than anthracene and that the same number of bound naphthalene molecules, therefore, results in a smaller additional mass in the coating and, thus, a smaller frequency shift or that the anthracene groups of the coating show a lower affinity to the somewhat different π-electron system of the naphthalene molecules. The difference in the size of the frequency shift between runs with anthracene and naphthalene gives no definite indication which effect is predominant. However, runs with benzo[*a*]pyrene and 1,2:5,6-dibenzanthracene show similar results. Both are five-membered PAHs and, therefore, have a higher molecular weight than anthracene but still show a decidedly lower response, as indicated by the low values of the apparent dissociation constant. This suggests that the coating selectively binds the target molecule, anthracence, over the larger PAHs, benzo[*a*]pyrene or 1,2:5,6-dibenzanthracene. The coating has less affinity for the larger PAHs, and this effect overrides the influence of their comparatively larger molecular weight. This indicates that the coating displays a degree of shape selectivity.

Dickert et al.[14] produced recognition element for PAHs via the formation of a molecular imprinted polymer of anthracene-coated QCMs. Their results indicated that the MIP recognition element displayed an affinity to several PAHs and showed a greater affinity for benzo[*a*]pyrene, 1,2:5,6-dibenzanthracene, chrysene, pyrene, and benzopyrelene over the target molecule anthracene, with the greatest affinity to chrysene. Unfortunately, it is not possible to directly compare our values of the apparent dissociation constant with those obtained by the molecular imprint approach of Dickert et al., because the values are not given. However, it can be seen that both the MIP approach and our ionic coating display an affinity to PAHs and that both approaches display some selectivity in terms of size and shape of PAH.

CONCLUSIONS

It is clear that quartz crystal sensors coated with a monolayer of aminothiols with an ionically bound anthracene group can be used to preferentially detect the PAH anthracene in the liquid phase with a sensitivity of 2 ppb. There are several possibilities to further improve the sensitivity.

First, it may be possible to increase the number of interaction sites on the QCM. To achieve this, the synthesis of the coating may be improved to give a higher yield. For instance, the effect of different amounts of the spacer 1-butanethiol may also be examined in order to achieve an optimal accessibility of the interaction sites.

Second, the mass sensitivity of the acoustic device can be improved. This may be achieved by increasing the resonance frequency of the sensor, because the sensor response to mass loading is proportional to the square of the operating frequency. The upper limit for quartz crystal microbalances operating at the fundamental frequency is around 10 MHz; the higher the

(18) Yilmaz, E.; Mosbach, K.; Haupt, K. *Anal. Commun.* **1999**, *36*, 167−170.

frequency, the thinner the crystal. Alternatively, surface acoustic wave devices may be employed that will extend the range of operating frequencies to over 1 GHz.[19,20]

For applications of the coated quartz crystal sensors in the field, future work to be considered would be to look for a way to break the ionic link that holds the PAH group and to replenish the coating with the same or a different group, creating a sensor that is capable of detecting different PAHs, such as benzo[*a*]-pyrene, which is considered to be the key marker compound for PAHs. The sensor is likely to respond to other environmental analytes; however, the ability of the sensor to respond preferentially to the target analyte compared with closely related analogues offers the potential to distinguish between PAHs and other analytes.

(19) Ji, H. S.; McNiven, S.; Ikebukuro, K.; Karube, I. *Anal. Chim. Acta* **1999**, *390*, 93−100.
(20) Jakoby, B.; Ismail, G. M.; Byfield, M. P.; Vellekoop, M. J. *Sens. Actuators, A* **1999**, *76*, 93−97.

Received for review May 7, 2002. Accepted January 29, 2003.

AC0257546